CHALMERS
UNIVERSITY OF TECHNOLOGY

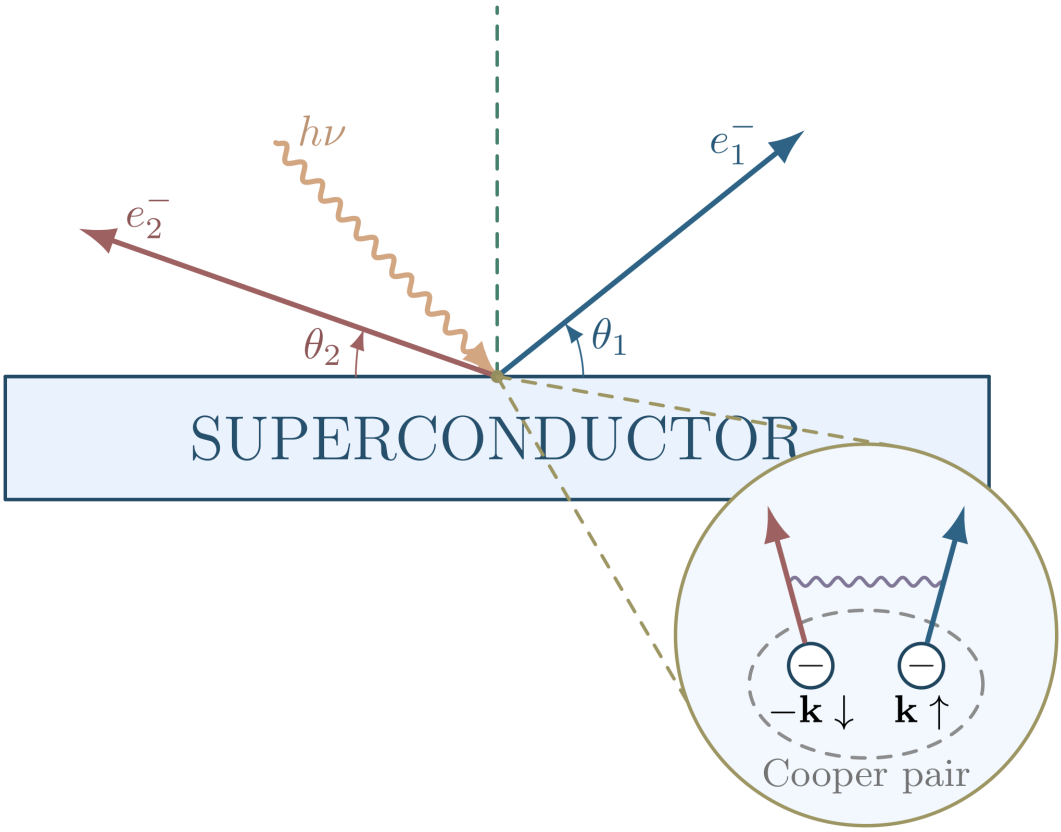

Cooper Pair Spectroscopy for Odd-Frequency Superconductors

Double Photoelectron Counting Rates from Green's-Function Theory

Master's thesis in Physics

JOHAN HERMANSSON

DEPARTMENT OF PHYSICS AND ASTRONOMY
CHALMERS UNIVERSITY OF TECHNOLOGY
Gothenburg, Sweden 2026
www.chalmers.se

Master's thesis 2026

Cooper Pair Spectroscopy for Odd-Frequency Superconductors

Double Photoelectron Counting Rates from Green's-Function Theory

JOHAN HERMANSSON

CHALMERS
UNIVERSITY OF TECHNOLOGY

Department of Physics and Astronomy
Division of Condensed Matter and Materials theory
Geilhufe Group
Chalmers University of Technology
Gothenburg, Sweden 2026

Cooper Pair Spectroscopy for Odd-Frequency Superconductors
Double Photoelectron Counting Rates from Green's-Function Theory
JOHAN HERMANSSON

Supervisor: Yulong Qiao, Department of Physics and Astronomy
Examiner: R. Matthias Geilhufe, Department of Physics and Astronomy

Master's Thesis 2026
Department of Physics and Astronomy
Division of Condensed Matter and Materials Theory
Geilhufe Group
Chalmers University of Technology
SE-412 96 Gothenburg
Sweden
Telephone +46 31 772 1000

Cover: Schematic representation of double photoelectron emission from a superconductor. It shows the anomalous contribution, in which two detected photoelectrons originate from the same Cooper pair.

Typeset in LaTeX
Gothenburg, Sweden 2026

Cooper Pair Spectroscopy for Odd-Frequency Superconductors
Double Photoelectron Counting Rates from Green's-Function Theory
JOHAN HERMANSSON
Department of Physics and Astronomy
Chalmers University of Technology

Abstract

In conventional spin-singlet superconductors with even parity, the anomalous pairing amplitude is even in frequency. Odd-frequency superconductivity is an unconventional superconducting state in which the pair amplitude is odd under exchange of time coordinates. Since superconducting pairing is encoded in two-particle correlations, double photoelectron spectroscopy provides a natural framework for probing such states through the simultaneous detection of two photoemitted electrons. When applied to superconducting samples, this approach is commonly referred to as Cooper pair spectroscopy. In this thesis, a Green's-function formulation of Cooper pair spectroscopy for odd-frequency superconductors is developed by extending the theoretical structure of angle-resolved photoemission spectroscopy to the double-photoemission case.

Starting from an expansion of the S-matrix, the double-photoelectron counting rate is derived to second order, which is the lowest order giving a non-vanishing contribution. The result separates into an anomalous contribution, expressed through greater anomalous Green's functions, and a normal contribution, expressed through lesser normal Green's functions. The anomalous part describes correlated emission associated with a single Cooper pair, while the normal part describes contributions from ordinary single-particle correlations.

The main result is that odd-frequency pairing leads to a different momentum structure in the anomalous contribution than conventional even-frequency pairing. In particular, the odd-frequency kernel contains a difference of screened Coulomb potentials, whereas the even-frequency case contains their sum. Consequently, for a symmetric screened Coulomb potential, the momentum dependence of the electron–photon coupling becomes essential for obtaining a finite odd-frequency anomalous contribution. The derived expression therefore identifies a key formal distinction between even- and odd-frequency superconductors in double photoelectron spectroscopy and provides a basis for future numerical and experimental investigations.

Keywords: Superconductivity, Odd-frequency pairing, Cooper pairs, Double photoelectron spectroscopy, Green's functions, Anomalous Green's functions, Counting rate.

Acknowledgements

I would like to sincerely thank my supervisor, Yulong Qiao, for his guidance throughout the project, for our many valuable discussions, and for always being available to answer my questions. I would also like to thank my examiner, R. Matthias Geilhufe, for proposing this interesting project and for providing valuable input throughout the work. I am also grateful to the other members of the Geilhufe group for creating a welcoming environment and for the feedback they have given me. Finally, I would like to thank my friends and family for their support.

Johan Hermansson, Gothenburg, June 2026

List of Acronyms

Below is the list of acronyms that have been used throughout this thesis listed in alphabetical order:

ARPES	Angle-resolved photoemission spectroscopy
BCS	Bardeen–Cooper–Schrieffer
DPE	Double photoelectron
PES	Photoemisson spectroscopy

Nomenclature

Below is a list of notation Green's functions, operators, variables, and superconducting symmetry labels used throughout this thesis.

Green's functions

$\mathcal{G}$	Matsubara normal Green's function
$\mathcal{F}$	Matsubara anomalous Green's function
G	Real-time time-ordered normal Green's function
F	Real-time time-ordered anomalous Green's function
$X^<$, $X^>$, X^R, X^A	Lesser, greater, retarded and advanced components of the Green's function X, where $X = G, F$

Operators

H	Full Hamiltonian
H_0	Free Hamiltonian
H_I	Interaction Hamiltonian
$c_{\mathbf{p}\sigma}$, $c^\dagger_{\mathbf{p}\sigma}$	Electron annihilation and creation operators
$d_{\mathbf{p}\sigma}$, $d^\dagger_{\mathbf{p}\sigma}$	Photoelectron annihilation and creation operators
$\mathcal{T}$	Time-ordering operator
$\mathcal{T}_\tau$	Imaginary-time-ordering operator

Variables

t	Real time
τ	Imaginary time
ω	Frequency

β	Inverse temperature, $\beta = 1/(k_B T)$

Superconducting symmetry labels

S	Spin-exchange symmetry
P^*	Parity/momentum-exchange symmetry
O	Orbital-exchange symmetry
T^*	Time/frequency-exchange symmetry

Contents

List of Figures

List of Tables

1

Introduction

Superconductivity is a macroscopic quantum phenomenon in which a material enters a phase characterized by dissipationless electrical transport and the expulsion of magnetic fields [1]. The first successful microscopic theory of superconductivity was developed by Bardeen, Cooper and Schrieffer, known as BCS theory [2]. In this theory, an effective attractive interaction between electrons close to the Fermi surface leads to the formation of Cooper pairs, whose condensate gives rise to the superconducting state [2], [3]. The properties of a superconductor are therefore closely related to the structure and symmetry of its Cooper pairs, such as their spin and orbital configurations, as well as the parity.

The symmetry of the superconducting state is encoded in the anomalous correlation function, which describes the propagation of two particles as a correlated pair. Due to the fermionic nature of electrons, this correlation function must be antisymmetric under the combined exchange of all quantum numbers [4]. In addition to spin, spatial and orbital indices, this classification also includes the exchange of time coordinates, or equivalently frequency. In standard BCS description, the superconducting pair amplitude is even under time exchange. However, superconducting states that are odd under time exchange are also allowed by the general symmetry constraint [4], [5]. Such odd-frequency superconducting states represent an unconventional form of superconductivity in which the pair amplitude changes sign under exchange of the two time coordinates, or equivalently under reversal of the relative time coordinate.

Experimentally identifying the symmetry of superconducting correlations is a central problem in the study of unconventional superconductors. Photoemission spectroscopy (PES) provides one of the most direct probes of the electronic structure of materials. In photoemission, an incoming photon transfers energy to an electron in the material, allowing it to escape into the vacuum. By measuring the kinetic energy of the emitted electrons, PES gives access to the binding energies and spectral weight of occupied electronic states [6]. In its angle-resolved form, ARPES additionally measures the emission angle, allowing the electronic structure to be resolved as a function of momentum [7]. ARPES has therefore become an important tool for studying superconductors, since the superconducting gap and its momentum dependence are reflected in the single-particle excitation spectrum [8].

However, ordinary photoemission is fundamentally a single-particle probe. While it provides access to spectral properties of individual electronic excitations, it does not directly resolve the two-particle correlations that define the internal structure of the Cooper pair [9], [10]. This limitation is particularly relevant for unconventional superconducting states, where essential information may be contained not only in

the magnitude of the superconducting gap, but also in the spin, momentum, orbital or time dependence of the anomalous pair amplitude [4], [11]. To access such correlations, one requires a technique capable of probing two emitted electrons together [9], [10].

Cooper pair spectroscopy, realized through double-photoelectron (DPE) spectroscopy, provides such a possibility [9]. In double photoemission, two electrons are emitted following the absorption of a photon, allowing the simultaneous detection of two photoelectrons [12]. Since the detected signal is sensitive to two-particle correlations, DPE offers a natural framework for investigating internal correlations of Cooper pairs. Previous theoretical studies of Cooper pair spectroscopy have primarily focused on even-frequency superconducting states [9], [10], [13], [14]. Extending the theoretical description of DPE to odd-frequency superconductivity is therefore of interest, both conceptually and in view of recent efforts to experimentally realize Cooper pair spectroscopy [15]. This thesis contributes to that extension by formulating the DPE counting rate in terms of Green's functions for an odd-frequency superconducting state.

1.1 Aim

This thesis aims to extend the theoretical description of Cooper pair spectroscopy to odd-frequency superconductors. In particular, the thesis addresses how the double-photoelectron counting rate differs between even-frequency superconductors and odd-frequency superconductors. The central research question is:

> How does the DPE counting rate differ between even- and odd-frequency superconducting pairing?

To answer this question, the DPE counting rate is derived using a Green's-function formulation based on an expansion of the S-matrix. The resulting expression is then analyzed for both even- and odd-frequency anomalous Green's functions, with emphasis on how the symmetry of the pairing state affects the formal structure of the counting rate.

1.2 Limitations

In this work, the odd-frequency superconducting state is assumed to be already established, and the microscopic mechanism responsible for realizing such pairing is not addressed. The analysis is restricted to a single-band pairing channel with spin-triplet, even-parity, odd-frequency symmetry. This restriction applies to the anomalous Green's function that enters the transition amplitude, and should not be understood as a restriction on the symmetry of the full superconducting order parameter. Consequently, the derived counting rate applies to this particular odd-frequency pairing channel, while other possible pairing symmetries are left for future work.

2

Theoretical Background

In this chapter, the theoretical background needed to describe DPE spectroscopy is introduced. Throughout this chapter, and in the remainder of this thesis, natural units with $\hbar = 1$ are used. The chapter begins with time-dependent perturbation theory, including the interaction picture, S-matrix expansion and Fermi's golden rule, which provide the framework for treating photoemission as a transition process and relating transition amplitudes to counting rates. Wick's theorem is then introduced to simplify expectation values containing several creation and annihilation operators, while Green's functions are used to describe the propagation of electrons, holes and anomalous superconducting correlations. The spectral function is discussed as the connection between Green's functions and photoemission spectra. Finally, ARPES is reviewed as a simpler single-particle photoemission process, serving as a reference point for the later treatment of DPE spectroscopy.

2.1 Perturbation Theory

Many quantum-mechanical systems of interest cannot be solved exactly. This is especially true in many-body physics, where interactions between particles or couplings to external probes often make the full Hamiltonian too complicated to diagonalize directly. Perturbation theory provides a systematic way of treating such problems when the Hamiltonian can be separated into a solvable part and a weak perturbation [16, ch. 5],

$$H = H_0 + V. \tag{2.1}$$

The eigenstates and eigenvalues of H_0 are assumed to be known, while the effect of V is included order by order.

The usefulness of this approach is that the dominant dynamics generated by H_0 can be treated exactly, while V is used to compute corrections and transition amplitudes [16, ch. 5]. In many-body theory, this perturbative viewpoint also underlies the S-matrix, Wick's theorem, and Green's function techniques [17, ch. 2]. These tools are essential for connecting microscopic Hamiltonians to experimentally measurable quantities, such as the spectral function relevant to photoemission experiments [7], [12].

2.1.1 Interaction Picture

There are three standard ways of formulating time evolution in quantum mechanics, referred to as pictures. These are the Schrödinger picture, the Heisenberg picture,

and the interaction picture, and quantities in these pictures will be distinguished by the labels S, H and I. In the Schrödinger picture, the state kets evolve with time, whereas the operators are time independent. In the Heisenberg picture, by contrast, the operators carry the time dependence while the state kets remain stationary [16, p. 75]. The interaction picture combines features of both: the time evolution generated by a chosen unperturbed Hamiltonian H_0 is assigned to the operators, while the remaining time evolution, generated by the interaction part of the Hamiltonian, is assigned to the state kets [16, p. 321], [18, pp. 83–84].

The time evolution of a Schrödinger-picture state ket is generated by the time-evolution operator $U(t, t_0)$, defined by

$$|\psi(t)\rangle_S = U(t, t_0)|\psi(t_0)\rangle_S. \tag{2.2}$$

To conserve probability, the time-evolution operator must be unitary [16, p. 63]. It therefore satisfies

$$U^\dagger(t, t_0)U(t, t_0) = U(t, t_0)U^\dagger(t, t_0) = 1. \tag{2.3}$$

Furthermore, the time evolution from t_3 to t_1 can be decomposed into successive evolutions via an intermediate time t_2, so that

$$U(t_1, t_2)U(t_2, t_3) = U(t_1, t_3). \tag{2.4}$$

In the Schrödinger picture, the time dependence carried by the state ket is governed by the Schrödinger equation

$$i\frac{\partial}{\partial t}|\psi(t)\rangle_S = H|\psi(t)\rangle_S. \tag{2.5}$$

Substituting the definition of the time-evolution operator gives

$$i\frac{\partial}{\partial t}U(t, t_0)|\psi(t_0)\rangle_S = HU(t, t_0)|\psi(t_0)\rangle_S. \tag{2.6}$$

Since the initial state $|\psi(t_0)\rangle_S$ is arbitrary, the time-evolution operator itself satisfies

$$i\frac{\partial}{\partial t}U(t, t_0) = HU(t, t_0). \tag{2.7}$$

For a time-independent Hamiltonian, this equation has the solution

$$U(t, t_0) = e^{-iH(t-t_0)}. \tag{2.8}$$

With $U(t, t_0)$ we can perform a unitary transformation to move a state ket from the Schrödinger picture to the Heisenberg picture, in which we define

$$|\psi(t_0)\rangle_H = U^\dagger(t, t_0)|\psi(t)\rangle_S = |\psi(t_0)\rangle_S. \tag{2.9}$$

We also define the Heisenberg operator from the unitary transformation

$$A^{(H)}(t) = U^\dagger(t, t_0)A^{(S)}(t_0)U(t, t_0) \tag{2.10}$$

where the picture label has been moved to the top for operators in order to avoid confusion with other labels. At $t = t_0$, states and operators are the same in the

Schrödinger and Heisenberg picture. Henceforth, we set $t_0 = 0$ for notational simplicity and write $U(t) = U(t, 0)$. With the simple expression for the time-evolution operator in Eq. (2.8), the Hamiltonian takes the same form in the Schrödinger and Heisenberg picture. Indeed, since the exponential in (2.8) is generated by the Hamiltonian itself, its Taylor expansion contains only powers of H. It therefore commutes with H, so that

$$H^{(H)} = U^\dagger(t) H^{(S)} U(t) = H^{(S)} U^\dagger(t) U(t) = H^{(S)}. \tag{2.11}$$

Thus, there is no need to distinguish between the Hamiltonian in the two pictures, and we will simply write H without an explicit picture label. Because the time-evolution operator is unitary, it also follows that expectation values are independent of the picture

$${}_S\langle\psi(t)|A^{(S)}|\psi(t)\rangle_S = \langle\psi(0)|U^\dagger(t)A^{(S)}U(t)|\psi(0)\rangle = {}_H\langle\psi|A^{(H)}(t)|\psi\rangle_H. \tag{2.12}$$

Differentiating Eq. (2.10) with respect to time gives Heisenberg's equation of motion. For a Schrödinger-picture operator with no explicit time dependence, this gives

$$i\frac{\mathrm{d}}{\mathrm{d}t}A^{(H)}(t) = \left[A^{(H)}(t), H\right]. \tag{2.13}$$

More generally, the Schrödinger-picture operator may itself depend explicitly on time. In that case, the equation of motion becomes

$$i\frac{\mathrm{d}}{\mathrm{d}t}A^{(H)}(t) = \left[A^{(H)}(t), H\right] + i\left(\frac{\partial A^{(S)}}{\partial t}\right)_H. \tag{2.14}$$

This explicit time dependence should not be confused with the time dependence generated by the Hamiltonian. Rather, it represents a time dependence already present in the Schrödinger-picture operator, analogous to the explicit time dependence of a classical quantity [19, p. 21].

In the interaction picture, where both state kets and operators are time dependent, the Hamiltonian is separated into two parts;

$$H = H_0 + V \tag{2.15}$$

where H_0 is the unperturbed part and V contains the interactions. H_0, which is often referred to as the free Hamiltonian, is usually selected such that it is exactly solvable [17, p. 67]. The time-evolution operator for the interaction picture is related to that of the Schrödinger picture by the transformation

$$U_0(t) = e^{-iH_0 t}. \tag{2.16}$$

Then, the state kets in the interaction picture evolves as

$$|\psi(t)\rangle_I = U_0^\dagger(t)|\psi(t)\rangle_S = U_0^\dagger(t)U(t)|\psi(0)\rangle_S, \tag{2.17}$$

and the operators evolves as

$$A^{(I)}(t) = U_0^\dagger(t) A^{(S)} U_0(t). \tag{2.18}$$

Therefore, the relation between the interaction picture and the Schrödinger picture is similar to that of the Heisenberg picture and the Schrödinger picture, except that the unitary operator U_0 only involves the free part of the Hamiltonian, rather than the full Hamiltonian. From Eq. (2.18) we see that

$$H_0^{(I)} = H_0^{(S)} \equiv H_0, \tag{2.19}$$

however, the interaction part V is not necessarily the same in the different pictures. If we insert Eq. (2.17) into the Schrödinger equation (2.5) we find

$$\begin{aligned} i\frac{\partial}{\partial t}|\psi(t)\rangle_I &= i\frac{\partial}{\partial t}\Big(U_0^\dagger(t)|\psi(t)\rangle_S\Big) \\ &= -U_0^\dagger(t)H_0|\psi(t)\rangle_S + U_0^\dagger(t)(H_0+V)|\psi(t)\rangle_S \\ &= U_0^\dagger(t)V\Big[U_0(t)U_0^\dagger(t)\Big]|\psi(t)\rangle_S \end{aligned}$$

and with Eqs. (2.17) and (2.18) we see that

$$i\frac{\partial}{\partial t}|\psi(t)\rangle_I = V^{(I)}(t)|\psi(t)\rangle_I, \tag{2.20}$$

which is the equation of motion for the state kets in the interaction picture. Unlike in the Schrödinger picture, where the state kets evolve under the full Hamiltonian, the evolution of the interaction-picture state kets is governed by the interaction Hamiltonian $V^{(I)}(t)$. This form is particularly useful for perturbation theory, since the unperturbed evolution generated by H_0 is treated exactly, while the remaining evolution can be expanded systematically in powers of $V^{(I)}(t)$ [17, pp. 67–69]. The corresponding differential form of the operator evolution follows directly from Eq. (2.18). For an operator with no explicit time dependence in the Schrödinger picture, differentiating (2.18) gives

$$i\frac{\mathrm{d}}{\mathrm{d}t}A^{(I)}(t) = \Big[A^{(I)}(t), H_0\Big]. \tag{2.21}$$

Having related the interaction picture to the Schrödinger picture, it is also useful to record its direct relation to the Heisenberg picture. Combining Eqs. (2.17) and (2.18) with the corresponding Heisenberg-picture definitions gives

$$|\psi(t)\rangle_I = U_I(t)|\psi(t)\rangle_H \tag{2.22}$$

for the state kets, and

$$A^{(I)}(t) = U_I(t)A^{(H)}(t)U_I^\dagger(t) \tag{2.23}$$

for operators. The unitary operator connecting the two pictures is

$$U_I(t) = e^{iH_0t}e^{-iHt}. \tag{2.24}$$

In what follows, explicit picture labels will be omitted unless required for clarity, and the relevant picture will be understood from the context.

2.1.2 S-matrix Expansion

In many-particle perturbation theory, the interaction-picture time evolution is often collected into a single operator known as the S-matrix. For finite times, this operator evolves the interaction-picture state from one time to another [17, pp. 70–71], while in the limit where the initial and final times are taken to the remote past and future, its matrix elements give asymptotic transition amplitudes between chosen initial and final states. The main advantage of introducing the S-matrix is that it admits a systematic expansion in powers of the interaction, which forms the basis for perturbative calculations [19, pp. 90–94].

The interaction-picture evolution operator $U_I(t)$ introduced in the previous section describes how the state changes due to the interaction term. It is therefore convenient to define the finite-time S-matrix as the operator that evolves an interaction-picture state from time t' to time t,

$$|\psi(t)\rangle = S(t,t')|\psi(t')\rangle. \tag{2.25}$$

Using $|\psi(t)\rangle = U_I(t)|\psi(0)\rangle$, this gives

$$S(t,t') = U_I(t)U_I^\dagger(t'). \tag{2.26}$$

Thus, $S(t,t')$ may be viewed as the interaction-picture time-evolution operator between the two times t' and t. It satisfies

1. $S(t,t) = 1$
2. $S^\dagger(t,t') = S(t',t)$
3. $S(t,t')S(t',t'') = S(t,t'')$,

where the second relation expresses the unitarity of the time evolution [17, pp. 70–71]. Taking the derivative of Eq. (2.26) with respect to time gives

$$i\frac{\partial}{\partial t}S(t,t') = V(t)S(t,t'), \tag{2.27}$$

where $V(t)$ is the interaction term in the interaction picture. Equation (2.27) has the formal solution [17, p. 70]

$$S(t,t') = \mathcal{T}\exp\left[-i\int_{t'}^{t}\mathrm{d}t_1\, V(t_1)\right], \tag{2.28}$$

where $\mathcal{T}$ denotes the time-ordering operator. The time-ordering operator arranges the operators with later times to the left. For bosonic operators, this can be written explicitly as

$$\mathcal{T}\Big[V(t)V(t')\Big] = \Theta(t-t')V(t)V(t') + \Theta(t'-t)V(t')V(t), \tag{2.29}$$

where the Heaviside step function is defined as

$$\Theta(t) = \begin{cases} 1, & t > 0, \\ 1/2, & t = 0, \\ 0, & t < 0. \end{cases} \tag{2.30}$$

The choice $\Theta(0) = 1/2$ is a convention that is useful when equal-time limits are encountered. For fermionic operators, the time-ordering operation must also account for the anticommutation of the operators. Consequently, a minus sign appears whenever the reordering requires an odd number of fermionic interchanges, as follows from the fermionic anticommutation relations [17, pp. 17–18]. The first terms in the expansion of the time-ordered exponential are

$$S(t,t') = 1 - i\int_{t'}^{t} \mathrm{d}t_1\, V(t_1) + \frac{(-i)^2}{2!}\int_{t'}^{t}\mathrm{d}t_1 \int_{t'}^{t}\mathrm{d}t_2\, \mathcal{T}\Big[V(t_1)V(t_2)\Big] + \cdots . \tag{2.31}$$

The Dyson series can be written in the compact form [19, p. 93]

$$S(t,t') = \sum_{n=0}^{\infty} \frac{(-i)^n}{n!}\int_{t'}^{t}\mathrm{d}t_1 \cdots \int_{t'}^{t}\mathrm{d}t_n\, \mathcal{T}\Big[V(t_1)\cdots V(t_n)\Big] = \sum_{n=0}^{\infty} S^{(n)}(t,t'), \tag{2.32}$$

with

$$S^{(n)}(t,t') = \frac{(-i)^n}{n!}\int_{t'}^{t}\mathrm{d}t_1 \cdots \int_{t'}^{t}\mathrm{d}t_n\, \mathcal{T}\Big[V(t_1)\cdots V(t_n)\Big], \tag{2.33}$$

where the notation $S^{(n)}$ denotes the contribution of order n in the interaction.

By taking the initial and final times to the remote past and future, the finite-time operator $S(t,t')$ gives the asymptotic transition amplitude between chosen initial and final states. If the initial state in the remote past is denoted by $|i\rangle$, then

$$|\psi(\infty)\rangle = S(\infty,-\infty)|i\rangle. \tag{2.34}$$

The amplitude for finding the system in the final state $|f\rangle$ is therefore

$$S_{fi} \equiv \langle f|S(\infty,-\infty)|i\rangle, \tag{2.35}$$

and the corresponding transition probability is proportional to

$$|S_{fi}|^2 = |\langle f|S(\infty,-\infty)|i\rangle|^2. \tag{2.36}$$

Thus, the same operator that describes finite-time interaction-picture evolution also provides the transition amplitudes between asymptotic many-body states.

2.1.3 Fermi's Golden Rule

Fermi's golden rule is a central result of time-dependent perturbation theory. It gives the transition rate induced by a weak perturbation between eigenstates of an unperturbed Hamiltonian [20]. Although commonly associated with Fermi, the result is usually traced back to Dirac's 1927 treatment of radiative transitions, while Fermi later helped establish the terminology of the "golden rule" [20]–[22]. We begin from the standard perturbative setup for deriving Fermi's golden rule [20], taking the perturbation to be constant after it is switched on. This gives the usual transition rate in terms of the matrix element $\langle f|V|i\rangle$ and the energy-conserving condition $E_f = E_i$. This form will later be used in the discussion of ARPES.

We consider a system described by

$$H(t) = H_0 + V(t) \tag{2.37}$$

where $V(t)$ is weak compared with H_0. If the system is initially prepared in an eigenstate $|i\rangle$ of H_0, the perturbation may induce transitions to other eigenstates $|f\rangle$. The corresponding transition probability is denoted $P_{fi}(t)$. The transition rate is defined as the rate of change of this probability,

$$w_{fi}(t) = \frac{\mathrm{d}P_{fi}(t)}{\mathrm{d}t}. \tag{2.38}$$

In the golden-rule limit considered below, $P_{fi}(t)$ becomes proportional to t, so that $w_{fi}(t)$ becomes time independent and will simply be denoted w_{fi}.

Although picture labels are generally suppressed, we keep them in the following step for clarity. Let $|i\rangle_0$ and $|f\rangle_0$ denote eigenstates of the unperturbed Hamiltonian H_0, with eigenvalues E_i and E_f, respectively,

$$H_0|i\rangle_0 = E_i|i\rangle_0, \qquad H_0|f\rangle_0 = E_f|f\rangle_0.$$

For a constant perturbation that is switched on at time $-t/2$, we take the Schrödinger-picture interaction Hamiltonian to be [16, p. 341]

$$V^{(S)}(t) = \begin{cases} 0, & t < -t/2, \\ V^{(S)}, & t \geq -t/2. \end{cases} \tag{2.39}$$

The corresponding interaction-picture perturbation is obtained through Eq. (2.18), hence

$$\begin{aligned} {}_0\langle f|V^{(I)}(t)|i\rangle_0 &= {}_0\langle f|e^{iH_0t}V^{(S)}e^{-iH_0t}|i\rangle_0 \\ &= {}_0\langle f|V^{(S)}|i\rangle_0 e^{i(E_f-E_i)t}. \end{aligned} \tag{2.40}$$

From this point onward, the subscript 0 and explicit picture labels are again omitted unless needed for clarity. We call $\Delta\omega = E_f - E_i$ so that we can write[1]

$$\langle f|V|i\rangle e^{i\Delta\omega t}. \tag{2.41}$$

Then from Eq. (2.33) we get the first order expansion term

$$S^{(1)}(t/2, -t/2) = -i\int_{-t/2}^{t/2} \mathrm{d}t'\, V(t') \tag{2.42}$$

such that the first-order finite-time transition amplitude is

$$S_{fi}^{(1)}(t) = -i\int_{-t/2}^{t/2} \mathrm{d}t'\, \langle f|V(t')|i\rangle \tag{2.43}$$

and using Eq. (2.41), this simplifies to

$$S_{fi}^{(1)}(t) = -i\langle f|V|i\rangle \int_{-t/2}^{t/2} \mathrm{d}t'\, e^{i\Delta\omega t'}. \tag{2.44}$$

[1] Remember that $E = \omega$ in units of $\hbar = 1$.

The time integral gives

$$S_{fi}^{(1)}(t) = -i\langle f|V|i\rangle \frac{2\sin(\Delta\omega t/2)}{\Delta\omega}. \tag{2.45}$$

To the first order approximation, the probability of the state making a transition from $|i\rangle$ to $|f\rangle$ at time t is

$$P_{fi}(t) = |S_{fi}^{(1)}(t)|^2. \tag{2.46}$$

More explicitly, the transition probability can be written as

$$\begin{aligned} P_{fi}(t) &= 4|\langle f|V|i\rangle|^2 \frac{\sin^2(\Delta\omega t/2)}{(\Delta\omega)^2} \\ &= 2t|\langle f|V|i\rangle|^2 \frac{\sin^2(\Delta\omega t/2)}{(\Delta\omega)^2 t/2}. \end{aligned} \tag{2.47}$$

The second line has been arranged so that the last factor has the form of a sinc-squared kernel. Defining

$$K_\alpha(x) = \frac{\sin^2(x\alpha)}{x^2\alpha}, \tag{2.48}$$

we identify $x = \Delta\omega$ and $\alpha = t/2$. This kernel acts as a finite-time approximation to the Dirac delta function. As illustrated in Fig. 2.1, $K_\alpha(x)$ becomes increasingly concentrated around $x = 0$ as α grows: its height increases while its width decreases, with the area under the curve remaining fixed. In the sense of distributions, one has [16, p. 343]

$$\lim_{\alpha\to\infty} K_\alpha(x) = \lim_{\alpha\to\infty} \frac{\sin^2(x\alpha)}{x^2\alpha} = \pi\delta(x). \tag{2.49}$$

Using $x = \Delta\omega$ and $\alpha = t/2$, Eq. (2.49) gives

$$\lim_{t\to\infty} \frac{\sin^2(\Delta\omega t/2)}{(\Delta\omega)^2 t/2} = \pi\delta(\Delta\omega). \tag{2.50}$$

Thus, in the long-time limit, the transition probability becomes linear in time,

$$P_{fi}(t) \simeq 2\pi t|\langle f|V|i\rangle|^2\delta(\Delta\omega). \tag{2.51}$$

Using Eq. (2.38), the transition rate is therefore

$$w_{fi} = 2\pi|\langle f|V|i\rangle|^2\delta(\Delta\omega). \tag{2.52}$$

Since $\Delta\omega = E_f - E_i$, this may equivalently be written as

$$w_{fi} = 2\pi|\langle f|V|i\rangle|^2\delta(E_f - E_i). \tag{2.53}$$

This is Fermi's golden rule for transitions induced by a constant perturbation. In the long-time limit, the finite-time sinc-squared peak becomes a delta function, so the transition probability is appreciable only when the final and initial states have the same energy, $E_f = E_i$ [16, pp. 341–346]. The factor $|\langle f|V|i\rangle|^2$ determines the strength with which the perturbation couples the initial and final states. The result should nevertheless be understood as an approximation: it assumes a weak perturbation and a regime in which the final states form an effective continuous set, while the transition probability remains small [20].

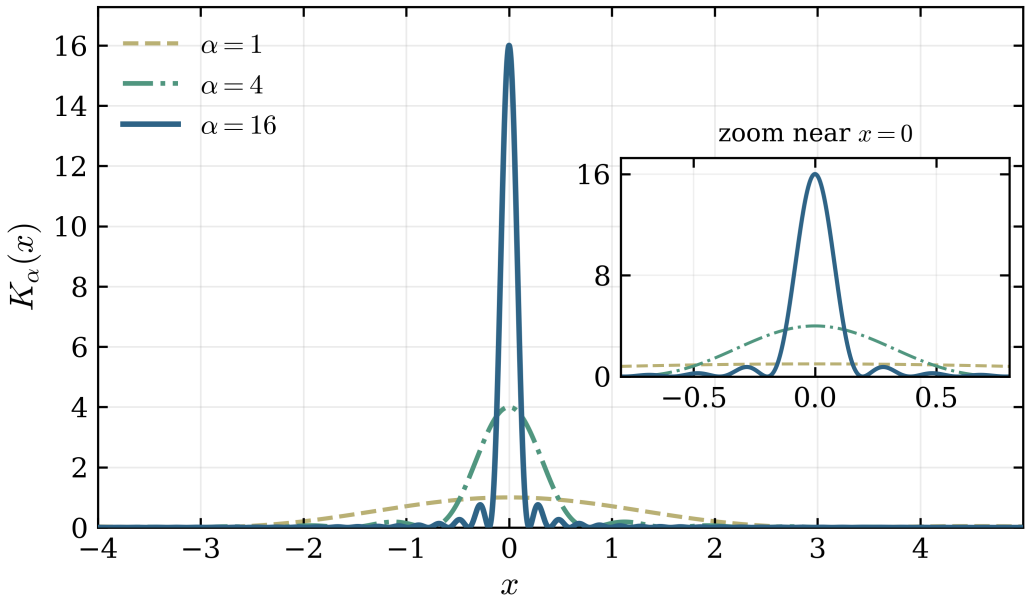

Figure 2.1: The sinc-squared kernel $K_\alpha(x) = \sin^2(x\alpha)/(x^2\alpha)$ for increasing values of α, with $K_\alpha(0)$ defined by the limit $K_\alpha(0) = \alpha$. As α increases, the kernel becomes increasingly concentrated around $x = 0$: its height grows while its width shrinks, with the total area remaining fixed. This illustrates the distributional convergence $K_\alpha(x) \to \pi\delta(x)$.

2.2 Wick's Theorem

In many-body calculations one often encounters expectation values containing more than two creation and annihilation operators. Direct evaluation of such objects becomes cumbersome as the number of operators increases. Wick's theorem provides a systematic way of rewriting such higher-order expectation values in terms of products of two-operator expectation values [23]. For a Gaussian reference state, the expectation value of a product of an even number of operators is given by the sum over all possible complete pairings of the operators. For fermionic operators, each term obtains a sign determined by the number of interchanges required to bring the paired operators together [17, pp. 76–81]. For example, given the fermionic operators A_i, the four-operator expectation value can be decomposed as

$$\langle|A_1A_2A_3A_4|\rangle = \langle|A_1A_2|\rangle\langle|A_3A_4|\rangle - \langle|A_1A_3|\rangle\langle|A_2A_4|\rangle + \langle|A_1A_4|\rangle\langle|A_2A_3|\rangle. \quad (2.54)$$

Here, $|\rangle$ denotes the zero-temperature reference state, and $\langle|$ denotes the corresponding bra. If the product is time ordered, the same pairing structure applies, but the two-operator expectation values are replaced by time-ordered ones. As discussed in Sec. 2.1.2, the time-ordering operator also includes the fermionic signs associated with reordering the operators in time. For two fermionic operators $A_i(t_i)$ and $A_j(t_j)$,

$$\mathcal{T}\Big[A_i(t_i)A_j(t_j)\Big] = \Theta(t_i - t_j)A_i(t_i)A_j(t_j) - \Theta(t_j - t_i)A_j(t_j)A_i(t_i). \quad (2.55)$$

Thus,

$$\begin{aligned}\langle|\mathcal{T}A_1A_2A_3A_4|\rangle = &\langle|\mathcal{T}A_1A_2|\rangle\langle|\mathcal{T}A_3A_4|\rangle \\ &- \langle|\mathcal{T}A_1A_3|\rangle\langle|\mathcal{T}A_2A_4|\rangle \\ &+ \langle|\mathcal{T}A_1A_4|\rangle\langle|\mathcal{T}A_2A_3|\rangle.\end{aligned} \tag{2.56}$$

The time-ordered and non-time-ordered decompositions therefore have the same pairing structure, while the two-operator factors differ because the time-ordered expectation values already contain the signs generated by fermionic time ordering.

Wick's theorem is exact when the expectation value is taken with respect to a Gaussian state, for example the ground state of a quadratic Hamiltonian [24]. If the state is not Gaussian, the same decomposition may still be used as a mean-field decoupling, but it is then an approximation in which higher-order connected correlations are neglected [25].

At finite temperature, the ground-state expectation value is replaced by a thermal average, also referred to as a thermodynamic average. In the grand-canonical ensemble, this average is defined as

$$\langle\langle A\rangle\rangle = \frac{1}{\mathcal{Z}}\,\mathrm{Tr}\Big(e^{-\beta K}A\Big) \tag{2.57}$$

with

$$\mathcal{Z} = \mathrm{Tr}\Big(e^{-\beta K}\Big), \qquad K = H - \mu N, \qquad \beta = \frac{1}{k_B T}, \tag{2.58}$$

where $\mathcal{Z}$ is the grand-canonical partition function, μ is the chemical potential and N is the particle-number operator. The symbol "Tr" denotes the trace, which is a sum over a complete set of many-body states,

$$\mathrm{Tr}(A) \equiv \sum_n \langle n|A|n\rangle. \tag{2.59}$$

Wick's theorem retains the same pairing structure at finite temperature, but the corresponding condition is that the thermal density matrix is Gaussian. This is the case when the operator appearing in the density matrix is quadratic in the creation and annihilation operators [26], [27]. If interactions are present in K, the thermal density matrix is generally not Gaussian, and the same qualifications as above apply: the Wick decomposition is no longer exact, but may be used as a mean-field decoupling.

2.3 Green's Functions

Green's functions provide a powerful framework for describing the dynamical and spectral properties of quantum many-body systems [28], [29]. The one-particle Green's function is particularly useful because it encodes the propagation of particle-like excitations and is directly related to the spectral function.

2.3.1 Zero-Temperature Formalism

For a many-body system at zero temperature, the single-particle Green's function for fermions is defined as [28], [30]

$$G(1,2) = -i\langle|\mathcal{T}\psi(1)\psi^\dagger(2)|\rangle, \tag{2.60}$$

where $|\rangle$ denotes the exact many-body ground state and $\mathcal{T}$ is the time-ordering operator. We use the compact notation $1 = (\mathbf{r}_1, \sigma_1, t_1)$, where $\mathbf{r}_1$ denotes the spatial coordinate, σ_1 the spin, and t_1 the time; the label 2 is defined analogously. The operator $\psi^\dagger(1)$ creates a particle at the space-time point 1, while $\psi(1)$ annihilates one. Thus, if the ground state contains N particles, which we may write explicitly as $|N\rangle$, then $\psi^\dagger(1)|N\rangle$ represents an $(N+1)$-particle state, whereas $\psi(1)|N\rangle$ represents an $(N-1)$-particle state.

The Green's function may therefore be interpreted as an amplitude for the propagation of a particle or a hole through the interacting many-body system [28]. When $t_1 > t_2$, the operator $\psi^\dagger(2)$ first adds a particle at position $\mathbf{r}_2$ with spin σ_2 at time t_2, and $\psi(1)$ later removes a particle at position $\mathbf{r}_1$ with spin σ_1 at time t_1. This part of the Green's function describes the propagation of an added particle from 2 to 1. When $t_2 > t_1$, the operator $\psi(1)$ first removes a particle at 1, creating a hole, and $\psi^\dagger(2)$ later adds a particle at 2, thereby filling the hole. This part describes the propagation of a hole from 1 to 2.

The time-ordered Green's function introduced above is only one of several closely related two-point Green's functions. They are all constructed from the same pair of fermionic field operators, but differ in how the two time arguments are ordered [17, pp. 96–97]. Since we will mainly be concerned with electrons, it is convenient to denote the corresponding annihilation and creation operators by $c(1)$ and $c^\dagger(1)$, respectively. We first introduce the greater and lesser Green's functions, from which the time-ordered, anti-time-ordered, retarded, and advanced Green's functions can be constructed [31], [32]. With this notation, the greater and lesser Green's functions are defined as

$$G^>(1,2) = -i\langle|c(1)c^\dagger(2)|\rangle, \tag{2.61}$$

$$G^<(1,2) = i\langle|c^\dagger(2)c(1)|\rangle. \tag{2.62}$$

The greater Green's function describes the propagation of an added particle, while the lesser Green's function describes the propagation of a hole. The time-ordered Green's function can then be written as

$$G^\mathcal{T}(1,2) = \Theta(t_1 - t_2)G^>(1,2) + \Theta(t_2 - t_1)G^<(1,2), \tag{2.63}$$

which is equivalent to the definition given in Eq. (2.60). In addition to the time-ordered Green's function, one may define the anti-time-ordered Green's function,

$$G^{\bar{\mathcal{T}}}(1,2) = \Theta(t_2 - t_1)G^>(1,2) + \Theta(t_1 - t_2)G^<(1,2), \tag{2.64}$$

as well as the retarded and advanced Green's functions,

$$G^R(1,2) = \Theta(t_1 - t_2)\Big[G^>(1,2) - G^<(1,2)\Big], \tag{2.65}$$

$$G^A(1,2) = \Theta(t_2 - t_1)\Big[G^<(1,2) - G^>(1,2)\Big]. \tag{2.66}$$

The retarded Green's function therefore vanishes unless $t_1 > t_2$, whereas the advanced Green's function vanishes unless $t_2 > t_1$. These two functions play a central role in the description of spectral properties [29], which will be discussed in Sec. 2.3.3. Unless otherwise stated, we will refer to the time-ordered Green's function simply as the Green's function.

2.3.2 Finite-Temperature Formalism

The zero-temperature formalism assumes that the system is in its exact many-body ground state. This is a useful idealization, and it is often sufficient when the temperature is small compared with the relevant energy scales of the problem. However, experiments are performed at nonzero temperatures, and thermal occupations and fluctuations can play an important role [17, p. 109]. It is therefore useful to formulate Green's functions in a way that describes thermal equilibrium rather than a single ground state. In the finite-temperature formalism, the ground-state expectation value is replaced by a thermal expectation value over a statistical ensemble, with the zero-temperature formalism recovered in the limit $T \to 0$, or equivalently $\beta \to \infty$. This formulation was introduced by Matsubara and is therefore commonly referred to as the Matsubara formalism [33].

For equilibrium systems, it is often more convenient to work in imaginary time than directly with real-time finite-temperature Green's functions, since the equilibrium density matrix is proportional to $e^{-\beta H}$, which can be viewed as an imaginary-time evolution operator. This connection allows much of the perturbative machinery used at zero temperature to be carried over to finite temperature [17, ch. 3]. In the Matsubara formalism, one introduces the imaginary time $\tau = it$ with the domain $-\beta \leq \tau \leq \beta$. For fermions, the finite-temperature, or Matsubara, Green's function is defined as

$$\mathcal{G}(1,2) = -\langle\langle \mathcal{T}_\tau c(1) c^\dagger(2) \rangle\rangle, \tag{2.67}$$

where now $1 = (\mathbf{r}_1, \sigma_1, \tau_1)$ and $\mathcal{T}_\tau$ orders operators along the imaginary-time axis, including the appropriate minus sign when fermionic operators are interchanged. The imaginary-time dependence of the operators is generated by $K = H - \mu N$,

$$c_\lambda(\tau) = e^{\tau K} c_\lambda e^{-\tau K}, \tag{2.68}$$

where $\lambda = (\mathbf{r}, \sigma)$ denotes the single-particle label. In thermal equilibrium, the Green's function is invariant under translations in imaginary time and therefore depends only on the difference $\tau_1 - \tau_2$ [17, pp. 112–114]. If the system is also spatially translationally invariant, it is diagonal in momentum space [34], so that it may be written in momentum space as $\mathcal{G}(\mathbf{p}, \tau_1 - \tau_2)$.

Because fermionic Matsubara Green's functions are anti-periodic in imaginary time,

$$\mathcal{G}(\tau + \beta) = -\mathcal{G}(\tau), \tag{2.69}$$

they can be expanded in terms of the fermionic Matsubara frequencies

$$\omega_n = \frac{(2n+1)\pi}{\beta}, \qquad n \in \mathbb{Z}. \tag{2.70}$$

The corresponding Fourier transform is

$$\mathcal{G}(i\omega_n) = \int_0^\beta \mathrm{d}\tau \, e^{i\omega_n \tau} \mathcal{G}(\tau), \tag{2.71}$$

with the inverse transform

$$\mathcal{G}(\tau) = \frac{1}{\beta} \sum_n e^{-i\omega_n \tau} \mathcal{G}(i\omega_n). \tag{2.72}$$

Although the Matsubara Green's function is defined in imaginary time, physical response functions are usually formulated in real time. In thermal equilibrium, this connection is made by analytic continuation from the discrete fermionic Matsubara frequencies, in Eq. (2.70), to real frequencies [17, pp. 118–128]. The retarded and advanced Green's functions are obtained as the boundary values

$$G^R(\omega) = \mathcal{G}(i\omega_n \to \omega + i\eta), \tag{2.73}$$
$$G^A(\omega) = \mathcal{G}(i\omega_n \to \omega - i\eta), \tag{2.74}$$

where η is infinitesimal and should be interpreted as the limit $\eta \to 0^+$. Thus, the imaginary-time formalism provides a convenient framework, where real-time quantities such as the retarded and advanced Green's functions are recovered by analytic continuation.

2.3.3 Spectral Function

The spectral function describes how single-particle excitations are distributed in energy and momentum. It therefore provides information about the energies and spectral weights of the particle- and hole-like excitations of an interacting many-body system [35]. In this sense, the spectral function connects the Green's function formalism to experimentally accessible excitation spectra. In particular, ARPES directly probes the occupied part of the momentum-resolved electronic spectral function, as discussed further in Sec. 2.4 [7].

For this reason, the spectral function is most naturally introduced through the retarded Green's function. With the convention used here, it is defined as

$$A(\mathbf{k}, \omega) = -\frac{1}{\pi} \operatorname{Im} G^R(\mathbf{k}, \omega). \tag{2.75}$$

To obtain an explicit expression for $A(\mathbf{k}, \omega)$, we first derive the Lehmann representation of the retarded Green's function.

We consider a system at zero temperature consisting of N identical fermions defined by its Hamiltonian H, and denote the many-body ground state by $|\Psi^N\rangle$. The retarded Green's function in Eq. (2.65) can then be written as

$$\begin{aligned} G^R_{\sigma\sigma'}(\mathbf{k}, t; \mathbf{k}', t') = &-i\Theta(t-t')\langle\Psi^N|c_{\mathbf{k}\sigma}(t)c^\dagger_{\mathbf{k}'\sigma'}(t')|\Psi^N\rangle \\ &- i\Theta(t-t')\langle\Psi^N|c^\dagger_{\mathbf{k}'\sigma'}(t')c_{\mathbf{k}\sigma}(t)|\Psi^N\rangle. \end{aligned} \tag{2.76}$$

To insert intermediate states, one must use the completeness relation in the appropriate particle-number sector. Since $c^\dagger_{\mathbf{k}'\sigma'}$ adds one electron to $|\Psi^N\rangle$, the first term involves eigenstates in the $(N+1)$-particle sector. Similarly, since $c_{\mathbf{k}\sigma}$ removes one electron, the second term involves eigenstates in the $(N-1)$-particle sector. Thus, we use

$$\sum_m |\Psi^{N+1}_m\rangle\langle\Psi^{N+1}_m| = \mathbf{1}_{N+1}, \qquad \sum_m |\Psi^{N-1}_m\rangle\langle\Psi^{N-1}_m| = \mathbf{1}_{N-1}. \tag{2.77}$$

In the following, the sector labels on the identity operators will be suppressed, and we write $\mathbf{1}_{N\pm1}$ simply as 1 when the particle-number sector is clear from the context.

Inserting these resolutions of the identity gives

$$\begin{aligned} G^R_{\sigma\sigma'}(\mathbf{k},t;\mathbf{k}',t') = &-i\Theta(t-t')\sum_m \langle\Psi^N|c_{\mathbf{k}\sigma}(t)|\Psi^{N+1}_m\rangle\langle\Psi^{N+1}_m|c^\dagger_{\mathbf{k}'\sigma'}(t')|\Psi^N\rangle \\ &- i\Theta(t-t')\sum_m \langle\Psi^N|c^\dagger_{\mathbf{k}'\sigma'}(t')|\Psi^{N-1}_m\rangle\langle\Psi^{N-1}_m|c_{\mathbf{k}\sigma}(t)|\Psi^N\rangle. \end{aligned} \tag{2.78}$$

The time dependence of the operators can be handled using Eq. (2.10), so that the two expectation values become

$$e^{i(E^N_0-E^{N+1}_m)t}e^{i(E^{N+1}_m-E^N_0)t'}\langle\Psi^N|c_{\mathbf{k}\sigma}|\Psi^{N+1}_m\rangle\langle\Psi^{N+1}_m|c^\dagger_{\mathbf{k}'\sigma'}|\Psi^N\rangle \tag{2.79}$$

$$e^{i(E^N_0-E^{N-1}_m)t'}e^{i(E^{N-1}_m-E^N_0)t}\langle\Psi^N|c^\dagger_{\mathbf{k}'\sigma'}|\Psi^{N-1}_m\rangle\langle\Psi^{N-1}_m|c_{\mathbf{k}\sigma}|\Psi^N\rangle. \tag{2.80}$$

Since the Hamiltonian is time independent and the ground state is stationary, the Green's function depends only on the time difference

$$s = t - t'. \tag{2.81}$$

Furthermore, we introduce

$$\epsilon^+_m = E^{N+1}_m - E^N_0 \qquad \text{and} \qquad \epsilon^-_m = E^N_0 - E^{N-1}_m \tag{2.82}$$

to facilitate the calculations. Thus, the retarded Green's function takes the form of

$$\begin{aligned} G^R_{\sigma\sigma'}(\mathbf{k},\mathbf{k}',s) = &-i\Theta(s)\sum_m e^{-i\epsilon^+_m s}\langle\Psi^N|c_{\mathbf{k}\sigma}|\Psi^{N+1}_m\rangle\langle\Psi^{N+1}_m|c^\dagger_{\mathbf{k}'\sigma'}|\Psi^N\rangle \\ &- i\Theta(s)\sum_m e^{-i\epsilon^-_m s}\langle\Psi^N|c^\dagger_{\mathbf{k}'\sigma'}|\Psi^{N-1}_m\rangle\langle\Psi^{N-1}_m|c_{\mathbf{k}\sigma}|\Psi^N\rangle. \end{aligned} \tag{2.83}$$

The goal is now to Fourier transform this expression to the frequency domain. To make the oscillatory time integral well defined, we introduce a convergence factor $\exp(-\eta s)$, where $\eta > 0$. As before, this factor should be understood in the limiting sense $\eta \to 0^+$ [17, pp. 121–124]. With this regularization factor, the Fourier transform becomes

$$\begin{aligned} G^R_{\sigma\sigma'}(\mathbf{k},\mathbf{k}',\omega) = -i\sum_m \int_0^\infty \mathrm{d}s \Big(&e^{i(\omega-\epsilon^+_m)s-\eta s}\langle\Psi^N|c_{\mathbf{k}\sigma}|\Psi^{N+1}_m\rangle\langle\Psi^{N+1}_m|c^\dagger_{\mathbf{k}'\sigma'}|\Psi^N\rangle \\ &+ e^{i(\omega-\epsilon^-_m)s-\eta s}\langle\Psi^N|c^\dagger_{\mathbf{k}'\sigma'}|\Psi^{N-1}_m\rangle\langle\Psi^{N-1}_m|c_{\mathbf{k}\sigma}|\Psi^N\rangle\Big), \end{aligned}$$

where we have used that the Heaviside step function restricts s to the domain $0 \le s < \infty$, and where we also interchanged the integration and summation order. The integral can be carried out using the result

$$\int_0^\infty \mathrm{d}s\, e^{ixs-\eta s} = \frac{i}{x+i\eta}. \tag{2.84}$$

With the identification $x = \omega - \epsilon^\pm_m$, the retarded Green's function is given by

$$\begin{aligned} G^R_{\sigma\sigma'}(\mathbf{k},\mathbf{k}',\omega) = \sum_m \Bigg(&\frac{\langle\Psi^N|c_{\mathbf{k}\sigma}|\Psi^{N+1}_m\rangle\langle\Psi^{N+1}_m|c^\dagger_{\mathbf{k}'\sigma'}|\Psi^N\rangle}{\omega - E^{N+1}_m + E^N_0 + i\eta} \\ &+ \frac{\langle\Psi^N|c^\dagger_{\mathbf{k}'\sigma'}|\Psi^{N-1}_m\rangle\langle\Psi^{N-1}_m|c_{\mathbf{k}\sigma}|\Psi^N\rangle}{\omega + E^{N-1}_m - E^N_0 + i\eta}\Bigg) \end{aligned} \tag{2.85}$$

in the frequency domain. This is the zero-temperature Lehmann representation of the retarded Green's function [28], [35]. The first term can be interpreted as the propagation of an added electron, whereas the second term describes the propagation of a hole created by removing an electron from the ground state.

Since the spectral function in Eq. (2.75) is written without explicit spin indices, we now restrict ourselves to the diagonal spin component of the Green's function and suppress the spin label. For a spatially translationally invariant system, the one-particle Green's function is diagonal in momentum space [34]. We therefore focus on the momentum-diagonal component and write

$$G^R(\mathbf{k},\omega) = \sum_m \frac{|\langle \Psi_m^{N+1}|c_{\mathbf{k}\sigma}^\dagger|\Psi^N\rangle|^2}{\omega - E_m^{N+1} + E_0^N + i\eta} + \sum_m \frac{|\langle \Psi_m^{N-1}|c_{\mathbf{k}\sigma}|\Psi^N\rangle|^2}{\omega + E_m^{N-1} - E_0^N + i\eta}, \tag{2.86}$$

where we have omitted the spin label.

We now want to extract the imaginary part of Eq. (2.86). Since the two terms have the same denominator structure, it is useful to consider the generic term of the form

$$\frac{\mathcal{M}}{x + i\eta}, \tag{2.87}$$

where $\mathcal{M}$ denotes a real, non-negative transition weight, given by the absolute square of the relevant matrix element, and x denotes the corresponding real energy difference appearing in the denominator. For the electron-addition part, these quantities are

$$\mathcal{M}_m^+ = |\langle \Psi_m^{N+1}|c_{\mathbf{k}\sigma}^\dagger|\Psi^N\rangle|^2, \qquad x_m^+ = \omega - E_m^{N+1} + E_0^N. \tag{2.88}$$

For the electron-removal part, they are

$$\mathcal{M}_m^- = |\langle \Psi_m^{N-1}|c_{\mathbf{k}\sigma}|\Psi^N\rangle|^2, \qquad x_m^- = \omega + E_m^{N-1} - E_0^N. \tag{2.89}$$

Thus, both calculations can be treated by considering

$$\frac{\mathcal{M}}{x + i\eta} = \mathcal{M}\frac{x - i\eta}{x^2 + \eta^2} = \mathcal{M}\frac{x}{x^2 + \eta^2} - i\mathcal{M}\frac{\eta}{x^2 + \eta^2}. \tag{2.90}$$

The imaginary part of the generic term is

$$\mathrm{Im}\,\frac{\mathcal{M}}{x + i\eta} = -\mathcal{M}\frac{\eta}{x^2 + \eta^2}. \tag{2.91}$$

The factor multiplying $\mathcal{M}$ is proportional to the normalized Lorentzian kernel. In the distributional sense,

$$\lim_{\eta\to 0^+} \frac{1}{\pi}\frac{\eta}{x^2 + \eta^2} = \delta(x). \tag{2.92}$$

Thus,

$$\mathrm{Im}\,\frac{\mathcal{M}}{x + i\eta} = -\pi\mathcal{M}\delta(x). \tag{2.93}$$

Using the definition of the spectral function in Eq. (2.75), we obtain

$$A(\mathbf{k},\omega) = \sum_m \mathcal{M}_m^+\delta(x_m^+) + \sum_m \mathcal{M}_m^-\delta(x_m^-). \tag{2.94}$$

where the two contributions originate from the electron-addition and electron-removal parts of the Green's function, respectively. It is therefore natural to decompose the spectral function as

$$A(\mathbf{k},\omega) = A^+(\mathbf{k},\omega) + A^-(\mathbf{k},\omega) \tag{2.95}$$

where

$$A^+(\mathbf{k},\omega) = \sum_m |\langle \Psi_m^{N+1}|c_{\mathbf{k}\sigma}^\dagger|\Psi^N\rangle|^2 \delta(\omega - E_m^{N+1} + E_0^N), \tag{2.96}$$

$$A^-(\mathbf{k},\omega) = \sum_m |\langle \Psi_m^{N-1}|c_{\mathbf{k}\sigma}|\Psi^N\rangle|^2 \delta(\omega + E_m^{N-1} - E_0^N). \tag{2.97}$$

Here, $A^+(\mathbf{k},\omega)$ is the electron-addition part of the spectral function, while $A^-(\mathbf{k},\omega)$ is the electron-removal part of the spectral function.

Although the Lehmann representation above was derived at zero temperature, this notation is useful because, in thermal equilibrium, the occupied and unoccupied spectral weights are selected by the Fermi–Dirac distribution. The removal part corresponds to the occupied spectral weight and is weighted by $f(\omega)$, reflecting that the state must be occupied before a particle can be removed [7]. The complementary unoccupied part is therefore weighted by $1 - f(\omega)$, so that

$$A^+(\mathbf{k},\omega) = \Big[1 - f(\omega)\Big] A(\mathbf{k},\omega), \qquad A^-(\mathbf{k},\omega) = f(\omega) A(\mathbf{k},\omega). \tag{2.98}$$

The Fermi–Dirac distribution,[2]

$$f(\omega) = \frac{1}{e^{\beta(\omega-\mu)} + 1} \tag{2.99}$$

gives the thermal occupation probability of a fermionic state with energy ω, where μ is the chemical potential and $\beta = 1/k_B T$. In the zero-temperature limit, this becomes a step function, so that states below the chemical potential are occupied and states above it are empty [36, pp. 266–277]. If energies are measured relative to the chemical potential, μ is set to zero, giving $f(\omega) = [\exp(\beta\omega) + 1]^{-1}$.

2.4 Angle-Resolved Photoemission Spectroscopy

Before turning to DPE, we first consider the simpler case of ARPES. In ARPES, a single incoming photon ejects one electron from the sample. This provides a useful reference point for the DPE process, in which the same photon instead leads to the emission of two electrons.

ARPES is based on the photoelectric effect which occurs when a photon is absorbed by an electron in a material, giving it enough energy to escape from the surface, as shown in Fig. 2.2. Through photoemission kinematics, the binding energy and crystal momentum of the electron prior to emission can be deduced [7], [8], [37].

Although an ARPES experiment is preformed using a photon beam, the elementary photoemission process is described as the absorption of a single photon by an

[2] We may sometimes refer to the Fermi–Dirac distribution simply as the Fermi function.

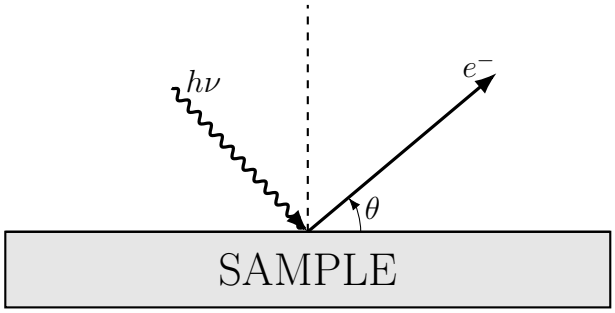

Figure 2.2: Schematic of the ARPES measurement geometry. An incident photon ($h\nu$) ejects a photoelectron (e^-) at an emission angle θ.

electron in the sample [7], [38]. We therefore consider one such photoemission event. The initial state of the sample is taken to be an N-electron state, while after emission the remaining sample is described by an $(N-1)$-electron state together with the emitted electron, which we refer to as the photoelectron. Since we do not consider spin-resolved ARPES here, we suppress spin indices throughout the following derivation.

The kinetic energy of the photoelectron after transmission through the surface barrier is given by the photoemission relation [7]

$$E_{\text{kin}} = \omega_{\mathbf{q}'} - \phi - |E_B|, \tag{2.100}$$

where $\omega_{\mathbf{q}'}$ is the photon energy with momentum $\mathbf{q}$, ϕ is the sample work function, and E_B is the binding energy measured relative to the Fermi level. Here E_{kin} is measured relative the vacuum level. It is therefore convenient to introduce the photoelectron energy measured from the Fermi level,

$$E_e = E_{\text{kin}} + \phi. \tag{2.101}$$

With this convention, the energy conservation condition may be written simply as

$$E_e = \omega_{\mathbf{q}'} - |E_B|. \tag{2.102}$$

We now turn from the kinematics of photoemission to the transition probability. The initial state is taken to consist of one photon and an N-electron state of the sample,

$$|i\rangle = |1_{\mathbf{q}'\lambda'}; \Psi_i^N\rangle, \tag{2.103}$$

where $\mathbf{q}$ and λ' denote the momentum and polarization of the incoming photon, respectively. After photoemission, the final state contains no photon, one emitted photoelectron with momentum $\mathbf{k}$, and an $(N-1)$-electron system. The final state can therefore be factorized as

$$|f\rangle = |\mathbf{k}; \Psi_m^{N-1}\rangle, \tag{2.104}$$

where Ψ_m^{N-1} denotes an eigenstate of the remaining sample with energy E_m^{N-1}. This factorization is justified within the sudden approximation, in which the photoelectron has sufficiently high final-state energy that it leaves the system before it can appreciably interact with the remaining $(N-1)$-electron system [8], [37].

With these definitions, the total initial energy is

$$E_i = E_i^N + \omega_{\mathbf{q}'}, \tag{2.105}$$

where E_i^N is the energy of the initial N-electron state of the sample and $\omega_{\mathbf{q}}$ is the photon energy. Similarly, the total final energy is

$$E_f = E_m^{N-1} + E_e, \tag{2.106}$$

where E_m^{N-1} is the energy of the remaining $(N-1)$-electron sample state and E_e is the photoelectron energy given in Eq. (2.102). Energy conservation therefore gives

$$E_i^N + \omega_{\mathbf{q}'} = E_f = E_m^{N-1} + E_e. \tag{2.107}$$

The photoemission process is induced by the coupling between the electrons and the electromagnetic field. The interaction Hamiltonian therefore describes the electron-photon interaction,

$$H_I = \frac{1}{2m}\Big(\mathbf{p} + \frac{e}{c}\mathbf{A}\Big)^2 - e\phi - \frac{\mathbf{p}^2}{2m} \tag{2.108}$$

and is treated as a perturbation [7], [37]. Here, m is the electron mass, $e > 0$ is the elementary charge and c is the speed of light in vacuum. For weak electromagnetic fields, we neglect terms quadratic in $\mathbf{A}$. Furthermore, working in the Coulomb gauge and neglecting the scalar potential, the leading contribution becomes

$$H_I \simeq \frac{e}{mc}\mathbf{A}\cdot\mathbf{p}. \tag{2.109}$$

Here $\mathbf{p}$ is the electron momentum operator, while ϕ and $\mathbf{A}$ are the electromagnetic scalar and vector potentials.

In second quantization, the vector potential can be expanded in photon modes as

$$\mathbf{A}(\mathbf{r}) = \sum_{\mathbf{q}}\sum_{\lambda}\sqrt{\frac{c^2}{2V\omega_{\mathbf{q}}}}\Big(\boldsymbol{\epsilon}_{\mathbf{q}\lambda}a_{\mathbf{q}\lambda}e^{i\mathbf{q}\cdot\mathbf{r}} + \boldsymbol{\epsilon}^*_{\mathbf{q}\lambda}a^\dagger_{\mathbf{q}\lambda}e^{-i\mathbf{q}\cdot\mathbf{r}}\Big). \tag{2.110}$$

Here $\omega_{\mathbf{q}} = c|\mathbf{q}|$, λ labels the photon polarization, and $a^\dagger_{\mathbf{q}\lambda}$ and $a_{\mathbf{q}\lambda}$ create and annihilate photons in the mode $(\mathbf{q},\lambda)$. Equivalently, after relabeling $\mathbf{q} \to -\mathbf{q}$ in the photon-creation term and choosing the polarization convention $\boldsymbol{\epsilon}^*_{\mathbf{q}} = \boldsymbol{\epsilon}_{-\mathbf{q}}$, the field can be written in the form used in electron–photon vertex formulations of photoemission [39],

$$\mathbf{A}(\mathbf{r}) = \sum_{\mathbf{q}}\sum_{\lambda}\sqrt{\frac{c^2}{2V\omega_{\mathbf{q}}}}\boldsymbol{\epsilon}_{\mathbf{q}\lambda}e^{i\mathbf{q}\cdot\mathbf{r}}\Big(a_{\mathbf{q}\lambda} + a^\dagger_{-\mathbf{q}\lambda}\Big). \tag{2.111}$$

Using the standard second-quantization identity for one-body operators [16, pp. 456–457],

$$\hat{\mathcal{O}} = \sum_{mn} b^\dagger_m b_n \langle \ell_m|\mathcal{O}|\ell_n\rangle, \tag{2.112}$$

the electron–photon interaction can be written as

$$H_I = \sum_{\mathbf{p},\mathbf{q}} \gamma(\mathbf{p},\mathbf{q}) c^\dagger_{\mathbf{p}+\mathbf{q}} c_{\mathbf{p}} \Big(a_{\mathbf{q}\lambda} + a^\dagger_{-\mathbf{q}\lambda} \Big), \tag{2.113}$$

which has the same absorption/emission structure as the electron–photon vertex used in used in Ref. [39]. Here, $\gamma(\mathbf{p},\mathbf{q})$ is the single-particle electron–photon coupling matrix element,

$$\gamma(\mathbf{p},\mathbf{q}) = \langle \phi^{\mathbf{p}}_f | \frac{e}{mc} \sqrt{\frac{c^2}{2V\omega_{\mathbf{q}}}} \boldsymbol{\epsilon}_{\mathbf{q}} e^{i\mathbf{q}\cdot\mathbf{r}} \cdot (-i\nabla) | \phi^{\mathbf{q}}_i \rangle. \tag{2.114}$$

Here, $|\phi^{\mathbf{q}}_i\rangle$ and $|\phi^{\mathbf{p}}_f\rangle$ denote the initial and final single-particle electron wave functions entering the electron–photon matrix element. The initial state describes the electron before photon absorption, while the final state describes the electron after photon absorption.

The transition rate from the initial state $|i\rangle$ to the final state $|f\rangle$ is then approximated by Fermi's golden rule. Using the form derived in Eq. (2.53), and the definitions above, we obtain

$$w_{fi} = 2\pi |\langle \Psi^{N-1}_m; \mathbf{k} | H_I | 1_{\mathbf{q}'\lambda'}; \Psi^N_i \rangle|^2 \delta(E_e + E^{N-1}_m - E^N_i - \omega_{\mathbf{q}'}). \tag{2.115}$$

Because there are no photons in the final state, only the photon-annihilation part of H_I contributes to the photoemission matrix element. Furthermore, if the detected photoelectron has momentum $\mathbf{k}$, we only keep the terms that create an electron in this outgoing state. The relevant matrix element is therefore

$$\begin{aligned} \langle \Psi^{N-1}_m; \mathbf{k} | H_I | 1_{\mathbf{q}'\lambda'}; \Psi^N_i \rangle &= \sum_{\mathbf{p},\mathbf{q}} \sum_{\lambda} \gamma(\mathbf{p},\mathbf{q}) \langle \Psi^{N-1}_m; \mathbf{k} | c^\dagger_{\mathbf{p}+\mathbf{q}} c_{\mathbf{p}} a_{\mathbf{q}\lambda} | 1_{\mathbf{q}'\lambda'}; \Psi^N_i \rangle \\ &= \sum_{\mathbf{p},\mathbf{q}} \sum_{\lambda} \gamma(\mathbf{p},\mathbf{q}) \delta_{\mathbf{p}+\mathbf{q},\mathbf{k}} \langle \Psi^{N-1}_m | c_{\mathbf{p}} | \Psi^N_i \rangle \langle 0_\gamma | a_{\mathbf{q}\lambda} | 1_{\mathbf{q}'\lambda'} \rangle \end{aligned} \tag{2.116}$$

where we only kept the terms that create an electron in the detected vacuum state $|\mathbf{k}\rangle$. For the photon energies commonly used in ARPES, the photon momentum is usually negligible compared with electronic crystal momenta. We therefore set the photon momentum to zero in the following [37]. Since translational symmetry is preserved parallel to a planar surface, the parallel component of the electron momentum is conserved up to a surface reciprocal lattice vector $\mathbf{G}_\parallel$. By contrast, translational symmetry is broken in the direction perpendicular to the surface, and $\mathbf{k}_\perp$ is therefore not conserved across the surface [7]. We therefore restrict the rest of this study to the in-plane momentum $\mathbf{k}_\parallel$. From this point onward, the symbol $\mathbf{k}$ denotes this conserved in-plane momentum

$$\mathbf{k} \equiv \mathbf{k}_\parallel. \tag{2.117}$$

The photon part of the matrix element enforces that the annihilation photon has the same momentum and polarization as the incoming photon,

$$\langle 0_\gamma | a_{\mathbf{q}\lambda} | 1_{\mathbf{q}',\lambda'} \rangle = \delta_{\mathbf{q},\mathbf{q}'} \delta_{\lambda,\lambda'}. \tag{2.118}$$

We denote this fixed photon momentum by $\mathbf{q}_0$. Although $\mathbf{q}_0$ is negligible in momentum conservation for the electronic states, it is not set to zero in the photon quantities such as the photon energy $\omega_{\mathbf{q}_0}$. Thus, whenever $\mathbf{q}_0$ appears added to an electronic crystal momentum, we approximate

$$\mathbf{k} \pm \mathbf{q}_0 \simeq \mathbf{k}, \tag{2.119}$$

while retaining $\omega_{\mathbf{q}_0}$ in the energy-conservation condition.

Using this in Eq. (2.116) and applying the approximations discussed above, gives

$$\langle \Psi_m^{N-1}; \mathbf{k} | H_I | 1_{\mathbf{q}'\lambda'}; \Psi_i^N \rangle \simeq M_{fi}(\mathbf{k}, \mathbf{q}_0) \langle \Psi_m^{N-1} | c_{\mathbf{k}} | \Psi_i^N \rangle. \tag{2.120}$$

Here $M_{fi}(\mathbf{k}, \mathbf{q}_0)$ denotes the single-particle photoemission matrix element, obtained from the electron–photon coupling $\gamma(\mathbf{k}, \mathbf{q}_0)$ after neglecting the photon momentum in the electronic momentum labels. Inserting Eq. (2.120) into Fermi's golden rule, Eq. (2.115), gives

$$w_{fi} \simeq 2\pi |M_{fi}(\mathbf{k}, \mathbf{q}_0)|^2 |\langle \Psi_m^{N-1} | c_{\mathbf{k}} | \Psi_i^N \rangle|^2 \delta(E_e + E_m^{N-1} - E_i^N - \omega_{\mathbf{q}_0}). \tag{2.121}$$

Explicitly, the matrix element is

$$M_{fi}(\mathbf{k}, \mathbf{q}_0) = \frac{e}{m} \sqrt{\frac{1}{2V\omega_{\mathbf{q}_0}}} \langle \phi_f^{\mathbf{k}} | \boldsymbol{\epsilon}_{\mathbf{q}_0\lambda'} e^{i\mathbf{q}_0 \cdot \mathbf{r}} \cdot \mathbf{p} | \phi_i^{\mathbf{k}} \rangle \tag{2.122}$$

where $\mathbf{p} = -i\nabla$. In the long-wavelength limit of the photon field, this reduces to

$$M_{fi}(\mathbf{k}, \mathbf{q}_0) \simeq \frac{e}{m} \sqrt{\frac{1}{2V\omega_{\mathbf{q}_0}}} \langle \phi_f^{\mathbf{k}} | \boldsymbol{\epsilon} \cdot \mathbf{p} | \phi_i^{\mathbf{k}} \rangle. \tag{2.123}$$

Here, $|\phi_i^{\mathbf{k}}\rangle$ and $|\phi_f^{\mathbf{k}}\rangle$ denote the single-particle electron wave functions before and after photon absorption, respectively. The common momentum label $\mathbf{k}$ follows from the momentum-conservation constraints in the transition amplitude.

The measured photocurrent is obtained by summing the transition rate over the initial and final states. Introducing

$$\omega = E_e - \omega_{\mathbf{q}_0}, \tag{2.124}$$

the photocurrent can be written as

$$J(\mathbf{k}, \omega) \propto \sum_{f,i} |M_{fi}(\mathbf{k}, \mathbf{q}_0)|^2 \sum_m |\langle \Psi_m^{N-1} | c_{\mathbf{k}} | \Psi_i^N \rangle|^2 \delta(\omega + E_m^{N-1} - E_i^N). \tag{2.125}$$

We recognize the last factor as the removal part of the spectral function, Eq. (2.97). Using Eq. (2.98), the photocurrent can then be expressed in terms of the full spectral function as

$$J(\mathbf{k}, \omega) \propto \sum_{f,i} |M_{fi}(\mathbf{k}, \mathbf{q}_0)|^2 A(\mathbf{k}, \omega) f(\omega). \tag{2.126}$$

This concludes the derivation of the ARPES photocurrent in the sudden approximation. The result shows how a one-electron photoemission process probes the occupied single-particle spectral function.

3

Superconducting Pairing

Superconductivity was first discovered in 1911 by Kammerlingh Onnes [40], and is most prominently characterized by the disappearance of electrical resistivity below a critical temperature T_c. As a result, currents can flow without dissipative losses [1]. However, it would take around 40 years before the first successful microscopic theory was formalized, which is known as BCS theory [2]. Microscopically, superconductivity is associated with correlations between electrons rather than with independent single-particle motion [41]. These correlations are described in terms of a superconducting pair amplitude, whose symmetry strongly influence the properties of the superconducting state [4].

The BCS framework provides the microscopic starting point for describing superconducting pairing and allows the pair amplitude to be obtained explicitly. We then turn to the symmetry properties of this amplitude, which provide a systematic way to distinguish different superconducting states. In particular, we discuss its classification in terms of spin, spatial, and frequency dependence, including the distinction between even- and odd-frequency superconductivity.

3.1 BCS Theory

Superconductivity as described by BCS theory involves the formation of bound electron pairs, known as Cooper pairs. These pairs are formed due to the presence of an attractive interaction near the Fermi surface, which in conventional superconductors arises from lattice vibrations, or equivalently from the exchange of phonons [1]. When an electron moves through the metal, it locally distorts the ionic lattice from its equilibrium positions due to the attractive interaction between the electron and the positive ions. Because the ions respond more slowly than the electron motion, this lattice distortion can persist after the electron has moved on, creating a region of enhanced positive charge density that can attract another electron [1]. The characteristic frequency scale of these lattice vibrations is set by the Debye frequency, ω_D, which therefore determines the energy range over which the phonon-mediated attraction is effective [1], [17, pp. 627–629].

This discussion motivates a simplified model for the effective attraction between electrons close to the Fermi surface. In the simple case, we can describe the potential responsible for this attractive interaction as [17, p. 629]

$$V(\mathbf{q}) = \begin{cases} -V_0 & |\xi_{\mathbf{p}}| < \omega_D, \\ 0 & |\xi_{\mathbf{p}}| > \omega_D, \end{cases} \tag{3.1}$$

where $\xi_{\mathbf{p}}$ is the electronic energy measured with respect to the Fermi level. It is defined as

$$\xi_{\mathbf{p}} = \epsilon_{\mathbf{p}} - \mu, \tag{3.2}$$

with μ being the chemical potential, and $\epsilon_{\mathbf{p}}$ is the single-particle dispersion. At low temperatures, $\mu \simeq E_F$. This approximation therefore restricts the attractive interaction to electronic states lying within an energy window of order ω_D around the Fermi surface. At this point, it is worth noting that this approximation is a weak-coupling model and is not expected to give a quantitatively reliable description of strongly electron–phonon coupled systems. In such cases, one generally has to retain more of the structure of the electron–phonon interaction, for example its frequency and momentum dependence, rather than replacing it by a constant attractive potential with a Debye window. However, for the system of interest, the electron–phonon interaction is weak, and this simple model should provide a suitable starting point. Having specified the effective interaction that allows two electrons to form a pair, we now turn to the quantum-statistical nature of such pairs.

Because electrons are identical fermions, they obey Fermi statistics, meaning that a many-electron state must be antisymmetric under the exchange of any two electrons. As a consequence, no two electrons can occupy the same complete quantum state, which is known as the Pauli exclusion principle [16, pp. 433–443]. Although the individual electrons are fermions, a two-electron pair can behave effectively like a boson rather than a fermion. This means that many such pairs can occupy the same collective quantum state. At sufficiently low temperatures, where Cooper pairs can form, they condense into a coherent many-body state that is responsible for the superconducting properties of the material [1].

Since the superconducting state is built from paired electrons, it is useful to first write down the ordinary single-particle Green's function in momentum space. From Eq. (2.67), this can be written as

$$\mathcal{G}(\mathbf{p}, \tau - \tau') = -\langle\langle \mathcal{T}_\tau c_{\mathbf{p}\sigma}(\tau) c^\dagger_{\mathbf{p}\sigma}(\tau') \rangle\rangle. \tag{3.3}$$

However, in the superconducting state it is not sufficient to describe only the propagation of individual particles, since the formation of Cooper pairs also implies correlations between the two electrons forming a pair. These pair correlations can be described by introducing the anomalous Green's function,

$$\mathcal{F}(\mathbf{p}, \tau - \tau') = \langle\langle \mathcal{T}_\tau c_{-\mathbf{p}\downarrow}(\tau) c_{\mathbf{p}\uparrow}(\tau') \rangle\rangle, \tag{3.4}$$

$$\mathcal{F}^\dagger(\mathbf{p}, \tau - \tau') = \langle\langle \mathcal{T}_\tau c^\dagger_{\mathbf{p}\uparrow}(\tau) c^\dagger_{-\mathbf{p}\downarrow}(\tau') \rangle\rangle, \tag{3.5}$$

which for conventional pairing relates electrons with opposite spin and opposite momenta. In the normal state, where Cooper pairs cannot form, these pair correlations are identically zero [17, p. 635]. These correlators are quite special in the sense that they include a pair of annihilation operators ($\mathcal{F}$), or a pair of creation operators ($\mathcal{F}^\dagger$), meaning that the states $|\rangle$ and $\langle|$ must have different particle numbers. For example, in (3.4), $|\rangle$ must have two more electrons than $\langle|$. This is possible in the BCS description because the superconducting ground state which breaks $U(1)$ symmetry is written as a coherent superposition of configurations with different numbers of Cooper pairs, and therefore also with different total electron numbers [17, p. 635].

In the following, we provide an outline for the derivation of an explicit expression of Eqs. (3.3), (3.4), and (3.5), as done in Ref. [17, pp. 635–641]. The details are provided in Appendix A. We assume the model Hamiltonian

$$H = \sum_{\mathbf{p}\sigma} \xi_{\mathbf{p}} c^\dagger_{\mathbf{p}\sigma} c_{\mathbf{p}\sigma} + \frac{1}{2\nu} \sum_{\mathbf{q}\mathbf{p}\mathbf{p}' ss'} V(\mathbf{q}) c^\dagger_{\mathbf{p}+\mathbf{q},s} c^\dagger_{\mathbf{p}'-\mathbf{q},s'} c_{\mathbf{p}'s'} c_{\mathbf{p}s}, \tag{3.6}$$

where ν represents the volume of the system. The derivation is done using the equation of motion, which for the Green's function in Eq. (3.3) is given by

$$\frac{\partial}{\partial\tau}\mathcal{G}(\mathbf{p},\tau-\tau') = -\delta(\tau-\tau') - \left\langle\!\!\left\langle \mathcal{T}_\tau \left[\frac{\partial}{\partial\tau} c_{\mathbf{p}\sigma}(\tau)\right] c^\dagger_{\mathbf{p}\sigma}(\tau') \right\rangle\!\!\right\rangle. \tag{3.7}$$

where the definition of the τ-ordered product has been used. This is where the delta function originates. The τ derivative of the annihilation operator can be found by using Heisenberg's equation of motion, giving

$$\frac{\mathrm{d}}{\mathrm{d}\tau} c_{\mathbf{p}\sigma}(\tau) = -\xi_{\mathbf{p}} c_{\mathbf{p}\sigma}(\tau) - \frac{1}{\nu} \sum_{\mathbf{q}\mathbf{p}'s'} V(\mathbf{q}) c^\dagger_{\mathbf{p}'-\mathbf{q},s'}(\tau) c_{\mathbf{p}'s'}(\tau) c_{\mathbf{p}-\mathbf{q},\sigma}(\tau). \tag{3.8}$$

Inserting this into Eq. (3.7) gives

$$\begin{aligned}\left(-\frac{\partial}{\partial\tau} - \xi_{\mathbf{p}}\right)\mathcal{G}(\mathbf{p},\tau-\tau') + \frac{1}{\nu}\sum_{\mathbf{q}\mathbf{p}'s'} V(\mathbf{q}) \\ \times \langle\!\langle \mathcal{T}_\tau c^\dagger_{\mathbf{p}'-\mathbf{q},s'}(\tau) c_{\mathbf{p}'s'}(\tau) c_{\mathbf{p}-\mathbf{q},\sigma}(\tau) c^\dagger_{\mathbf{p},\sigma}(\tau')\rangle\!\rangle = \delta(\tau-\tau').\end{aligned} \tag{3.9}$$

Here, the four-operator object can be reduced to products of two-objects using Wick's theorem. To simplify this further, we assume that long-wavelength phonons give a zero potential. Then $V(\mathbf{q}=0)=0$, which results in the pairing that occurs at $\mathbf{p}=0$ vanishes. Since Wick's theorem is not exact in our case, we will continue by working in the Wick-factorization approximation described in Sec. 2.2. In this approximation, we find that the second term of Eq. (3.9) simplifies to

$$\begin{aligned}&\frac{1}{\nu}\sum_{\mathbf{q}\mathbf{p}'s'} V(\mathbf{q}) \langle\!\langle \mathcal{T}_\tau c^\dagger_{\mathbf{p}'-\mathbf{q},s'}(\tau) c_{\mathbf{p}'s'}(\tau) c_{\mathbf{p}-\mathbf{q},\sigma}(\tau) c^\dagger_{\mathbf{p},\sigma}(\tau')\rangle\!\rangle \\ &\qquad = \frac{1}{\nu}\sum_{\mathbf{q}} V(\mathbf{q}) \Big[\mathcal{G}(\mathbf{p},\tau-\tau') n_{\mathbf{p}-\mathbf{q}} - \mathcal{F}(\mathbf{p}-\mathbf{q},0)\mathcal{F}^\dagger(\mathbf{p},\tau-\tau')\Big].\end{aligned} \tag{3.10}$$

The first contribution corresponds to an exchange correction to the electron self-energy, arising from the effective phonon-induced interaction between electrons. The corresponding self-energy term is

$$\Sigma_x = -\frac{1}{\nu}\sum_{\mathbf{q}} V(\mathbf{q}) n_{\mathbf{p}-\mathbf{q}}. \tag{3.11}$$

Since this contribution changes only weakly when going from the normal state to the superconducting state, it is neglected in the weak-coupling approximation. In the second term, we find the combination

$$\Delta(\mathbf{p}) = -\frac{1}{\nu}\sum_{\mathbf{p}} V(\mathbf{p}) \mathcal{F}(\mathbf{p}-\mathbf{q},\tau=0), \tag{3.12}$$

which denotes the gap function. With the attractive potential defined in Eq. (3.1), the right-hand side is positive, so $\Delta(\mathbf{p})$ is positive. This quantity sets the superconducting energy scale and enters directly in the quasiparticle excitation spectrum. With this, Eq. (3.9) becomes

$$\left(-\frac{\partial}{\partial\tau}-\xi_{\mathbf{p}}\right)\mathcal{G}(\mathbf{p},\tau-\tau')+\Delta(\mathbf{p})\mathcal{F}^{\dagger}(\mathbf{p},\tau-\tau')=\delta(\tau-\tau'). \tag{3.13}$$

There are two unknowns in this equation, $\mathcal{G}$ and $\mathcal{F}^{\dagger}$. To solve this, we need to find a coupled equation, which can be obtained from the equation of motion of $\mathcal{F}^{\dagger}$.

Taking the τ derivative of $\mathcal{F}^{\dagger}$, we find its equation of motion

$$\frac{\partial}{\partial\tau}\mathcal{F}^{\dagger}(\mathbf{p},\tau-\tau')=\left\langle\left\langle\mathcal{T}_{\tau}\left[\frac{\partial}{\partial\tau}c^{\dagger}_{\mathbf{p}\uparrow}(\tau)\right]c^{\dagger}_{-\mathbf{p}\downarrow}(\tau')\right\rangle\right\rangle. \tag{3.14}$$

In contrast to Eq. (3.7), this equation lacks the term $\delta(\tau-\tau')$ that vanishes in the calculations. The τ evolution of $\mathcal{F}^{\dagger}$ is described by the τ evolution of the creation operator, which can be computed as

$$\frac{\mathrm{d}}{\mathrm{d}\tau}c^{\dagger}_{\mathbf{p}\sigma}(\tau)=\xi_{\mathbf{p}}c_{\mathbf{p}\sigma}(\tau)+\frac{1}{\nu}\sum_{\mathbf{q}\mathbf{p}'s'}V(\mathbf{q})c^{\dagger}_{\mathbf{p}-\mathbf{q},\sigma}(\tau)c^{\dagger}_{\mathbf{p}'+\mathbf{q},s'}(\tau)c_{\mathbf{p}'s'}(\tau). \tag{3.15}$$

Inserting this into Eq. (3.14) gives

$$\left(-\frac{\partial}{\partial\tau}+\xi_{\mathbf{p}}\right)\mathcal{F}^{\dagger}(\mathbf{p},\tau-\tau')+\frac{1}{\nu}\sum_{\mathbf{q}\mathbf{p}'s}V(\mathbf{q})\langle\langle\mathcal{T}_{\tau}c^{\dagger}_{\mathbf{p}-\mathbf{q},\sigma}(\tau)c^{\dagger}_{\mathbf{p}'+\mathbf{q},s'}(\tau)c_{\mathbf{p}'s'}(\tau)c^{\dagger}_{-\mathbf{p}\downarrow}(\tau')\rangle\rangle=0. \tag{3.16}$$

As before, there is a four-operator object. This can be rewritten as products of two-operator objects using Wick's theorem, which is again an approximation. From this approximation we get three terms, one that requires $\mathbf{p}=0$, which vanishes by the same argument as before. One term with the exchange potential in Eq. (3.11) which is again neglected. Lastly, we get the quantity $\Delta^{\dagger}(\mathbf{p})$. This gives the equation of motion

$$\left(-\frac{\partial}{\partial\tau}+\xi_{\mathbf{p}}\right)\mathcal{F}^{\dagger}(\mathbf{p},\tau-\tau')+\Delta^{\dagger}(\mathbf{p})\mathcal{G}(\mathbf{p},\tau-\tau')=0. \tag{3.17}$$

We assume that the gap function is real, leading to $\Delta^{\dagger}(\mathbf{p})=\Delta(\mathbf{p})$.

From the definition of the inverse Fourier transform in Eq. (2.72), the inverse Fourier transforms of $\mathcal{G}$, $\mathcal{F}$ and $\mathcal{F}^{\dagger}$ are defined as

$$\mathcal{G}(\mathbf{p},\tau)=\frac{1}{\beta}\sum_{n}e^{-i\omega_n\tau}\mathcal{G}(\mathbf{p},i\omega_n), \tag{3.18}$$

$$\mathcal{F}(\mathbf{p},\tau)=\frac{1}{\beta}\sum_{n}e^{-i\omega_n\tau}\mathcal{F}(\mathbf{p},i\omega_n), \tag{3.19}$$

$$\mathcal{F}^{\dagger}(\mathbf{p},\tau)=\frac{1}{\beta}\sum_{n}e^{-i\omega_n\tau}\mathcal{F}^{\dagger}(\mathbf{p},i\omega_n). \tag{3.20}$$

Using these transformations in Eqs. (3.9) and (3.16), they are transformed to the two algebraic equations

$$(i\omega_n - \xi_{\mathbf{p}})\mathcal{G}(\mathbf{p}, i\omega_n) + \Delta(\mathbf{p})\mathcal{F}^\dagger(\mathbf{p}, i\omega_n) = 1, \tag{3.21}$$

$$(i\omega_n + \xi_{\mathbf{p}})\mathcal{F}^\dagger(\mathbf{p}, i\omega_n) + \Delta(\mathbf{p})\mathcal{G}(\mathbf{p}, i\omega_n) = 0. \tag{3.22}$$

These can be solved, giving

$$\mathcal{G}(\mathbf{p}, i\omega_n) = -\frac{i\omega_n + \xi_{\mathbf{p}}}{\omega_n^2 + \xi_{\mathbf{p}}^2 + \Delta^2(\mathbf{p})}, \tag{3.23}$$

$$\mathcal{F}(\mathbf{p}, i\omega_n) = \mathcal{F}^\dagger(\mathbf{p}, i\omega_n) = \frac{\Delta(\mathbf{p})}{\omega_n^2 + \xi_{\mathbf{p}}^2 + \Delta^2(\mathbf{p})}. \tag{3.24}$$

The equation of motion for $\mathcal{F}$ is obtained in the same manner as for $\mathcal{F}^\dagger$. In the convention used here, with a real positive gap function, both anomalous Green's functions reduce to the same expression, hence the equivalence in Eq. (3.24). This concludes the outline of the derivation presented in Ref. [17, pp. 635–641].

Before we move on, it is useful to introduce the excitation energy of the superconductor [17, p. 639]

$$E_{\mathbf{p}} = \sqrt{\xi_{\mathbf{p}}^2 + \Delta^2(\mathbf{p})}. \tag{3.25}$$

In the conventional s-wave case, the gap function is independent of momentum and can therefore be written as $\Delta(\mathbf{p}) = \Delta$ at a fixed temperature. The elementary excitations of the superconducting state are quasiparticles with energy $E_{\mathbf{p}}$. Since $\xi_{\mathbf{p}}^2 \geq 0$, this energy is minimized at the Fermi surface, where $\xi_{\mathbf{p}} = 0$, giving $E_{\mathbf{p}} \geq \Delta$. Thus, Δ represents the minimum energy required to create a single quasiparticle. However, because the electrons in the superconducting ground state are paired, breaking a pair creates two excited quasiparticles. In the conventional BCS case, the paired states have opposite momenta, so the energy for such a pair-breaking excitation is therefore $E_{\mathbf{p}} + E_{-\mathbf{p}} \geq 2\Delta$. The superconducting energy gap is consequently given by $E_g \equiv 2\Delta$ [17, pp. 639–640].

3.2 Pairing Symmetries

The anomalous Green's function was introduced in Eq. (3.4) of the previous section for the simple BCS case. There, it was written in momentum space and imaginary time, and the orbital indices were left out. More generally, it can be written as

$$F_{\alpha\beta,ab}(\mathbf{r}_1, t_1; \mathbf{r}_2, t_2) = \langle\langle \mathcal{T} c_{\alpha,a}(\mathbf{r}_1, t_1) c_{\beta,b}(\mathbf{r}_2, t_2) \rangle\rangle, \tag{3.26}$$

where α and β label spin indices, a and b label orbital indices, and $\mathbf{r}_1$, $\mathbf{r}_2$ and t_1, t_2 denote spatial and time coordinates, respectively [4]. From Fermi statistics, we know that the exchange of two fermions induces a sign change, so that

$$F_{\alpha\beta,ab}(\mathbf{r}_1, t_1; \mathbf{r}_2, t_2) = -F_{\beta\alpha,ba}(\mathbf{r}_2, t_2; \mathbf{r}_1, t_1), \tag{3.27}$$

which corresponds to interchanging all quantum numbers of the two fermions. However, the exchange of a single quantum number does not need to produce the sign

change by itself. It is only under the combined exchange of all quantum numbers that the anomalous Green's function must be antisymmetric [4], [5], [42]. The exchange of individual quantum numbers can be divided into a set of four symmetry operations: spin exchange (S), parity (P^*), orbital exchange (O) and time exchange (T^*). Since the combined action of these operators must induce a sign change, we can schematically write this relation as

$$SP^*OT^* = -1. \tag{3.28}$$

Therefore, the pairing symmetry of the superconducting state is determined by the symmetry properties of the anomalous Green's function. In what follows, we will exclusively consider single-band pairing symmetries, meaning that the anomalous Green's function is even under orbital exchange, i.e. $O = +1$.

Consider a superconducting state that is odd under spin exchange ($S = -1$) and even under parity exchange ($P^* = +1$). Then, from Eq. (3.28), we can deduce that this state must be even under the exchange of time coordinates ($T^* = +1$). Such a superconducting state is called an even-frequency superconductor. If the superconducting state was instead even under spin exchange ($S = +1$), it would be forced to have an odd time-exchange symmetry ($T^* = -1$) by Eq. (3.28). This type of pairing state is known as an odd-frequency superconducting state [4]. There are four possible pairing states for the single-band system considered here. These have been compiled in Tab. 3.1. The first two correspond to even-frequency pairing, whereas the last two correspond to odd-frequency pairing. All superconducting states considered in this thesis are even under parity exchange, and hence belong to the first row for the even-frequency case and the third row for the odd-frequency case.

Table 3.1: Possible pairing symmetries for the superconducting state. Here, the time-exchange (T^*) symmetry determines whether the superconducting state is even or odd in frequency. Hence, the first two rows correspond to even-frequency states, and the last two rows correspond to odd-frequency states.

Symmetry factors				
S	P^*	O	T^*	SP^*OT^*
-1	$+1$	$+1$	$+1$	-1
$+1$	-1	$+1$	$+1$	-1
$+1$	$+1$	$+1$	-1	-1
-1	-1	$+1$	-1	-1

By introducing the relative spatial coordinate $\mathbf{r} = \mathbf{r}_1 - \mathbf{r}_2$, the action of P^* corresponds to $\mathbf{r} \to -\mathbf{r}$. In this form, the earlier use of the term parity becomes natural. Similarly, introducing the relative-time variable $s = t_1 - t_2$, the action of T^* corresponds to $s \to -s$, that is, a reversal of the relative time [4].[1] Thus, an

[1] These operations should not be confused with ordinary spatial inversion or time-reversal symmetry.

anomalous Green's-function component that is odd in frequency satisfies

$$F_{\alpha\beta,ab}(\mathbf{r}, s) = -F_{\alpha\beta,ab}(\mathbf{r}, -s). \tag{3.29}$$

Since a function that is antisymmetric in a coordinate vanishes when that coordinate is zero, this implies $F_{\alpha\beta,ab}(\mathbf{r}, 0) = 0$ for a purely odd-frequency component. Here, we encounter a conceptual difference between conventional BCS pairing and odd-frequency pairing. From the definition of the gap function in Eq. (3.12), it is clear that the equal-time anomalous amplitude entering the conventional BCS gap definition vanishes for a purely odd-frequency component. This does not necessarily mean that the superconducting state is gapless in the odd-frequency case, although it can be [4].

Since $F(s)$ is odd in the relative time, its relative-time derivative is even and can therefore be nonzero at $s = 0$, provided the equal-time limit is well defined. In the Matsubara formulation, the analogous statement is made by considering the derivative with respect to the relative imaginary-time coordinate. Thus, although the equal-time anomalous amplitude itself vanishes for a purely odd-frequency component, the slope of the anomalous amplitude at equal relative time may be nonzero. This motivates an alternative way of characterizing the odd-frequency gap structure in terms of the appropriate equal-time contribution to the relative-time derivative of the anomalous Green's function, rather than in terms of the equal-time anomalous amplitude itself [43]. It is this distinction between the equal-time anomalous amplitude and the relative-time structure of the anomalous Green's function that separates odd-frequency pairing from the conventional BCS case [4], [43].

4

Double Photoelectron Spectroscopy of Odd-Frequency Pairing

The chapter is organized as follows. First, the DPE setup and the corresponding photoemission Hamiltonian are introduced. The S-matrix expansion developed in Sec. 2.1.2 is then applied to the DPE process, where the leading nonzero contribution is the second-order term in the interaction Hamiltonian. This term is used to derive a general expression for the counting rate in terms of Green's functions. The resulting expression is then used to compare the general structure of the anomalous and normal contributions for even- and odd-frequency pairing. Finally, the BCS limit is evaluated explicitly and compared with the known even-frequency result, providing a consistency check of the Green's-function formulation.

4.1 DPE Setup and Interaction Hamiltonian

Similar to ARPES, DPE is based on the photoelectric effect. However, in DPE, absorption of a single photon results in the emission of two outgoing electrons rather than one, as illustrated in Fig. 4.1. In the following, these emitted electrons are referred to as photoelectrons in order to distinguish them from the conduction electrons in the sample.

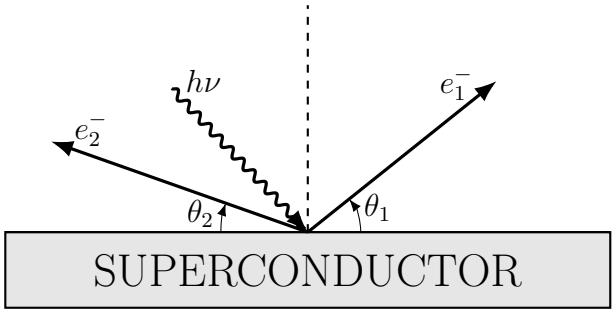

Figure 4.1: Schematic of the DPE measurement geometry. An incident photon ($h\nu$) impinges on a superconductor, leading to the ejection of photoelectron (e_1^-) at an emission angle θ_1 and photoelectron (e_2^-) at an emission angle θ_2.

There are two sequential mechanisms by which a single photon may give rise to the emission of two electrons [10], [44]. In the first scenario, the photon is initially

absorbed by a valence-band electron, which is excited into a free photoelectron state. The resulting photoelectron can subsequently interact with another valence electron and provide sufficient energy for its emission. In the second scenario, the photon removes an electron from a core level, leaving behind a core hole. When this vacancy is filled by a valence electron, the released energy can be transferred to another valence electron, which is then emitted via an Auger process. However, the present discussion is limited to DPE spectroscopy performed with relatively low-photon-energy, laser-based XUV sources. Under these conditions, direct access to core-level states is not expected [10]; consequently, the Auger-like pathway is neglected and the discussion focuses on the valence-band process.

In the following derivation, the photoemission process is treated within the sudden approximation. The detected photoelectrons are described by plane-wave final states, while the electronic states in the sample are described as conduction-electron states. Energies of the conduction electrons are measured relative to the Fermi energy, which is taken as the zero of energy. Equivalently, we work with $\xi_{\mathbf{k}} = \epsilon_{\mathbf{k}} - \mu$, with $\mu = 0$ in this convention.

The superconducting state considered here is modeled as a minimal BCS-like single-band odd-frequency pairing state. The anomalous pair amplitude entering the transition amplitude is taken to have spin-triplet, even-parity symmetry. Using the symmetry notation introduced in Sec. 3.2, this corresponds to

$$S = +1, \qquad P^* = +1, \qquad O = +1, \qquad T^* = -1. \tag{4.1}$$

These symmetry labels indicate that the pair amplitude is spin-symmetric, momentum-even, single-band, and odd in relative time or frequency. Since $P^* = +1$ only specifies even momentum parity, this symmetry classification includes, for example, both s-wave and d-wave pairing structure [11]. In this minimal model, the normal Green's function is taken to be spin diagonal.

Following the model used in Ref. [10], we write the Schrödinger-picture Hamiltonian as

$$H = H_0 + H_I, \tag{4.2}$$

where H_0 is described by

$$H_0 = \sum_{\mathbf{q},\nu} \omega_{\mathbf{q}} a^\dagger_{\mathbf{q}\nu} a_{\mathbf{q}\nu} + \sum_{\mathbf{k},\sigma} \epsilon_{\mathbf{k}} d^\dagger_{\mathbf{k}\sigma} d_{\mathbf{k}\sigma} + H_{\mathrm{SC}}. \tag{4.3}$$

At this stage, H_{SC} is left unspecified, since the counting rate can be expressed generally in terms of Green's functions without choosing a particular model. An explicit form of H_{SC} is only needed when these Green's functions are evaluated or when the result is further simplified. The interaction Hamiltonian is taken as

$$H_I = \sum_{\mathbf{k},\mathbf{q},\sigma,\nu} \gamma_\nu(\mathbf{k},\mathbf{q}) d^\dagger_{\mathbf{k}+\mathbf{q},\sigma} c_{\mathbf{k}\sigma} (a_{\mathbf{q}\nu} + a^\dagger_{-\mathbf{q}\nu}) + \sum_{\mathbf{k},\mathbf{p},\mathbf{q},\alpha,\beta} V(\mathbf{q}) d^\dagger_{\mathbf{k}+\mathbf{q},\alpha} d^\dagger_{\mathbf{p}-\mathbf{q},\beta} d_{\mathbf{p}\beta} c_{\mathbf{k}\alpha} + \mathrm{H.c.}, \tag{4.4}$$

where H.c. denotes the Hermitian conjugate. The operators $d^\dagger_{\mathbf{k}\sigma}$ and $d_{\mathbf{k}\sigma}$ create and annihilate a photoelectron with momentum $\mathbf{k}$ and spin σ, respectively; while $c^\dagger_{\mathbf{k}\sigma}$ and $c_{\mathbf{k}\sigma}$ create and annihilate a conduction electron in the sample. Similarly, $a^\dagger_{\mathbf{q}\nu}$ and $a_{\mathbf{q}\nu}$ create and annihilate a photon with momentum $\mathbf{q}$ and polarization ν. The first term

describes the coupling between the radiation field and the conduction electrons, with $\gamma_\nu(\mathbf{k},\mathbf{q})$ denoting the effective electron–photon coupling matrix element. The second term describes the electron–electron scattering process that leads to the emission of a second photoelectron, mediated by the screened Coulomb interaction $V(\mathbf{q})$.

We next define the states entering the transition amplitude. The initial state $|i\rangle$ describes the system before photoemission, with the sample in an N-electron many-body state, one incoming photon, and no photoelectrons. The final state $|f\rangle$ describes the system after the DPE process, with the sample left in an $(N-2)$-electron many-body state, no remaining photons, and two photoelectrons. These states are written as

$$|i\rangle = |\Phi_i^N\rangle|1_{\mathbf{q}'\lambda'}\rangle_\gamma|0\rangle_{pe}, \tag{4.5}$$

$$|f\rangle = |\Phi_f^{N-2}\rangle|0\rangle_\gamma|\mathbf{k}_1',\sigma_1';\mathbf{k}_2',\sigma_2'\rangle_{pe}. \tag{4.6}$$

Having specified the initial and final states, we now identify which terms in the S-matrix expansion can connect them. For notational convenience, we separate the interaction Hamiltonian into the electron–photon coupling H_γ and the electron–electron scattering rate H_{ee}, defined by

$$H_\gamma = \sum_{\mathbf{k},\mathbf{q},\sigma,\nu} \gamma_\nu(\mathbf{k},\mathbf{q}) d^\dagger_{\mathbf{k}+\mathbf{q},\sigma} c_{\mathbf{k}\sigma}(a_{\mathbf{q}\nu} + a^\dagger_{-\mathbf{q}\nu}), \tag{4.7}$$

$$H_{ee} = \sum_{\mathbf{k},\mathbf{p},\mathbf{q},\alpha,\beta} V(\mathbf{q}) d^\dagger_{\mathbf{k}+\mathbf{q},\alpha} d^\dagger_{\mathbf{p}-\mathbf{q},\beta} d_{\mathbf{p}\beta} c_{\mathbf{k}\alpha}. \tag{4.8}$$

Thus,

$$H_I = H_\gamma + H_{ee} + H_\gamma^\dagger + H_{ee}^\dagger \tag{4.9}$$

Using Eq. (2.18), the interaction terms are expressed in the interaction picture before being inserted into the S-matrix expansion.

From the S-matrix expansion in Eq. (2.32), we see that the zeroth-order term cannot contribute since the initial and final states contain different photon and photoelectron occupations. The first-order term also vanishes: the electron–photon part of H_I can create only one photoelectron, whereas the electron–electron scattering term requires an already existing photoelectron in the initial state. Thus, the lowest-order non-vanishing contribution is obtained from the second-order term, in which photon absorption is followed by electron–electron scattering. The second-order term is thus given by

$$S^{(2)}(\infty,-\infty) = -\frac{1}{2}\int_{-\infty}^{\infty} \mathrm{d}t_1\, \mathrm{d}t_2\, \mathcal{T}\Big\{[H_\gamma(t_1) + H_{ee}(t_1) + H_\gamma^\dagger(t_1) + H_{ee}^\dagger(t_1)] \times [H_\gamma(t_2) + H_{ee}(t_2) + H_\gamma^\dagger(t_2) + H_{ee}^\dagger(t_2)]\Big\}. \tag{4.10}$$

Expanding the product gives several combinations of H_γ, H_{ee}, and their Hermitian conjugates. However, only terms with one H_γ and one H_{ee} can connect the states $|i\rangle$ and $|f\rangle$: the former absorbs the incoming photon and creates the first photoelectron, while the latter creates the second photoelectron through electron–electron scattering. Thus, the only contributing products are $H_{ee}(t_1)H_\gamma(t_2)$ and $H_\gamma(t_1)H_{ee}(t_2)$. Since the two terms are related by the interchange of the integration variables t_1

and t_2, they give equal contributions under the time-ordering operation. The factor $1/2$ is therefore cancelled, and the contribution relevant for the DPE process can be written as

$$S^{(2)}(\infty,-\infty) = -\int_{-\infty}^{\infty} \mathrm{d}t_1\ \mathrm{d}t_2\, \mathcal{T}\Bigg[\sum_{\mathbf{k}_2,\mathbf{p},\mathbf{l}}\sum_{\sigma,\bar{\sigma}} V(\mathbf{l}) d^\dagger_{\mathbf{k}_2+\mathbf{l},\bar{\sigma}}(t_1) d^\dagger_{\mathbf{p}-\mathbf{l},\sigma}(t_1) d_{\mathbf{p}\sigma}(t_1) c_{\mathbf{k}_2\bar{\sigma}}(t_1) \times \sum_{\mathbf{k}_1,\sigma_1}\sum_{\mathbf{q},\nu} \gamma_\nu(\mathbf{k}_1,\mathbf{q}) d^\dagger_{\mathbf{k}_1+\mathbf{q},\sigma_1}(t_2) c_{\mathbf{k}_1\sigma_1}(t_2) a_{\mathbf{q}\nu}(t_2)\Bigg]. \tag{4.11}$$

The DPE counting rate is obtained from the transition probability per unit time for detecting two photoelectrons with momenta and spins $(\mathbf{k}'_1,\sigma'_1)$ and $(\mathbf{k}'_2,\sigma'_2)$. Since the final many-body state of the sample is not resolved experimentally, we sum over all final states $|\Phi_f^{N-2}\rangle$. The initial states of the sample are thermally averaged, giving the second-order contribution to the counting rate [10]

$$P^{(2)}(\mathbf{k}'_1,\sigma'_1,\mathbf{k}'_2,\sigma'_2) = \frac{1}{Z}\sum_{i,f}\frac{e^{-\beta E_i}}{\Delta t}|\langle f|S^{(2)}(\infty,-\infty)|i\rangle|^2, \tag{4.12}$$

where Z is the partition function and Δt denotes the duration of the photoemission process.

4.2 Counting Rate in Terms of Green's Functions

We now evaluate the second-order transition amplitude that enters the DPE counting rate. The photon beam is taken to be incident over a time interval of duration Δt, centered at $t=0$, giving

$$\int_{-\Delta t/2}^{\Delta t/2}\mathrm{d}t_2\int_{t_2}^{\infty}\mathrm{d}t_1 \sum_{\mathbf{k}_2,\mathbf{p},\mathbf{l}}\sum_{\sigma,\bar{\sigma}} V(\mathbf{l}) \sum_{\mathbf{k}_1,\sigma_1}\sum_{\mathbf{q},\nu}\gamma_\nu(\mathbf{k}_1,\mathbf{q}) \times \langle f|d^\dagger_{\mathbf{k}_2+\mathbf{l},\bar{\sigma}}(t_1) d^\dagger_{\mathbf{p}-\mathbf{l},\sigma}(t_1) d_{\mathbf{p}\sigma}(t_1) c_{\mathbf{k}_2\bar{\sigma}}(t_1) d^\dagger_{\mathbf{k}_1+\mathbf{q},\sigma_1}(t_2) c_{\mathbf{k}_1\sigma_1}(t_2) a_{\mathbf{q}\nu}(t_2)|i\rangle. \tag{4.13}$$

The overall sign is omitted, as it drops out of the counting rate. To handle the time dependence of the operators, we use Eq. (2.18). Since the photon and photoelectron parts of H_0 are diagonal in the corresponding number operators, their interaction-picture time dependence is simply

$$d^\dagger_{\mathbf{k}}(t) = e^{i\epsilon_{\mathbf{k}}t} d^\dagger_{\mathbf{k}}, \qquad d_{\mathbf{k}}(t) = e^{-i\epsilon_{\mathbf{k}}t} d_{\mathbf{k}}, \tag{4.14}$$

$$a^\dagger_{\mathbf{k}}(t) = e^{i\omega_{\mathbf{k}}t} a^\dagger_{\mathbf{k}}, \qquad a_{\mathbf{k}}(t) = e^{-i\omega_{\mathbf{k}}t} a_{\mathbf{k}}. \tag{4.15}$$

The conduction-electron operators are instead evolved with H_{SC}. Since this Hamiltonian is not assumed diagonal in the $c_{\mathbf{k},\sigma}$ operators, their time dependence cannot in general reduce to a simple phase factor. We therefore keep $c_{\mathbf{k},\sigma}(t)$ explicitly. The corresponding transition amplitude is then simplified to

$$\int_{-\Delta t/2}^{\Delta t/2}\mathrm{d}t_2\int_{t_2}^{\infty}\mathrm{d}t_1 \sum_{\mathbf{k}_2,\mathbf{p},\mathbf{l}}\sum_{\sigma,\bar{\sigma}} V(\mathbf{l}) \sum_{\mathbf{k}_1,\sigma_1}\sum_{\mathbf{q},\nu}\gamma_\nu(\mathbf{k}_1,\mathbf{q}) e^{-i\omega_{\mathbf{q}}t_2} e^{i\epsilon_{\mathbf{k}_1}t_2} e^{i(-\epsilon_{\mathbf{p}}+\epsilon_{\mathbf{p}-\mathbf{l}}+\epsilon_{\mathbf{k}_2+\mathbf{l}})t_1} \times \langle f|d^\dagger_{\mathbf{k}_2+\mathbf{l},\bar{\sigma}} d^\dagger_{\mathbf{p}-\mathbf{l},\sigma} d_{\mathbf{p}\sigma} c_{\mathbf{k}_2\bar{\sigma}}(t_1) d^\dagger_{\mathbf{k}_1+\mathbf{q},\sigma_1} c_{\mathbf{k}_1\sigma_1}(t_2) a_{\mathbf{q}\nu}|i\rangle. \tag{4.16}$$

Since the Hilbert space factorizes into sample, photon, and photoelectron sectors, the matrix element can be separated into contributions from each sector. Using the fermionic anticommutation relations to collect the photoelectron operators, and denoting the momentum of the incoming photon by $\mathbf{q}_0'$, we obtain

$$\begin{aligned}
&{}_{pe}\langle \mathbf{k}_1', \sigma_1'; \mathbf{k}_2', \sigma_2'|\,{}_\gamma\langle 0|\,\langle \Phi_f^{N-2}|d^\dagger_{\mathbf{k}_2+\mathbf{l},\bar\sigma} d^\dagger_{\mathbf{p}-\mathbf{l},\sigma} d_{\mathbf{p}\sigma} c_{\mathbf{k}_2\bar\sigma}(t_1) d^\dagger_{\mathbf{k}_1+\mathbf{q},\sigma_1} c_{\mathbf{k}_1\sigma_1}(t_2) a_{\mathbf{q}\nu}|\Phi_i^N\rangle |1_{\mathbf{q}_0'\lambda'}\rangle_\gamma |0\rangle_{pe} \\
&= -{}_{pe}\langle \mathbf{k}_1', \sigma_1'; \mathbf{k}_2', \sigma_2'|d^\dagger_{\mathbf{k}_2+\mathbf{l},\bar\sigma} d^\dagger_{\mathbf{p}-\mathbf{l},\sigma} d_{\mathbf{p}\sigma} d^\dagger_{\mathbf{k}_1+\mathbf{q},\sigma_1}|0\rangle_{pe}\,{}_\gamma\langle 0|a_{\mathbf{q}\nu}|1_{\mathbf{q}_0'\lambda'}\rangle_\gamma \\
&\quad \times \langle \Phi_f^{N-2}|c_{\mathbf{k}_2\bar\sigma}(t_1) c_{\mathbf{k}_1\sigma_1}(t_2)|\Phi_i^N\rangle,
\end{aligned} \tag{4.17}$$

The minus sign arises from interchanging $c_{\mathbf{k}_2\bar\sigma}(t_1)$ with $d^\dagger_{\mathbf{k}_1+\mathbf{q},\sigma_1}$. The photon matrix element fixes the momentum and polarization of the photon operator to those of the incoming photon,

$${}_\gamma\langle 0|a_{\mathbf{q}\nu}|1_{\mathbf{q}_0'\lambda'}\rangle_\gamma = \delta_{\mathbf{q}\mathbf{q}_0'}\delta_{\nu\lambda'} \tag{4.18}$$

Since $\mathbf{q}_0'$ is small compared with the electronic momenta, we neglect it in the photoelectron momenta appearing in the matrix element. The photon energy is retained throughout. We now simplify the photoelectron matrix element in the same way. First,

$$d_{\mathbf{p}\sigma} d^\dagger_{\mathbf{k}_1,\sigma_1}|0\rangle_{pe} = \delta_{\mathbf{p}\mathbf{k}_1}\delta_{\sigma\sigma_1}|0\rangle_{pe}, \tag{4.19}$$

which fixes $\mathbf{p} = \mathbf{k}_1$ and $\sigma = \sigma_1$. The remaining two-photoelectron overlap is then

$$\begin{aligned}
&{}_{pe}\langle \mathbf{k}_1', \sigma_1'; \mathbf{k}_2', \sigma_2'|d^\dagger_{\mathbf{k}_2+\mathbf{l},\bar\sigma} d^\dagger_{\mathbf{p}-\mathbf{l},\sigma}|0\rangle_{pe} \\
&= \delta_{\mathbf{k}_1',\mathbf{k}_2+\mathbf{l}}\delta_{\sigma_1'\bar\sigma}\delta_{\mathbf{k}_2',\mathbf{k}_1-\mathbf{l}}\delta_{\sigma_2',\sigma} - \delta_{\mathbf{k}_1',\mathbf{k}_1-\mathbf{l}}\delta_{\sigma_1',\sigma}\delta_{\mathbf{k}_2',\mathbf{k}_2+\mathbf{l}}\delta_{\sigma_2',\bar\sigma}.
\end{aligned} \tag{4.20}$$

The minus sign in the second term follows from the antisymmetry of the two-photoelectron state. Substituting the photon and photoelectron matrix elements into the transition amplitude yields

$$\begin{aligned}
&\int_{-\Delta t/2}^{\Delta t/2} \mathrm{d}t_2 \int_{t_2}^{\infty} \mathrm{d}t_1 \sum_{\mathbf{k}_2,\mathbf{p},\mathbf{l}} \sum_{\sigma,\bar\sigma} V(\mathbf{l}) \sum_{\mathbf{k}_1,\sigma_1} \sum_{\mathbf{q},\nu} \gamma_\nu(\mathbf{k}_1,\mathbf{q}) e^{-i\omega_{\mathbf{q}} t_2} e^{i\epsilon_{\mathbf{k}_1} t_2} e^{i(-\epsilon_{\mathbf{p}}+\epsilon_{\mathbf{p}-\mathbf{l}}+\epsilon_{\mathbf{k}_2+\mathbf{l}})t_1} \\
&\quad \times \delta_{\mathbf{q}\mathbf{q}_0'}\delta_{\nu\lambda'}\delta_{\mathbf{p}\mathbf{k}_1}\delta_{\sigma\sigma_1}\Big(\delta_{\mathbf{k}_1',\mathbf{k}_2+\mathbf{l}}\delta_{\sigma_1'\bar\sigma}\delta_{\mathbf{k}_2',\mathbf{k}_1-\mathbf{l}}\delta_{\sigma_2',\sigma} - \delta_{\mathbf{k}_1',\mathbf{k}_1-\mathbf{l}}\delta_{\sigma_1',\sigma}\delta_{\mathbf{k}_2',\mathbf{k}_2+\mathbf{l}}\delta_{\sigma_2',\bar\sigma}\Big) \\
&\quad \times \langle \Phi_f^{N-2}|c_{\mathbf{k}_2\bar\sigma}(t_1) c_{\mathbf{k}_1\sigma_1}(t_2)|\Phi_i^N\rangle.
\end{aligned} \tag{4.21}$$

The Kronecker deltas collapse the sums over $\mathbf{q}$, ν, $\mathbf{p}$, σ, and the remaining photoelectron momenta, giving the transition amplitude

$$\begin{aligned}
&\langle f|S^{(2)}(\infty,-\infty)|i\rangle \\
&= -\int_{-\Delta t/2}^{\Delta t/2} \mathrm{d}t_2 \int_{t_2}^{\infty} \mathrm{d}t_1 \sum_{\mathbf{k}_2,\mathbf{k}_1} \delta_{\mathbf{k}_1'+\mathbf{k}_2'-\mathbf{k}_1-\mathbf{k}_2,0} e^{-i\omega_{\mathbf{q}_0'} t_2} e^{i\epsilon_{\mathbf{k}_1} t_2} e^{i(-\epsilon_{\mathbf{k}_1}+\epsilon_{\mathbf{k}_2'}+\epsilon_{\mathbf{k}_1'})t_1} \\
&\qquad \times \gamma_{\lambda'}(\mathbf{k}_1,\mathbf{q}_0')\Big[V(\mathbf{k}_1-\mathbf{k}_2')\langle \Phi_f^{N-2}|c_{\mathbf{k}_2\sigma_1'}(t_1) c_{\mathbf{k}_1\sigma_2'}(t_2)|\Phi_i^N\rangle \\
&\qquad\qquad - V(\mathbf{k}_1-\mathbf{k}_1')\langle \Phi_f^{N-2}|c_{\mathbf{k}_2\sigma_2'}(t_1) c_{\mathbf{k}_1\sigma_1'}(t_2)|\Phi_i^N\rangle\Big],
\end{aligned} \tag{4.22}$$

where the remaining Kronecker delta enforces momentum conservation.

The expression above is general within the assumptions stated so far. We now specialize to the zero-center-of-mass channel, which is the channel relevant for the superconducting correlations considered in this work. This implies

$$\mathbf{k}_1 = -\mathbf{k}_2, \qquad \mathbf{k}_1' = -\mathbf{k}_2'. \tag{4.23}$$

We neglect the photon momentum in the electron–photon coupling, since it is small compared to the electronic momenta, while retaining the photon energy. For notational compactness, we therefore write

$$\gamma_{\lambda'}(\mathbf{k}_1, \mathbf{q}_0') \equiv \gamma(\mathbf{k}_1), \tag{4.24}$$

where the polarization index is suppressed. For compactness, we relabel the independent incoming and outgoing momenta as

$$\mathbf{k}_1 \equiv \mathbf{p}, \qquad \mathbf{k}_1' \equiv \mathbf{k}'. \tag{4.25}$$

With these definitions, the transition amplitude becomes

$$\begin{aligned}
&\langle f|S^{(2)}(\infty,-\infty)|i\rangle \\
&= -\int_{-\Delta t/2}^{\Delta t/2} \mathrm{d}t_2 \int_{t_2}^{\infty} \mathrm{d}t_1 \sum_{\mathbf{p}} e^{i(\epsilon_{\mathbf{p}}-\omega_{\mathbf{q}})t_2} e^{i(-\epsilon_{\mathbf{p}}+2\epsilon_{\mathbf{k}'})t_1} \gamma(\mathbf{p}) \\
&\times \Big[V(\mathbf{p}+\mathbf{k}') \langle \Phi_f^{N-2}| c_{-\mathbf{p}\sigma_1'}(t_1) c_{\mathbf{p}\sigma_2'}(t_2) |\Phi_i^N\rangle - V(\mathbf{p}-\mathbf{k}') \langle \Phi_f^{N-2}| c_{-\mathbf{p}\sigma_2'}(t_1) c_{\mathbf{p}\sigma_1'}(t_2) |\Phi_i^N\rangle \Big],
\end{aligned} \tag{4.26}$$

where we have used that $\epsilon_{\mathbf{k}} = \epsilon_{-\mathbf{k}}$.

We now form the transition probability by taking the modulus squared of the transition amplitude. To keep the resulting expression compact, we introduce the following shorthand notation:

$$\mathcal{K} \equiv \langle \Phi_f^{N-2}| c_{-\mathbf{p}\sigma_1'}(t_1) c_{\mathbf{p}\sigma_2'}(t_2) |\Phi_i^N\rangle, \quad \mathcal{K}^\dagger \equiv \langle \Phi_i^N| c^\dagger_{\mathbf{p}'\sigma_2'}(t_2') c^\dagger_{-\mathbf{p}'\sigma_1'}(t_1') |\Phi_f^{N-2}\rangle, \tag{4.27}$$

$$\mathcal{R} \equiv \langle \Phi_f^{N-2}| c_{-\mathbf{p}\sigma_2'}(t_1) c_{\mathbf{p}\sigma_1'}(t_2) |\Phi_i^N\rangle, \quad \mathcal{R}^\dagger \equiv \langle \Phi_i^N| c^\dagger_{\mathbf{p}'\sigma_1'}(t_2') c^\dagger_{-\mathbf{p}'\sigma_2'}(t_1') |\Phi_f^{N-2}\rangle. \tag{4.28}$$

For compactness, we define the phase factor

$$\mathcal{A} \equiv \mathcal{A}(\mathbf{p}, \mathbf{k}', \mathbf{q}, t_1, t_2) = e^{i(\epsilon_{\mathbf{p}}-\omega_{\mathbf{q}})t_2} e^{i(-\epsilon_{\mathbf{p}}+2\epsilon_{\mathbf{k}'})t_1}. \tag{4.29}$$

The modulus square of the transition amplitude is then

$$\begin{aligned}
&|\langle f|S^{(2)}(\infty,-\infty)|i\rangle|^2 \\
&\quad = \int_{-\Delta t/2}^{\Delta t/2} \mathrm{d}t_2 \int_{t_2}^{\infty} \mathrm{d}t_1 \int_{-\Delta t'/2}^{\Delta t'/2} \mathrm{d}t_2' \int_{t_2'}^{\infty} \mathrm{d}t_1' \sum_{\mathbf{p},\mathbf{p}'} \mathcal{A}\mathcal{A}^\dagger \gamma(\mathbf{p}) \gamma^\dagger(\mathbf{p}') \\
&\qquad \times \Big[V(\mathbf{p}+\mathbf{k}') V(\mathbf{p}'+\mathbf{k}') \mathcal{K}^\dagger \mathcal{K} + V(\mathbf{p}-\mathbf{k}') V(\mathbf{p}'-\mathbf{k}') \mathcal{R}^\dagger \mathcal{R} \\
&\qquad\quad - V(\mathbf{p}+\mathbf{k}') V(\mathbf{p}'-\mathbf{k}') \mathcal{R}^\dagger \mathcal{K} - V(\mathbf{p}-\mathbf{k}') V(\mathbf{p}'+\mathbf{k}') \mathcal{K}^\dagger \mathcal{R} \Big].
\end{aligned} \tag{4.30}$$

After summing over the unobserved final many-body states and thermally averaging over the initial states, the sample part of the squared transition amplitude can be organized into normal and anomalous equilibrium correlation functions $F^>$ and

$G^<$. These Green's functions are defined with respect to the same thermal average over the initial sample-state ensemble. The first is the greater anomalous Green's function, defined as

$$F^>(\mathbf{p}, t_1, t_2) = i\langle\langle c_{-\mathbf{p}\sigma_1'}(t_1) c_{\mathbf{p}\sigma_2'}(t_2)\rangle\rangle, \tag{4.31}$$

$$F^{\dagger>}(\mathbf{p}, t_1, t_2) = i\langle\langle c^\dagger_{\mathbf{p}\sigma_2'}(t_1) c^\dagger_{-\mathbf{p}\sigma_1'}(t_2)\rangle\rangle, \tag{4.32}$$

and the latter is the lesser Green's function defined in Eq. (2.62). To illustrate how the sample-state sums are rewritten in terms of Green's functions, we show one representative contraction explicitly. The corresponding algebra for all four terms is collected in Appendix B. Consider, for example, the contribution

$$\frac{1}{Z}\sum_{i,f} e^{-\beta E_i} \mathcal{K}^\dagger \mathcal{K} = \langle\langle c^\dagger_{\mathbf{p}'\sigma_2'}(t_2') c^\dagger_{-\mathbf{p}'\sigma_1'}(t_1') c_{-\mathbf{p}\sigma_1'}(t_1) c_{\mathbf{p}\sigma_2'}(t_2)\rangle\rangle. \tag{4.33}$$

Using Wick's theorem described in Sec. 2.2, this becomes

$$\begin{aligned}\frac{1}{Z}\sum_{i,f} e^{-\beta E_i} \mathcal{K}^\dagger \mathcal{K} \approx{}& \langle\langle c^\dagger_{\mathbf{p}'\sigma_2'}(t_2') c^\dagger_{-\mathbf{p}'\sigma_1'}(t_1')\rangle\rangle \langle\langle c_{-\mathbf{p}\sigma_1'}(t_1) c_{\mathbf{p}\sigma_2'}(t_2)\rangle\rangle \\ &- \langle\langle c^\dagger_{\mathbf{p}'\sigma_2'}(t_2') c_{-\mathbf{p}\sigma_1'}(t_1)\rangle\rangle \langle\langle c^\dagger_{-\mathbf{p}'\sigma_1'}(t_1') c_{\mathbf{p}\sigma_2'}(t_2)\rangle\rangle \\ &+ \langle\langle c^\dagger_{\mathbf{p}'\sigma_2'}(t_2') c_{\mathbf{p}\sigma_2'}(t_2)\rangle\rangle \langle\langle c^\dagger_{-\mathbf{p}'\sigma_1'}(t_1') c_{-\mathbf{p}\sigma_1'}(t_1)\rangle\rangle.\end{aligned} \tag{4.34}$$

The first term corresponds to greater anomalous Green's functions, and with the symmetries described in Eq. (4.1), it can be written as $F^{\dagger>}F^>$. This represents the emission of two electrons from the same Cooper pair, while the remaining terms are lesser Green's functions and correspond to the emission of two electrons from different Cooper pairs. For the superconducting state considered here, the normal Green's function is diagonal in spin. We therefore write

$$\begin{aligned}\frac{1}{Z}\sum_{i,f} e^{-\beta E_i} \mathcal{K}^\dagger \mathcal{K} \approx{}& F^{\dagger>}(\mathbf{p}', t_1' - t_2') F^>(\mathbf{p}, t_1 - t_2) \\ &+ \delta_{\mathbf{p},-\mathbf{p}'}\delta_{\sigma_1'\sigma_2'} G^<(\mathbf{p}, t_1 - t_2') G^<(-\mathbf{p}, t_2 - t_1') \\ &- \delta_{\mathbf{p}\mathbf{p}'} G^<(\mathbf{p}, t_2 - t_2') G^<(-\mathbf{p}, t_1 - t_1'),\end{aligned} \tag{4.35}$$

with

$$G^<(\mathbf{p}, t - t') = i\langle\langle c^\dagger_{\mathbf{k}\sigma}(t') c_{\mathbf{k}\sigma}(t)\rangle\rangle. \tag{4.36}$$

Each of the four products $\mathcal{K}^\dagger\mathcal{K}$, $\mathcal{R}^\dagger\mathcal{R}$, $\mathcal{R}^\dagger\mathcal{K}$, and $\mathcal{K}^\dagger\mathcal{R}$ contains one anomalous term proportional to the greater anomalous Green's-function pair $F^{\dagger>}F^>$. After applying the superconducting symmetry relations, the relative sign of these anomalous terms depend on the frequency symmetry of the pair amplitude. For the odd-frequency state considered here, defined by Eq. (4.1), all four anomalous terms acquire the same relative sign. For comparison, an even-frequency single-band spin-singlet state with even-parity pairing has the symmetry structure

$$S = -1, \qquad P^* = +1, \qquad O = +1, \qquad T^* = +1. \tag{4.37}$$

Table 4.1: Relative sign of the anomalous terms proportional to $-F^{\dagger>}F^{>}$ in the four contributions to the squared transition amplitude. The signs are shown after applying the superconducting symmetry relations for the odd-frequency state in Eq. (4.1) and for the even-frequency comparison state in Eq. (4.37).

Contribution	Odd-frequency state	Even-frequency state
$\mathcal{K}^\dagger\mathcal{K}$	$+$	$+$
$\mathcal{R}^\dagger\mathcal{R}$	$+$	$+$
$\mathcal{R}^\dagger\mathcal{K}$	$+$	$-$
$\mathcal{K}^\dagger\mathcal{R}$	$+$	$-$

This includes both *s*-wave and *d*-wave singlet states, since both are even under inversion of the relative momentum. In that case, two of the anomalous terms acquire the opposite relative sign. The resulting sign structure is summarized in Tab. 4.1; the explicit contractions are given in Appendix B.

In the following, all expressions are evaluated within the Wick-factorization approximation described in Sec. 2.2. Within this approximation, we decompose the counting rate as

$$P^{(2)} = P^{(2)}_{\text{anom}} + P^{(2)}_{\text{norm}}. \tag{4.38}$$

4.2.1 The Anomalous Contribution to the Counting Rate

We first consider the part of the counting rate containing anomalous Green's functions. After the sample-state sums have been evaluated, this contribution takes the form

$$\begin{aligned} P^{(2)}_{\text{anom}} = \frac{1}{\Delta t}\int_{-\Delta t/2}^{\Delta t/2}\mathrm{d}t_2\int_{t_2}^{\infty}\mathrm{d}t_1\int_{-\Delta t'/2}^{\Delta t'/2}\mathrm{d}t_2'\int_{t_2'}^{\infty}\mathrm{d}t_1'\sum_{\mathbf{p},\mathbf{p}'}\mathcal{A}\mathcal{A}^\dagger\gamma(\mathbf{p})\gamma^\dagger(\mathbf{p}') \\ \times\Big[V(\mathbf{p}+\mathbf{k}')-V(\mathbf{p}-\mathbf{k}')\Big]\Big[V(\mathbf{p}'+\mathbf{k}')-V(\mathbf{p}'-\mathbf{k}')\Big] \\ \times\Big[-F^{\dagger>}(\mathbf{p}',t_2'-t_1')\Big]F^{>}(\mathbf{p},t_1-t_2). \end{aligned} \tag{4.39}$$

From the definitions of the greater anomalous Green's functions in Eqs. (4.31) and (4.32), it follows that

$$\Big[F^{>}(\mathbf{p},t_1-t_2)\Big]^\dagger = -F^{\dagger>}(\mathbf{p},t_2-t_1). \tag{4.40}$$

The anomalous contribution therefore has the form of an amplitude multiplied by its Hermitian conjugate. We can then rewrite it as

$$P^{(2)}_{\text{anom}} = \frac{1}{\Delta t}\left|\int_{-\Delta t/2}^{\Delta t/2}\mathrm{d}t_2\int_{t_2}^{\infty}\mathrm{d}t_1\sum_{\mathbf{p}}\mathcal{A}W_{\text{odd}}(\mathbf{p},\mathbf{k}')F^{>}(\mathbf{p},t_1-t_2)\right|^2, \tag{4.41}$$

where we have introduced the kernel

$$W_{\text{odd}}(\mathbf{p},\mathbf{k}') = \gamma(\mathbf{p})\Big[V(\mathbf{p}+\mathbf{k}')-V(\mathbf{p}-\mathbf{k}')\Big]. \tag{4.42}$$

The relative minus sign between the two terms follows from the odd-frequency sign structure summarized in Tab. 4.1. For an even-frequency state with the symmetry structure in Eq. (4.37), the same calculation would instead give

$$W_{\text{even}}(\mathbf{p},\mathbf{k}') = \gamma(\mathbf{p})\Big[V(\mathbf{p}+\mathbf{k}') + V(\mathbf{p}-\mathbf{k}')\Big]. \tag{4.43}$$

Since $V(\mathbf{q})$ is even in momentum, the odd-frequency kernel contains an antisymmetric combination $V(\mathbf{p}+\mathbf{k}') - V(\mathbf{p}-\mathbf{k}')$. In particular, if $\gamma(\mathbf{p})$ is replaced by a momentum-independent constant, an approximation used in Ref. [10], the anomalous odd-frequency contribution vanishes after summing over $\mathbf{p}$. Retaining the momentum dependence of $\gamma(\mathbf{p})$ is therefore essential for obtaining a finite anomalous DPE signal in this case.

To further simplify Eq. (4.41), we introduce the relative time

$$s = t_1 - t_2. \tag{4.44}$$

The anomalous contribution to the counting rate can then be written as

$$P^{(2)}_{\text{anom}} = \frac{1}{\Delta t}\left|\int_{-\Delta t/2}^{\Delta t/2} \mathrm{d}t_2\, e^{i(2\epsilon_{\mathbf{k}'}-\omega_{\mathbf{q}})t_2}\right|^2 \times \left|\int_0^\infty \mathrm{d}s \sum_{\mathbf{p}} e^{i(2\epsilon_{\mathbf{k}'}-\epsilon_{\mathbf{p}})s} W_{\text{odd}}(\mathbf{p},\mathbf{k}') F^{>}(\mathbf{p},s)\right|^2. \tag{4.45}$$

Here, the change of variables separates the dependence on the absolute time t_2 from the dependence on the relative time s. The first factor gives

$$\frac{1}{\Delta t}\left|\int_{-\Delta t/2}^{\Delta t/2} \mathrm{d}t_2\, e^{i(2\epsilon_{\mathbf{k}'}-\omega_{\mathbf{q}})t_2}\right|^2 = 2\frac{\sin^2\left[(2\epsilon_{\mathbf{k}'}-\omega_{\mathbf{q}})\Delta t/2\right]}{(2\epsilon_{\mathbf{k}'}-\omega_{\mathbf{q}})^2\Delta t/2}. \tag{4.46}$$

Using Eq. (2.49), this becomes, in the long-time limit,

$$2\pi\delta(2\epsilon_{\mathbf{k}'}-\omega_{\mathbf{q}}). \tag{4.47}$$

To simplify the second factor, we Fourier transform the anomalous correlation

$$F^{>}(\mathbf{p},s) = \frac{1}{2\pi}\int_{-\infty}^{\infty} \mathrm{d}\omega\, e^{-i\omega s} F^{>}(\mathbf{p},\omega). \tag{4.48}$$

Using the energy-conservation condition imposed by the delta function, $2\epsilon_{\mathbf{k}'}-\omega_{\mathbf{q}}$, the anomalous contribution becomes

$$P^{(2)}_{\text{anom}} = 2\pi\delta(\omega_{\mathbf{q}}-2\epsilon_{\mathbf{k}'})\left|\frac{1}{2\pi}\sum_{\mathbf{p}} W_{\text{odd}}(\mathbf{p},\mathbf{k}')\int_0^\infty \mathrm{d}s\, e^{i(\omega_{\mathbf{q}}-\epsilon_{\mathbf{p}})s}\int_{-\infty}^{\infty}\mathrm{d}\omega\, e^{-i\omega s}F^{>}(\mathbf{p},\omega)\right|^2. \tag{4.49}$$

Here, the delta function enforces energy conservation between the absorbed photon and the two detected photoelectrons, and its constraint has been used in the remaining phase factor. We have also used $\delta(x) = \delta(-x)$ to write the argument in this form.

4.2.2 The Normal Contribution to the Counting Rate

To keep the normal contribution compact, we define

$$\mathbf{p}_\pm = \mathbf{p} \pm \mathbf{k}', \qquad \mathbf{p}'_\pm = \mathbf{p}' \pm \mathbf{k}', \qquad K(\mathbf{p}_\pm, \mathbf{p}'_\pm) = V(\mathbf{p}_\pm)V(\mathbf{p}'_\pm). \tag{4.50}$$

The signs in the two arguments are independent; e.g.,

$$K(\mathbf{p}_+, \mathbf{p}'_-) = V(\mathbf{p} + \mathbf{k}')V(\mathbf{p}' - \mathbf{k}'). \tag{4.51}$$

The normal contribution to the counting rate can then be written as

$$\begin{aligned} P^{(2)}_{\text{norm}} = \frac{1}{\Delta t}\int_{-\Delta t/2}^{\Delta t/2} \mathrm{d}t_2 \int_{t_2}^{\infty} \mathrm{d}t_1 \int_{-\Delta t'/2}^{\Delta t'/2} \mathrm{d}t'_2 \int_{t'_2}^{\infty} \mathrm{d}t'_1 \sum_{\mathbf{p},\mathbf{p}'} \mathcal{A}\mathcal{A}^\dagger \gamma(\mathbf{p})\gamma^\dagger(\mathbf{p}') \\ \times \Big\{ K(\mathbf{p}_+, \mathbf{p}'_+)\Big[\delta_{\mathbf{p},-\mathbf{p}'}\delta_{\sigma'_1\sigma'_2} G^<(\mathbf{p}, t_1 - t'_2)G^<(-\mathbf{p}, t_2 - t'_1) \\ - \delta_{\mathbf{p}\mathbf{p}'} G^<_{\sigma'_2}(\mathbf{p}, t_2 - t'_2)G^<_{\sigma'_1}(-\mathbf{p}, t_1 - t'_1).\Big] \\ + K(\mathbf{p}_-, \mathbf{p}'_-)\Big[\delta_{\mathbf{p},-\mathbf{p}'}\delta_{\sigma'_1\sigma'_2} G^<(\mathbf{p}, t_1 - t'_2)G^<(-\mathbf{p}, t_2 - t'_1) \\ - \delta_{\mathbf{p}\mathbf{p}'} G^<_{\sigma'_1}(\mathbf{p}, t_2 - t'_2)G^<_{\sigma'_2}(-\mathbf{p}, t_1 - t'_1).\Big] \\ - K(\mathbf{p}_+, \mathbf{p}'_-)\Big[\delta_{\mathbf{p},-\mathbf{p}'} G^<_{\sigma'_1}(\mathbf{p}, t_1 - t'_2)G^<_{\sigma'_2}(-\mathbf{p}, t_2 - t'_1) \\ - \delta_{\mathbf{p}\mathbf{p}'}\delta_{\sigma'_1\sigma'_2} G^<(\mathbf{p}, t_2 - t'_2)G^<(-\mathbf{p}, t_1 - t'_1).\Big] \\ - K(\mathbf{p}_-, \mathbf{p}'_+)\Big[\delta_{\mathbf{p},-\mathbf{p}'} G^<_{\sigma'_2}(\mathbf{p}, t_1 - t'_2)G^<_{\sigma'_1}(-\mathbf{p}, t_2 - t'_1) \\ - \delta_{\mathbf{p}\mathbf{p}'}\delta_{\sigma'_1\sigma'_2} G^<(\mathbf{p}, t_2 - t'_2)G^<(-\mathbf{p}, t_1 - t'_1).\Big]\Big\}, \end{aligned} \tag{4.52}$$

where we have suppressed the spin label in the terms proportional to $\delta_{\sigma'_1\sigma'_2}$, since the detected spins are constrained to be equal. The terms that are not proportional to $\delta_{\sigma'_1\sigma'_2}$, where already diagonal in spin. Here, we have kept the spin label in order to distinguish between the σ'_1, and σ'_2 channels.

The Kronecker deltas collapse the $\mathbf{p}'$-sum into two channels, $\mathbf{p}' = -\mathbf{p}$ and $\mathbf{p}' = \mathbf{p}$. Since $\mathcal{A}$ depends on momentum only through the even dispersion $\epsilon_{\mathbf{p}} = \epsilon_{-\mathbf{p}}$, both channels give the same factor $\mathcal{A}^\dagger$. The normal contribution can therefore be written compactly as

$$\begin{aligned} P^{(2)}_{\text{norm}} = \frac{1}{\Delta t}\int_{-\Delta t/2}^{\Delta t/2} \mathrm{d}t_2 \int_{t_2}^{\infty} \mathrm{d}t_1 \int_{-\Delta t'/2}^{\Delta t'/2} \mathrm{d}t'_2 \int_{t'_2}^{\infty} \mathrm{d}t'_1 \\ \times \sum_{\mathbf{p}} \mathcal{A}\mathcal{A}^\dagger \gamma(\mathbf{p})\Big[\gamma^\dagger(-\mathbf{p})\mathcal{N}_- + \gamma^\dagger(\mathbf{p})\mathcal{N}_+\Big]. \end{aligned} \tag{4.53}$$

Here, $\mathcal{N}_-$ collects the terms arising from the $\mathbf{p}' = -\mathbf{p}$ channel, while $\mathcal{N}_+$ collects the terms arising from the $\mathbf{p}' = \mathbf{p}$ channel. They are given by

$$\begin{aligned} \mathcal{N}_- = \delta_{\sigma'_1\sigma'_2}\Big[K(\mathbf{p}_+, -\mathbf{p}_-) + K(\mathbf{p}_-, -\mathbf{p}_+)\Big]G^<(\mathbf{p}, t_1 - t'_2)G^<(-\mathbf{p}, t_2 - t'_1) \\ - K(\mathbf{p}_+, -\mathbf{p}_+)G^<_{\sigma'_1}(\mathbf{p}, t_1 - t'_2)G^<_{\sigma'_2}(-\mathbf{p}, t_2 - t'_1) \\ - K(\mathbf{p}_-, -\mathbf{p}_-)G^<_{\sigma'_2}(\mathbf{p}, t_1 - t'_2)G^<_{\sigma'_1}(-\mathbf{p}, t_2 - t'_1), \end{aligned} \tag{4.54}$$

and

$$\begin{aligned}\mathcal{N}_+ = \delta_{\sigma_1'\sigma_2'}\Big[K(\mathbf{p}_+,\mathbf{p}_-) + K(\mathbf{p}_-,\mathbf{p}_+)\Big]G^<(\mathbf{p},t_2-t_2')G^<(-\mathbf{p},t_1-t_1') \\ - K(\mathbf{p}_+,\mathbf{p}_+)G^<_{\sigma_2'}(\mathbf{p},t_2-t_2')G^<_{\sigma_1'}(-\mathbf{p},t_1-t_1') \\ - K(\mathbf{p}_-,\mathbf{p}_-)G^<_{\sigma_1'}(\mathbf{p},t_2-t_2')G^<_{\sigma_2'}(-\mathbf{p},t_1-t_1').\end{aligned} \tag{4.55}$$

In Eq. (4.54), the notation $-\mathbf{p}_\pm$ should be understood as the corresponding shifted momentum after imposing $\mathbf{p}' = -\mathbf{p}$. Explicitly,

$$-\mathbf{p}_+ = -\mathbf{p} + \mathbf{k}', \qquad -\mathbf{p}_- = -\mathbf{p} - \mathbf{k}'. \tag{4.56}$$

In contrast to the anomalous contribution, the normal contribution does not acquire additional sign changes from the pairing symmetries. The superconducting-state dependence instead enters through the normal Green's function.

For practical evaluations, it is useful to express the normal contribution in frequency space, since explicit forms of the lesser Green's functions are typically available in this representation. We Fourier transform each lesser Green's function according to

$$G^<_\sigma(\mathbf{p},t-t') = \frac{1}{2\pi}\int_{-\infty}^{\infty}\mathrm{d}\omega\, e^{-i\omega(t-t')}G^<_\sigma(\mathbf{p},\omega). \tag{4.57}$$

After inserting this into Eq. (4.53), the time integrations can be used to eliminate two of the frequency variables. The remaining result can therefore be written in terms of two independent frequencies, ω_1 and ω_2. The intermediate steps are collected in Appendix B.3, while the final expression is

$$P^{(2)}_{\mathrm{norm}} = \frac{1}{2\pi}\int_{-\infty}^{\infty}\mathrm{d}\omega_1\int_{-\infty}^{\infty}\mathrm{d}\omega_2\sum_{\mathbf{p}}\gamma(\mathbf{p})\Big[\gamma^\dagger(-\mathbf{p})\mathcal{D}_1\mathcal{C}_1 + \gamma^\dagger(\mathbf{p})\mathcal{D}_2\mathcal{C}_2\Big]. \tag{4.58}$$

The dependence of the compact factors $\omega_{1,2}$, $\mathbf{p}$, $\mathbf{k}'$, and $\mathbf{q}$ is left implicit in Eq. (4.58). The factors $\mathcal{C}_{1,2}$ contain the frequency-domain products of the lesser Green's functions and are given by

$$\begin{aligned}\mathcal{C}_1 &\equiv \mathcal{C}_1(\omega_1;\mathbf{p},\mathbf{k}',\mathbf{q}) \\ &= \delta_{\sigma_1'\sigma_2'}\Big[K(\mathbf{p}_+,-\mathbf{p}_-) + K(\mathbf{p}_-,-\mathbf{p}_+)\Big]G^<(\mathbf{p},\omega_1)G^<(-\mathbf{p},2\epsilon_{\mathbf{k}'}-\omega_{\mathbf{q}}-\omega_1) \\ &\quad - K(\mathbf{p}_+,-\mathbf{p}_+)G^<_{\sigma_1'}(\mathbf{p},\omega_1)G^<_{\sigma_2'}(-\mathbf{p},2\epsilon_{\mathbf{k}'}-\omega_{\mathbf{q}}-\omega_1) \\ &\quad - K(\mathbf{p}_-,-\mathbf{p}_-)G^<_{\sigma_2'}(\mathbf{p},\omega_1)G^<_{\sigma_1'}(-\mathbf{p},2\epsilon_{\mathbf{k}'}-\omega_{\mathbf{q}}-\omega_1),\end{aligned} \tag{4.59}$$

and

$$\begin{aligned}\mathcal{C}_2 &\equiv \mathcal{C}_2(\omega_2;\mathbf{p},\mathbf{k}',\mathbf{q}) \\ &= \delta_{\sigma_1'\sigma_2'}\Big[K(\mathbf{p}_+,\mathbf{p}_-) + K(\mathbf{p}_-,\mathbf{p}_+)\Big]G^<(\mathbf{p},\omega_2)G^<(-\mathbf{p},2\epsilon_{\mathbf{k}'}-\omega_{\mathbf{q}}-\omega_2) \\ &\quad - K(\mathbf{p}_+,\mathbf{p}_+)G^<_{\sigma_2'}(\mathbf{p},\omega_2)G^<_{\sigma_1'}(-\mathbf{p},2\epsilon_{\mathbf{k}'}-\omega_{\mathbf{q}}-\omega_2) \\ &\quad - K(\mathbf{p}_-,\mathbf{p}_-)G^<_{\sigma_1'}(\mathbf{p},\omega_2)G^<_{\sigma_2'}(-\mathbf{p},2\epsilon_{\mathbf{k}'}-\omega_{\mathbf{q}}-\omega_2).\end{aligned} \tag{4.60}$$

The remaining factors $\mathcal{D}_{1,2}$ arise from the time integrations and are defined as

$$\mathcal{D}_1 \equiv \mathcal{D}_1(\omega_1;\mathbf{p},\mathbf{k}',\mathbf{q}) = \frac{1}{-\epsilon_{\mathbf{p}}+2\epsilon_{\mathbf{k}'}-\omega_1+i\eta}\frac{1}{-\epsilon_{\mathbf{p}}+\omega_{\mathbf{q}}+\omega_1-i\eta}, \tag{4.61}$$

and

$$\mathcal{D}_2 \equiv \mathcal{D}_2(\omega_2; \mathbf{p}, \mathbf{k}', \mathbf{q}) = \left| \frac{1}{\omega_{\mathbf{q}} - \epsilon_{\mathbf{p}} + \omega_2 + i\eta} \right|^2 . \tag{4.62}$$

Equation (4.58) gives the normal contribution to the second-order DPE counting rate in a frequency-domain form suitable for inserting explicit expressions for the lesser Green's function. Since the anomalous contribution was obtained in Eq. (4.49), this completes the decomposition of the counting rate into its anomalous and normal parts.

4.2.3 Differences Between Even- and Odd-Frequency Contributions

We have found an expression for the anomalous contribution to the counting rate in Eq. (4.49) in terms of anomalous Green's functions, and an expression for the normal contribution in Eq. (4.58) in terms of normal Green's functions. In these expressions, the temperature dependence is encoded directly in the Green's functions. Both expressions can be generalized straightforwardly to odd- and even-frequency superconductors. One difference between the corresponding counting rates is therefore encoded in the explicit form of the Green's functions. These functions can be difficult to determine, especially for odd-frequency superconductors, where the pairing gap, or more generally the order parameter, must be treated differently from the familiar BCS case.

Apart from the explicit form of the Green's functions, a further difference between even- and odd-frequency superconductors appears in the anomalous contribution to the counting rate. This difference is encoded in the kernel W, given in Eqs. (4.42) and (4.43). In the odd-frequency case, the kernel contains an antisymmetric combination of the effective screened Coulomb potential $V(\mathbf{q})$, whereas in the even-frequency case the corresponding combination is symmetric. Consequently, the momentum dependence of the effective electron–photon coupling matrix element $\gamma(\mathbf{p})$ is crucial for obtaining a nonzero anomalous contribution in the odd-frequency case. In particular, $\gamma(\mathbf{p})$ cannot in general be approximated as momentum independent, in contrast to the even-frequency case.

As a separate observation, the frequency symmetry of the anomalous Green's function can also be reflected in the corresponding anomalous spectral function. This statement, however, relies on an additional assumption and is not needed for the preceding discussion of the counting rate. We define the anomalous spectral function as

$$A_F(\omega) = -\frac{1}{\pi} \operatorname{Im} F^R(\omega). \tag{4.63}$$

The retarded and advanced Green's functions are related by

$$G^R(\omega) = \left[G^A(\omega) \right]^*, \tag{4.64}$$

for real frequencies [17, pp. 119–120]. If we assume, for the purpose of the present spectral-function argument, that the anomalous Green's function satisfies the corresponding relation

$$F^R(\omega) = \left[F^A(\omega) \right]^*, \tag{4.65}$$

where $*$ denotes ordinary complex conjugation, one finds that the spectral function has the opposite frequency symmetry to the Matsubara anomalous Green's function $\mathcal{F}(i\omega_n)$. Thus, under this assumption, an even-frequency $\mathcal{F}(i\omega_n)$ gives an anti-symmetric spectral function, whereas an odd-frequency $\mathcal{F}(i\omega_n)$ gives a symmetric spectral function. This condition is satisfied, for example, in the conventional BCS case when the superconducting phase is chosen such that the gap parameter is real. In this case, the anomalous Green's functions obey $\mathcal{F} = \mathcal{F}^\dagger$, as shown explicitly in Eq. (3.24). More generally, however, the anomalous Green's function may have a more complicated internal structure, so the opposite-symmetry relation should not be regarded as universal. The detailed derivation is given in Appendix C.

4.3 Counting Rate in the BCS Limit

The Green's function formulation derived in the previous section expresses the counting rate in terms of the normal and anomalous Green's functions of the superconducting state. As a consistency check, we now evaluate this expression using the BCS Green's functions derived in Sec. 3.1. These Green's functions were written for a real, even-frequency gap function $\Delta(\mathbf{p})$, and therefore have the same mean-field structure as the Green's functions of a spin-singlet d-wave superconductor, with the difference contained in the explicit momentum dependence of the gap. This allows us to compare the present Green's-function approach with the result obtained in Ref. [10] for a d-wave even-frequency superconductor using a Bogoliubov transformation. To make this comparison, we work in the opposite-spin channel,

$$\sigma_1' = -\sigma_2'. \tag{4.66}$$

In this channel, the terms proportional to $\delta_{\sigma_1'\sigma_2'}$ vanish. For the BCS Green's functions derived in Sec. 3.1, the normal Green's function is diagonal in spin space. For equal spin indices, the two diagonal components are equal,

$$\mathcal{G}_\uparrow = \mathcal{G}_\downarrow. \tag{4.67}$$

Thus, whenever a normal Green's function appears with equal spin indices, the explicit spin label can be suppressed. Furthermore, to match the comparison with Ref. [10], we approximate the effective electron–photon matrix element as momentum independent, $\gamma(\mathbf{p}) \to \gamma_0$.

Equations (4.49) and (4.58) are expressed in terms of greater and lesser Green's functions, whereas the BCS Green's functions in Eqs. (3.23) and (3.24) were derived in the Matsubara formalism. Before inserting the explicit BCS expressions into the counting rate, we therefore need to relate the Matsubara Green's functions to the corresponding real-frequency greater and lesser Green's functions. The retarded and advanced Green's functions are obtained from the Matsubara Green's function through the analytic continuations given in Eqs. (2.73) and (2.74), respectively. In thermal equilibrium, the greater and lesser components can then be related to the spectral function, or equivalently to the imaginary part of the retarded Green's

function, through

$$G^{>}(\omega) = 2i\Big[1 - f(\omega)\Big]\,\mathrm{Im}\,G^{R}(\omega), \tag{4.68}$$

$$G^{<}(\omega) = -2i f(\omega)\,\mathrm{Im}\,G^{R}(\omega), \tag{4.69}$$

where $f(\omega)$ is the Fermi–Dirac distribution. These equilibrium relations are a form of the fluctuation-dissipation theorem [29], [34]. In the following, we will assume that the corresponding equilibrium relations can also be applied to the anomalous Green's functions.

Using the relations above, the greater anomalous Green's function becomes

$$F^{>}(\mathbf{p},\omega) = 2\pi i\frac{\Delta(\mathbf{p})}{2E_{\mathbf{p}}}\Big\{\Big[1 - f(E_{\mathbf{p}})\Big]\delta(\omega - E_{\mathbf{p}}) - f(E_{\mathbf{p}})\delta(\omega + E_{\mathbf{p}})\Big\}, \tag{4.70}$$

where $E_{\mathbf{p}} = \sqrt{\xi_{\mathbf{p}}^2 + \Delta^2(\mathbf{p})}$ is the quasiparticle excitation energy of the superconductor, as introduced in Eq. (3.25). The detailed derivation is given in Appendix D.1. To obtain the normal lesser Green's function, we first rewrite the BCS Green's function in terms of the coherence factors [17, p. 640]

$$u_{\mathbf{p}}^2 = \frac{1}{2}\left(1 + \frac{\xi_{\mathbf{p}}}{E_{\mathbf{p}}}\right), \tag{4.71}$$

$$v_{\mathbf{p}}^2 = \frac{1}{2}\left(1 - \frac{\xi_{\mathbf{p}}}{E_{\mathbf{p}}}\right), \tag{4.72}$$

$$u_{\mathbf{p}}v_{\mathbf{p}} = \frac{1}{2}\left(1 - \frac{\xi_{\mathbf{p}}^2}{E_{\mathbf{p}}^2}\right)^{1/2} = \frac{\Delta(\mathbf{p})}{2E_{\mathbf{p}}}, \tag{4.73}$$

$$u_{\mathbf{p}}^2 + v_{\mathbf{p}}^2 = 1. \tag{4.74}$$

With these definitions, the Matsubara Green's function in Eq. (3.23) can be written as

$$\mathcal{G}(\mathbf{p}, i\omega_n) = \frac{u_{\mathbf{p}}^2}{i\omega_n - E_{\mathbf{p}}} + \frac{v_{\mathbf{p}}^2}{i\omega_n + E_{\mathbf{p}}}. \tag{4.75}$$

Applying the equilibrium relation for $G^{<}$ then gives

$$G^{<}(\mathbf{p},\omega) = 2\pi i f(\omega)\Big[u_{\mathbf{p}}^2\delta(\omega - E_{\mathbf{p}}) + v_{\mathbf{p}}^2\delta(\omega + E_{\mathbf{p}})\Big], \tag{4.76}$$

with the details given in Appendix D.2.

With the explicit expressions for the greater anomalous and normal lesser Green's functions at hand, we can now evaluate the anomalous and normal contributions to the counting rate. The derivations are rather lengthy and are therefore given in Appendix D.3 for the anomalous contribution and in Appendix D.4 for the normal contribution. The anomalous contribution is found to be

$$\begin{aligned} P_{\mathrm{anom}}^{(2)} = 8\pi\delta(\omega_{\mathbf{q}} - 2\epsilon_{\mathbf{k}'})\Bigg|\gamma_0\sum_{\mathbf{p}} V(\mathbf{k}' - \mathbf{p})\frac{\Delta(\mathbf{p})}{2E_{\mathbf{p}}} \\ \times\left[\frac{f(E_{\mathbf{p}})}{\omega_{\mathbf{q}} + E_{\mathbf{p}} - \epsilon_{\mathbf{p}} + i\eta} - \frac{1 - f(E_{\mathbf{p}})}{\omega_{\mathbf{q}} - E_{\mathbf{p}} - \epsilon_{\mathbf{p}} + i\eta}\right]\Bigg|^2. \end{aligned} \tag{4.77}$$

This contribution is supported at $\omega_{\mathbf{q}} = 2\epsilon_{\mathbf{k}'}$, as expected for the superconducting zero-excess-energy channel. A detailed comparison with Ref. [10] will be made after the normal contribution has also been evaluated.

The normal contribution can be split into two parts

$$P^{(2)}_{\mathrm{norm}} = P^{(2)}_{\mathrm{norm},1} + P^{(2)}_{\mathrm{norm},2}. \tag{4.78}$$

The first term is given by

$$\begin{aligned} P^{(2)}_{\mathrm{norm},1} = 8\pi\gamma_0^2 \sum_{\mathbf{p}} \Bigg[& \delta(\omega_{\mathbf{q}} - 2\epsilon_{\mathbf{k}'} - 2E_{\mathbf{p}}) \left| \frac{V(\mathbf{k}' - \mathbf{p}) v_{\mathbf{p}}^2}{\omega_{\mathbf{q}} - \epsilon_{\mathbf{p}} - E_{\mathbf{p}} + i\eta} \right|^2 \Big[1 - f(E_{\mathbf{p}})\Big] \Big[1 - f(E_{\mathbf{p}})\Big] \\ & + \delta(\omega_{\mathbf{q}} - 2\epsilon_{\mathbf{k}'} + 2E_{\mathbf{p}}) \left| \frac{V(\mathbf{k}' - \mathbf{p}) u_{\mathbf{p}}^2}{\omega_{\mathbf{q}} - \epsilon_{\mathbf{p}} + E_{\mathbf{p}} + i\eta} \right|^2 f(E_{\mathbf{p}}) f(E_{\mathbf{p}}) \Bigg]. \end{aligned} \tag{4.79}$$

Thus, if we define the excess energy as $\Delta\omega = \omega_{\mathbf{q}} - 2\epsilon_{\mathbf{k}'}$, this contribution is supported at $\Delta\omega = \pm 2E_{\mathbf{p}}$. The positive-excess branch, $\Delta\omega = 2E_{\mathbf{p}}$, is weighted by $[1 - f(E_{\mathbf{p}})]^2$. Since $1 - f(E_{\mathbf{p}})$ is the probability that a fermionic quasiparticle state is unoccupied, this branch corresponds to the normal contribution in which the relevant quasiparticle states are initially empty. The negative-excess branch, $\Delta\omega = -2E_{\mathbf{p}}$, is weighted by $f(E_{\mathbf{p}})^2$ and therefore requires occupied quasiparticle states. The second term is given by

$$\begin{aligned} P^{(2)}_{\mathrm{norm},2} = 4\pi\gamma_0^2 \sum_{\mathbf{p}} \delta(\omega_{\mathbf{q}} - 2\epsilon_{\mathbf{k}'}) & \left| V(\mathbf{k}' - \mathbf{p}) \frac{\Delta(\mathbf{p})}{2E_{\mathbf{p}}} \right|^2 f(E_{\mathbf{p}}) \Big[1 - f(E_{\mathbf{p}})\Big] \\ \times & \left| \frac{1}{\omega_{\mathbf{q}} - \epsilon_{\mathbf{p}} + E_{\mathbf{p}} + i\eta} + \frac{1}{\omega_{\mathbf{q}} - \epsilon_{\mathbf{p}} - E_{\mathbf{p}} + i\eta} \right|^2. \end{aligned} \tag{4.80}$$

This is supported at $\omega_{\mathbf{q}} = 2\epsilon_{\mathbf{k}'}$ and is proportional to $f(E_{\mathbf{p}})[1 - f(E_{\mathbf{p}})]$. Although this contribution occurs at the same excess energy as the anomalous condensate contribution, it should not be interpreted as arising from the emission of two electrons from the same Cooper pair. That coherent pair contribution is encoded in the anomalous Green's functions. Instead, $P^{(2)}_{\mathrm{norm},2}$ originates from mixed particlelike and holelike poles of the normal Green's functions and represents a finite-temperature quasiparticle background.

We can now compare the result with the finite-temperature expressions in Ref. [10]. Since the anomalous contribution was obtained by applying Wick's theorem to the thermal four-operator average, it is written in terms of thermally averaged anomalous amplitudes. Its structure is therefore schematically of the form $P^{(2)}_{\mathrm{anom}} \sim |\langle\langle \mathcal{I} \rangle\rangle|^2$. Here, $\mathcal{I}$ is only a placeholder used to indicate the position of the thermal average. By contrast, the superconducting contribution $P^{(2)}_{\mathrm{SC}}$ in Eq. (A8) of Ref. [10] is written as a thermal average of the modulus squared matrix element, $P^{(2)}_{\mathrm{SC}} \sim \langle\langle |\mathcal{I}|^2 \rangle\rangle$. The same symbol $\mathcal{I}$ need not denote the same explicit expression in both cases. These two quantities are not equivalent at finite temperature, so $P^{(2)}_{\mathrm{anom}}$ should not be compared directly with $P^{(2)}_{\mathrm{SC}}$ alone. The mixed normal contribution $P^{(2)}_{\mathrm{norm},2}$ is also supported at $\omega_{\mathbf{q}} = 2\epsilon_{\mathbf{k}'}$ and must therefore be included in the zero-excess-energy

part of the comparison. Thus, the appropriate finite-temperature comparison to Eq. (A8) of Ref. [10] is with the combined contribution $P^{(2)}_{\mathrm{anom}} + P^{(2)}_{\mathrm{norm},2}$, while $P^{(2)}_{\mathrm{norm},1}$ corresponds to the two-Cooper-pair contribution $P^{(2)}_{\mathrm{2cp}}$ in Eq. (A12) of Ref. [10].

Taken together, this comparison shows that the Green's-function formulation reproduces the same organization into zero- and finite-excess-energy channels as the Bogoliubov approach in the BCS mean-field limit. This provides a consistency check of the Green's-function approach before applying it to pairing states where the explicit Green's functions, and in the odd-frequency case also the kernel structure, take a different form.

5

Conclusion

In this thesis, we have extended the theoretical description of Cooper pair spectroscopy to an odd-frequency superconducting state. More specifically, we considered a spin-triplet, even-parity, single-band odd-frequency pairing channel characterized by $S = +1$, $P^* = +1$, $O = +1$, and $T^* = -1$. The central aim was to determine how the double-photoelectron counting rate differs between even- and odd-frequency superconducting pairing.

To address this question, we formulated the DPE counting rate in terms of superconducting Green's functions. This provides a natural language for the problem, since the normal and anomalous Green's functions directly encode the single-particle and pair correlations of the superconducting state. In particular, the anomalous Green's function carries the symmetry of the pair amplitude, making it possible to analyze how spin, spatial, orbital and frequency symmetries enter the counting rate. The Green's-function formulation also provides an alternative to the Bogoliubov-transformation approach used in previous work, although the explicit analysis in this thesis was restricted to the BCS case and to the odd-frequency pairing channel specified above.

Starting from an expansion of the S-matrix, we derived the counting rate to second order in the interaction Hamiltonian, which is the lowest order giving a non-vanishing DPE contribution. The resulting expression separates into an anomalous part and a normal part. The anomalous contribution is expressed in terms of greater anomalous Green's functions and describes correlated emission associated with a single Cooper pair. The normal contribution is expressed in terms of lesser normal Green's functions and describes contributions arising from ordinary single-particle correlations.

The main result is that the odd-frequency character of the anomalous Green's function changes the momentum structure of the anomalous contribution. In the even-frequency case, the kernel contains a symmetric combination of screened Coulomb potentials. In the odd-frequency case considered here, the corresponding kernel instead contains an antisymmetric combination. Consequently, for a symmetric screened Coulomb interaction, a momentum-independent electron–photon matrix element gives a vanishing odd-frequency anomalous contribution. A finite anomalous signal therefore requires additional momentum dependence, for example through the electron–photon coupling. This provides a formal distinction between even- and odd-frequency superconducting correlations in the DPE counting rate.

As a consistency check, the Green's-function formulation was also evaluated in the BCS limit for a real, even-frequency gap function. This allowed the result to be compared with the Bogoliubov-transformation approach used in previous work on

double photoemission from conventional superconductors. In this limit, the anomalous contribution reproduces the expected zero-excess-energy structure associated with coherent pair emission, while the normal contribution separates into a two-Cooper-pair continuum and a finite-temperature quasiparticle background. This comparison provides a useful check on the formalism and clarifies the physical interpretation of the different terms in the counting rate: the anomalous contribution describes emission of electrons originating from the same Cooper pair, while the normal contribution contains both the emission of electrons from different Cooper pairs and a finite-temperature quasiparticle background.

A natural direction for future work would be to evaluate the counting rate explicitly for an odd-frequency superconducting state. This would require explicit expressions for both the anomalous and normal Green's functions associated with the odd-frequency pairing, and would allow the DPE signal to be studied for specific models or candidate materials. A complementary direction would be to make a more general comparison between the anomalous contributions for even- and odd-frequency pairing. This could be done by approximating the anomalous Green's function near zero relative time, giving a rough but material-independent comparison of how the different frequency symmetries enter the anomalous transition amplitude.

Bibliography

[1] A. Altland and B. D. Simons, *Condensed Matter Field Theory*, 2nd ed. Cambridge, UK: Cambridge University Press, 2010, pp. 265–300.

[2] J. Bardeen, L. N. Cooper, and J. R. Schrieffer, "Theory of superconductivity," *Physical review*, vol. 108, no. 5, p. 1175, 1957. DOI: 10.1103/PhysRev.108.1175.

[3] L. N. Cooper, "Bound electron pairs in a degenerate fermi gas," *Phys. Rev.*, vol. 104, pp. 1189–1190, 4 Nov. 1956. DOI: 10.1103/PhysRev.104.1189.

[4] J. Linder and A. V. Balatsky, "Odd-frequency superconductivity," *Rev. Mod. Phys.*, vol. 91, p. 045 005, 4 Dec. 2019. DOI: 10.1103/RevModPhys.91.045005.

[5] V. Berezinskii, "New model of the anisotropic phase of superfluid he3," *Jetp Lett*, vol. 20, no. 9, pp. 287–289, 1974.

[6] S. Hüfner, S. Schmidt, and F. Reinert, "Photoelectron spectroscopy—an overview," *Nuclear Instruments and Methods in Physics Research Section A: Accelerators, Spectrometers, Detectors and Associated Equipment*, vol. 547, no. 1, pp. 8–23, 2005, Proceedings of the Workshop on Hard X-ray Photoelectron Spectroscopy, ISSN: 0168-9002. DOI: https://doi.org/10.1016/j.nima.2005.05.008.

[7] J. A. Sobota, Y. He, and Z.-X. Shen, "Angle-resolved photoemission studies of quantum materials," *Rev. Mod. Phys.*, vol. 93, p. 025 006, 2 May 2021. DOI: 10.1103/RevModPhys.93.025006.

[8] A. Damascelli, Z. Hussain, and Z.-X. Shen, "Angle-resolved photoemission studies of the cuprate superconductors," *Rev. Mod. Phys.*, vol. 75, pp. 473–541, 2 Apr. 2003. DOI: 10.1103/RevModPhys.75.473.

[9] K. A. Kouzakov and J. Berakdar, "Photoinduced emission of cooper pairs from superconductors," *Phys. Rev. Lett.*, vol. 91, p. 257 007, 25 Dec. 2003. DOI: 10.1103/PhysRevLett.91.257007.

[10] F. Mahmood, T. Devereaux, P. Abbamonte, and D. K. Morr, "Distinguishing finite-momentum superconducting pairing states with two-electron photoemission spectroscopy," *Phys. Rev. B*, vol. 105, p. 064 515, 6 Feb. 2022. DOI: 10.1103/PhysRevB.105.064515.

[11] M. Sigrist and K. Ueda, "Phenomenological theory of unconventional superconductivity," *Rev. Mod. Phys.*, vol. 63, pp. 239–311, 2 Apr. 1991. DOI: 10.1103/RevModPhys.63.239.

[12] N. Fominykh, J. Henk, J. Berakdar, P. Bruno, H. Gollisch, and R. Feder, "Theory of two-electron photoemission from surfaces," *Solid State Communications*, vol. 113, no. 12, pp. 665–669, 2000, ISSN: 0038-1098. DOI: https://doi.org/10.1016/S0038-1098(99)00568-2.

[13] K. Kouzakov and J. Berakdar, "Mechanisms of superconductivity studied by two-particle emission," *Journal of Electron Spectroscopy and Related Phenomena*, vol. 161, no. 1, pp. 121–124, 2007, Many particle spectroscopy of atoms, molecules, clusters and surfaces, ISSN: 0368-2048. DOI: https://doi.org/10.1016/j.elspec.2007.02.007.

[14] K. H. Wong, A. Patwardhan, P. Abbamonte, F. Mahmood, and D. K. Morr, "Two-electron photoemission spectroscopy in topological superconductors," *Phys. Rev. B*, vol. 109, p. 094 503, 9 Mar. 2024. DOI: 10.1103/PhysRevB.109.094503.

[15] KTH, *Cooper pair spectroscopy (cops)*, Accessed on: 2026-05-15, 2025. [Online]. Available: https://www.kth.se/profile/oscar/page/cooper-pair-spectroscopy-cops.

[16] J. J. Sakurai and J. Napolitano, *Modern Quantum Mechanics*, 3rd ed. Cambridge, UK: Cambridge University Press, 2020.

[17] G. D. Mahan, *Many-Particle Physics*, 3rd ed. New York, NY, USA: Springer, 2000.

[18] M. E. Peskin and D. V. Schroeder, *An Introduction To Quantum Field Theory*, 1st ed. Boca Raton, FL, USA: CRC Press, 1995.

[19] F. Mandl and G. Shaw, *Quantum Field Theory*, 2nd ed. Chichester, UK: John Wiley & Sons Inc, 2010.

[20] J. M. Zhang and Y. Liu, "Fermi's golden rule: Its derivation and breakdown by an ideal model," *European Journal of Physics*, vol. 37, no. 6, p. 065 406, Oct. 2016. DOI: 10.1088/0143-0807/37/6/065406.

[21] P. A. M. Dirac, "The quantum theory of the emission and absorption of radiation," *Proceedings of the Royal Society of London. Series A, Containing Papers of a Mathematical and Physical Character*, vol. 114, no. 767, pp. 243–265, Mar. 1927, ISSN: 0950-1207. DOI: 10.1098/rspa.1927.0039.

[22] E. Fermi, *Nuclear Physics*, Revised ed. Chicago, IL, USA: University of Chicago Press, 1950, p. 142.

[23] G. C. Wick, "The evaluation of the collision matrix," *Phys. Rev.*, vol. 80, pp. 268–272, 2 Oct. 1950. DOI: 10.1103/PhysRev.80.268.

[24] J. K. Pachos and C. Vlachou, "Quantifying fermionic interactions from the violation of Wick's theorem," *Quantum*, vol. 6, p. 840, Oct. 2022, ISSN: 2521-327X. DOI: 10.22331/q-2022-10-13-840.

[25] D. Vollhardt, "Dynamical mean-field theory for correlated electrons," *Annalen der Physik*, vol. 524, no. 1, pp. 1–19, 2012. DOI: https://doi.org/10.1002/andp.201100250.

[26] M. Gaudin, "Une démonstration simplifiée du théorème de wick en mécanique statistique," *Nuclear Physics*, vol. 15, pp. 89–91, 1960, ISSN: 0029-5582. DOI: https://doi.org/10.1016/0029-5582(60)90285-6.

[27] T. Evans and D. Steer, "Wick's theorem at finite temperature," *Nuclear Physics B*, vol. 474, no. 2, pp. 481–496, 1996, ISSN: 0550-3213. DOI: https://doi.org/10.1016/0550-3213(96)00286-6.

[28] G. Onida, L. Reining, and A. Rubio, "Electronic excitations: Density-functional versus many-body green's-function approaches," *Rev. Mod. Phys.*, vol. 74, pp. 601–659, 2 Jun. 2002. DOI: 10.1103/RevModPhys.74.601.

[29] V. Špička, B. Velický, and A. Kalvová, "Electron systems out of equilibrium: Nonequilibrium green's function approach," *International Journal of Modern Physics B*, vol. 28, no. 23, p. 1 430 013, 2014. DOI: 10.1142/S0217979214300138.

[30] L. Hedin, "New method for calculating the one-particle green's function with application to the electron-gas problem," *Phys. Rev.*, vol. 139, A796–A823, 3A Aug. 1965. DOI: 10.1103/PhysRev.139.A796.

[31] V. Turkowski and J. K. Freericks, "Nonequilibrium perturbation theory of the spinless falicov-kimball model: Second-order truncated expansion in U," *Phys. Rev. B*, vol. 75, p. 125 110, 12 Mar. 2007. DOI: 10.1103/PhysRevB.75.125110.

[32] J. K. Freericks and V. M. Turkowski, "Steady-state nonequilibrium dynamical mean-field theory and the quantum boltzmann equation," *Journal of Physics: Conference Series*, vol. 35, no. 1, p. 39, Apr. 2006. DOI: 10.1088/1742-6596/35/1/004.

[33] T. Matsubara, "A new approach to quantum-statistical mechanics," *Progress of Theoretical Physics*, vol. 14, no. 4, pp. 351–378, Oct. 1955, ISSN: 0033-068X. DOI: 10.1143/PTP.14.351.

[34] J. K. Freericks, "An introduction to many-body green's functions in and out of equilibrium," in *Many-Body Methods for Real Materials*, ser. Modeling and Simulation, E. Pavarini, E. Koch, and S. Zhang, Eds., vol. 9, Jülich, Germany: Forschungszentrum Jülich GmbH, Institute of Advanced Simulation, 2019, ch. 13.

[35] J. Rizzo, F. Libbi, F. Tacchino, P. J. Ollitrault, N. Marzari, and I. Tavernelli, "One-particle green's functions from the quantum equation of motion algorithm," *Phys. Rev. Res.*, vol. 4, p. 043 011, 4 Oct. 2022. DOI: 10.1103/PhysRevResearch.4.043011.

[36] D. V. Schroeder, *An Introduction to Thermal Physics*. Oxford, UK: Oxford University Press, 2021.

[37] A. Damascelli, "Probing the electronic structure of complex systems by arpes," *Physica Scripta*, vol. 2004, no. T109, p. 61, Jan. 2004. DOI: 10.1238/Physica.Topical.109a00061.

[38] F. Boschini, M. Zonno, and A. Damascelli, "Time-resolved arpes studies of quantum materials," *Rev. Mod. Phys.*, vol. 96, p. 015 003, 1 Feb. 2024. DOI: 10.1103/RevModPhys.96.015003.

[39] Y. Su and C. Zhang, "Coincidence angle-resolved photoemission spectroscopy: Proposal for detection of two-particle correlations," *Phys. Rev. B*, vol. 101, p. 205 110, 20 May 2020. DOI: 10.1103/PhysRevB.101.205110.

[40] H. Kamerlingh Onnes, "Further experiments with liquid helium. C. On the change of electric resistance of pure metals at very low temperatures etc. IV. The resistance of pure mercury at helium temperatures," *KNAW Proceedings*, vol. 13 II, pp. 1274–1276, 1911. [Online]. Available: https://dwc.knaw.nl/DL/publications/PU00013358.pdf.

[41] A. V. Balatsky, I. Vekhter, and J.-X. Zhu, "Impurity-induced states in conventional and unconventional superconductors," *Rev. Mod. Phys.*, vol. 78, pp. 373–433, 2 May 2006. DOI: 10.1103/RevModPhys.78.373.

[42] A. Balatsky and E. Abrahams, "New class of singlet superconductors which break the time reversal and parity," *Phys. Rev. B*, vol. 45, 13125(R)–13128(R), 22 Jun. 1992. DOI: 10.1103/PhysRevB.45.13125.

[43] E. Abrahams, A. Balatsky, D. J. Scalapino, and J. R. Schrieffer, "Properties of odd-gap superconductors," *Phys. Rev. B*, vol. 52, pp. 1271–1278, 2 Jul. 1995. DOI: 10.1103/PhysRevB.52.1271.

[44] Y. Su, K. Cao, and C. Zhang, "Coincidence detection probability of (γ, $2e$) photoemission measurement," *Journal of Physics: Condensed Matter*, vol. 36, no. 50, p. 505 602, Oct. 2024. DOI: 10.1088/1361-648X/ad7e74.

A

Derivational Details for the BCS Green's Functions

In this appendix, we provide the derivational details for the normal and anomalous Green's functions appearing in the BCS theory discussed in Sec. 3.1. These details are omitted from the main text in order to keep the discussion of BCS theory compact. The appendix is organized into four sections: the first section derives the imaginary-time evolution of the creation and annihilation operators, the second and third sections derive the equations of motion for the normal and anomalous Green's functions, respectively, and the final section uses the coupled equations of motion to obtain the explicit expressions for the normal and anomalous Green's functions.

A.1 Imaginary-Time Evolution of Creation and Annihilation Operators

We want to compute the time derivative of $c_{\mathbf{k}\sigma}$, which can be done as

$$\frac{\mathrm{d}}{\mathrm{d}\tau}c_{\mathbf{k}\sigma}(\tau) = [H, c_{\mathbf{k}\sigma}(\tau)] = e^{H\tau}\Big([H_0, c_{\mathbf{k}\sigma}] + [H_I, c_{\mathbf{k}\sigma}]\Big)e^{-H\tau}. \tag{A.1}$$

The first commutation can be computed as

$$\begin{aligned}
[H_0, c_{\mathbf{k}\sigma}] &= (H_0 c_{\mathbf{k}\sigma} - c_{\mathbf{k}\sigma}H_0) \\
&= \left(\sum_{\mathbf{k}'\sigma'} \xi_{\mathbf{k}'} c^\dagger_{\mathbf{k}'\sigma'} c_{\mathbf{k}'\sigma'}\right) c_{\mathbf{k}\sigma} - c_{\mathbf{k}\sigma}\left(\sum_{\mathbf{k}'\sigma'} \xi_{\mathbf{k}'} c^\dagger_{\mathbf{k}'\sigma'} c_{\mathbf{k}'\sigma'}\right) \\
&= \sum_{\mathbf{k}'\sigma'} \xi_{\mathbf{k}'} c^\dagger_{\mathbf{k}'\sigma'} c_{\mathbf{k}'\sigma'} c_{\mathbf{k}\sigma} - \sum_{\mathbf{k}'\sigma'} \xi_{\mathbf{k}'} c_{\mathbf{k}\sigma} c^\dagger_{\mathbf{k}'\sigma'} c_{\mathbf{k}'\sigma'} \\
&= \sum_{\mathbf{k}'\sigma'} \xi_{\mathbf{k}'} c^\dagger_{\mathbf{k}'\sigma'} c_{\mathbf{k}'\sigma'} c_{\mathbf{k}\sigma} - \sum_{\mathbf{k}'\sigma'} \xi_{\mathbf{k}'} \left\{c_{\mathbf{k}\sigma}, c^\dagger_{\mathbf{k}'\sigma'}\right\} c_{\mathbf{k}'\sigma'} + \sum_{\mathbf{k}'\sigma'} \xi_{\mathbf{k}'} c^\dagger_{\mathbf{k}'\sigma'} c_{\mathbf{k}\sigma} c_{\mathbf{k}'\sigma'} \\
&= \sum_{\mathbf{k}'\sigma'} \xi_{\mathbf{k}'} c^\dagger_{\mathbf{k}'\sigma'} c_{\mathbf{k}'\sigma'} c_{\mathbf{k}\sigma} - \sum_{\mathbf{k}'\sigma'} \xi_{\mathbf{k}'} c^\dagger_{\mathbf{k}'\sigma'} c_{\mathbf{k}'\sigma'} c_{\mathbf{k}\sigma} - \sum_{\mathbf{k}'\sigma'} \xi_{\mathbf{k}'} \delta_{\mathbf{k}\mathbf{k}'}\delta_{\sigma\sigma'} c_{\mathbf{k}'\sigma'} \\
&= -\xi_{\mathbf{k}} c_{\mathbf{k}\sigma},
\end{aligned} \tag{A.2}$$

so that

$$e^{H\tau}\,[H_0, c_{\mathbf{k}\sigma}]\,e^{-H\tau} = -\xi_{\mathbf{k}} c_{\mathbf{k}\sigma}(\tau). \tag{A.3}$$

The second term can be computed as

$$[H_I, c_{\mathbf{k}\sigma}] = \frac{1}{2\nu}\sum_{\mathbf{qpp}'ss'} V(\mathbf{q})\Big(c^\dagger_{\mathbf{p}+\mathbf{q},s}c^\dagger_{\mathbf{p}'-\mathbf{q},s'}c_{\mathbf{p}'s'}c_{\mathbf{p}s}c_{\mathbf{k}\sigma} - c_{\mathbf{k}\sigma}c^\dagger_{\mathbf{p}+\mathbf{q},s}c^\dagger_{\mathbf{p}'-\mathbf{q},s'}c_{\mathbf{p}'s'}c_{\mathbf{p}s}\Big). \tag{A.4}$$

Using the relation $cc^\dagger = \left\{c, c^\dagger\right\} - c^\dagger c$, we can rewrite it as

$$\begin{aligned}
&\left\{c_{\mathbf{k}\sigma}, c^\dagger_{\mathbf{p}+\mathbf{q},s}\right\} c^\dagger_{\mathbf{p}'-\mathbf{q},s'}c_{\mathbf{p}'s'}c_{\mathbf{p}s} - c^\dagger_{\mathbf{p}+\mathbf{q},s}c_{\mathbf{k}\sigma}c^\dagger_{\mathbf{p}'-\mathbf{q},s'}c_{\mathbf{p}'s'}c_{\mathbf{p}s}\\
&= \left\{c_{\mathbf{k}\sigma}, c^\dagger_{\mathbf{p}+\mathbf{q},s}\right\} c^\dagger_{\mathbf{p}'-\mathbf{q},s'}c_{\mathbf{p}'s'}c_{\mathbf{p}s} - c^\dagger_{\mathbf{p}+\mathbf{q},s}\left\{c_{\mathbf{k}\sigma}, c^\dagger_{\mathbf{p}'-\mathbf{q},s'}\right\} c_{\mathbf{p}'s'}c_{\mathbf{p}s} + c^\dagger_{\mathbf{p}+\mathbf{q},s}c^\dagger_{\mathbf{p}'-\mathbf{q},s'}c_{\mathbf{k}\sigma}c_{\mathbf{p}'s'}c_{\mathbf{p}s}\\
&= \delta_{\mathbf{k},\mathbf{p}+\mathbf{q}}\delta_{\sigma s}c^\dagger_{\mathbf{p}'-\mathbf{q},s'}c_{\mathbf{p}'s'}c_{\mathbf{p}s} - \delta_{\mathbf{k},\mathbf{p}'-\mathbf{q}}\delta_{\sigma s'}c^\dagger_{\mathbf{p}+\mathbf{q},s}c_{\mathbf{p}'s'}c_{\mathbf{p}s} + c^\dagger_{\mathbf{p}+\mathbf{q},s}c^\dagger_{\mathbf{p}'-\mathbf{q},s'}c_{\mathbf{p}'s'}c_{\mathbf{p}s}c_{\mathbf{k}\sigma}.
\end{aligned} \tag{A.5}$$

Putting this back into Eq. (A.4) gives

$$\begin{aligned}
[H_I, c_{\mathbf{k}\sigma}] = \frac{1}{2\nu}\sum_{\mathbf{qpp}'ss'} V(\mathbf{q})\Big(&c^\dagger_{\mathbf{p}+\mathbf{q},s}c^\dagger_{\mathbf{p}'-\mathbf{q},s'}c_{\mathbf{p}'s'}c_{\mathbf{p}s}c_{\mathbf{k}\sigma} - \Big[\delta_{\mathbf{k},\mathbf{p}+\mathbf{q}}\delta_{\sigma s}c^\dagger_{\mathbf{p}'-\mathbf{q},s'}c_{\mathbf{p}'s'}c_{\mathbf{p}s}\\
&- \delta_{\mathbf{k},\mathbf{p}'-\mathbf{q}}\delta_{\sigma s'}c^\dagger_{\mathbf{p}+\mathbf{q},s}c_{\mathbf{p}'s'}c_{\mathbf{p}s} + c^\dagger_{\mathbf{p}+\mathbf{q},s}c^\dagger_{\mathbf{p}'-\mathbf{q},s'}c_{\mathbf{p}'s'}c_{\mathbf{p}s}c_{\mathbf{k}\sigma}\Big]\Big).
\end{aligned} \tag{A.6}$$

The first and the last term cancel, giving

$$\begin{aligned}
&-\frac{1}{2\nu}\sum_{\mathbf{qp}'s'} V(\mathbf{q})c^\dagger_{\mathbf{p}'-\mathbf{q},s'}c_{\mathbf{p}'s'}c_{\mathbf{k}-\mathbf{q},\sigma} + \frac{1}{2\nu}\sum_{\mathbf{qp}s} V(\mathbf{q})c^\dagger_{\mathbf{p}+\mathbf{q},s}c_{\mathbf{k}+\mathbf{q},\sigma}c_{\mathbf{p}s}\\
&= -\frac{1}{2\nu}\sum_{\mathbf{qp}'s'} V(\mathbf{q})c^\dagger_{\mathbf{p}'-\mathbf{q},s'}c_{\mathbf{p}'s'}c_{\mathbf{k}-\mathbf{q},\sigma} - \frac{1}{2\nu}\sum_{\mathbf{qp}s} V(\mathbf{q})c^\dagger_{\mathbf{p}+\mathbf{q},s}c_{\mathbf{p}s}c_{\mathbf{k}+\mathbf{q},\sigma}.
\end{aligned} \tag{A.7}$$

By relabeling $\mathbf{p}' \to \mathbf{k}'$ in the first term and $\mathbf{p} \to \mathbf{k}'$, $s \to s'$ and $\mathbf{q} \to -\mathbf{q}$ in the second term, we can write this as

$$-\frac{1}{2\nu}\sum_{\mathbf{qk}'s'} V(\mathbf{q})c^\dagger_{\mathbf{k}'-\mathbf{q},s'}c_{\mathbf{k}'s'}c_{\mathbf{k}-\mathbf{q},\sigma} - \frac{1}{2\nu}\sum_{\mathbf{qk}'s'} V(-q)c^\dagger_{\mathbf{k}'-\mathbf{q},s'}c_{\mathbf{k}'s'}c_{\mathbf{k}-\mathbf{q},\sigma} \tag{A.8}$$

and using that $V(\mathbf{q}) = V(-q)$ is symmetric, we find

$$[H_I, c_{\mathbf{k}\sigma}] = -\frac{1}{\nu}\sum_{\mathbf{qk}'s'} V(\mathbf{q})c^\dagger_{\mathbf{k}'-\mathbf{q},s'}c_{\mathbf{k}'s'}c_{\mathbf{k}-\mathbf{q},\sigma}. \tag{A.9}$$

The time dependent contribution of the second term is then given by

$$\begin{aligned}
e^{H\tau}\left[H_I, c_{\mathbf{k}\sigma}\right]e^{-H\tau} &= -e^{H\tau}\frac{1}{\nu}\sum_{\mathbf{qk}'s'} V(\mathbf{q})c^\dagger_{\mathbf{k}'-\mathbf{q},s'}c_{\mathbf{k}'s'}c_{\mathbf{k}-\mathbf{q},\sigma}e^{-H\tau}\\
&= -\frac{1}{\nu}\sum_{\mathbf{qk}'s'} V(\mathbf{q})e^{H\tau}c^\dagger_{\mathbf{k}'-\mathbf{q},s'}e^{-H\tau}e^{H\tau}c_{\mathbf{k}'s'}e^{-H\tau}e^{H\tau}c_{\mathbf{k}-\mathbf{q},\sigma}e^{-H\tau}\\
&= -\frac{1}{\nu}\sum_{\mathbf{qk}'s'} V(\mathbf{q})c^\dagger_{\mathbf{k}'-\mathbf{q},s'}(\tau)c_{\mathbf{k}'s'}(\tau)c_{\mathbf{k}-\mathbf{q},\sigma}(\tau).
\end{aligned} \tag{A.10}$$

With Eqs. (A.3) and (A.10), the imaginary-time derivative in Eq. (A.1) is given by

$$\frac{\mathrm{d}}{\mathrm{d}\tau}c_{\mathbf{k}\sigma}(\tau) = [H, c_{\mathbf{k}\sigma}(\tau)] = -\xi_{\mathbf{k}}c_{\mathbf{k}\sigma}(\tau) - \frac{1}{\nu}\sum_{\mathbf{q}\mathbf{k}'s'} V(\mathbf{q})c^{\dagger}_{\mathbf{k}'-\mathbf{q},s'}(\tau)c_{\mathbf{k}'s'}(\tau)c_{\mathbf{k}-\mathbf{q},\sigma}(\tau). \tag{A.11}$$

The steps for finding the imaginary-time derivative of $c^{\dagger}_{\mathbf{k}\sigma}$ are virtually the same. They result in

$$\frac{\mathrm{d}}{\mathrm{d}\tau}c^{\dagger}_{\mathbf{k}\sigma} = \xi_{\mathbf{k}}c^{\dagger}_{\mathbf{k}\sigma}(\tau) + \frac{1}{\nu}\sum_{\mathbf{q}\mathbf{k}'s'} V(\mathbf{q})c^{\dagger}_{\mathbf{k}-\mathbf{q},\sigma}(\tau)c^{\dagger}_{\mathbf{k}'+\mathbf{q},s'}(\tau)c_{\mathbf{k}'s'}(\tau). \tag{A.12}$$

A.2 Equation of Motion for the Normal Green's Function

Computing the τ derivative of Eq. (3.3) gives

$$\begin{aligned}\frac{\partial}{\partial\tau}\mathcal{G}(\mathbf{k},\tau-\tau') &= -\frac{\partial}{\partial\tau}\Big[\Theta(\tau-\tau')\langle\langle c_{\mathbf{k}\sigma}(\tau)c^{\dagger}_{\mathbf{k}\sigma}(\tau')\rangle\rangle - \Theta(\tau'-\tau)\langle\langle c^{\dagger}_{\mathbf{k}\sigma}(\tau')c_{\mathbf{k}\sigma}(\tau)\rangle\rangle\Big] \\ &= -\delta(\tau-\tau')\langle\langle c_{\mathbf{k}\sigma}(\tau)c^{\dagger}_{\mathbf{k}\sigma}(\tau')\rangle\rangle - \Theta(\tau-\tau')\left\langle\left\langle \frac{\partial c_{\mathbf{k}\sigma}(\tau)}{\partial\tau}c^{\dagger}_{\mathbf{k}\sigma}(\tau')\right\rangle\right\rangle \\ &\quad - \delta(\tau'-\tau)\langle\langle c^{\dagger}_{\mathbf{k}\sigma}(\tau')c_{\mathbf{k}\sigma}(\tau)\rangle\rangle + \Theta(\tau'-\tau)\left\langle\left\langle c^{\dagger}_{\mathbf{k}\sigma}(\tau')\frac{\partial c_{\mathbf{k}\sigma}(\tau)}{\partial\tau}\right\rangle\right\rangle.\end{aligned} \tag{A.13}$$

Here, it is worth noting that $\delta(\tau-\tau') = \delta(\tau'-\tau)$ is symmetric. Therefore, we can simplify those two terms as follows

$$\begin{aligned}&\delta(\tau-\tau')\langle\langle c_{\mathbf{k}\sigma}(\tau)c^{\dagger}_{\mathbf{k}\sigma}(\tau')\rangle\rangle + \delta(\tau'-\tau)\langle\langle c^{\dagger}_{\mathbf{k}\sigma}(\tau')c_{\mathbf{k}\sigma}(\tau)\rangle\rangle \\ &= \delta(\tau-\tau')\left\langle\left\langle\left\{c_{\mathbf{k}\sigma}(\tau), c^{\dagger}_{\mathbf{k}\sigma}(\tau')\right\}\right\rangle\right\rangle \\ &= \delta(\tau-\tau'),\end{aligned} \tag{A.14}$$

where we have used $\langle\langle a+b\rangle\rangle = \langle\langle a\rangle\rangle + \langle\langle b\rangle\rangle$ and where we also used that the delta function enforces equal time, so that we can use the anticommutation relation for fermions. We may also notice from Eq. (A.13) that

$$\begin{aligned}\left\langle\left\langle \mathcal{T}_{\tau}\frac{\partial c_{\mathbf{k}\sigma}(\tau)}{\partial\tau}c^{\dagger}_{\mathbf{k}\sigma}(\tau')\right\rangle\right\rangle &= \Theta(\tau-\tau')\left\langle\left\langle \frac{\partial c_{\mathbf{k}\sigma}(\tau)}{\partial\tau}c^{\dagger}_{\mathbf{k}\sigma}(\tau')\right\rangle\right\rangle \\ &\quad - \Theta(\tau'-\tau)\left\langle\left\langle c^{\dagger}_{\mathbf{k}\sigma}(\tau')\frac{\partial c_{\mathbf{k}\sigma}(\tau)}{\partial\tau}\right\rangle\right\rangle.\end{aligned} \tag{A.15}$$

With these two simplifications, Eq. (A.13) can be written as

$$\frac{\partial}{\partial\tau}\mathcal{G}(\mathbf{k},\tau-\tau') = -\delta(\tau-\tau') - \left\langle\left\langle \mathcal{T}_{\tau}\frac{\partial c_{\mathbf{k}\sigma}(\tau)}{\partial\tau}c^{\dagger}_{\mathbf{k}\sigma}(\tau')\right\rangle\right\rangle. \tag{A.16}$$

Using the result of Eq. (A.11) in Eq. (A.16) gives

$$\begin{aligned}\frac{\partial}{\partial\tau}\mathcal{G}(\mathbf{k},\tau-\tau') = -\delta(\tau-\tau') + \xi_{\mathbf{k}}\langle\langle\mathcal{T}_\tau c_{\mathbf{k}\sigma}(\tau)c^\dagger_{\mathbf{k}\sigma}(\tau')\rangle\rangle \\ + \frac{1}{\nu}\sum_{\mathbf{q}\mathbf{k}'s'} V(\mathbf{q})\langle\langle\mathcal{T}_\tau c^\dagger_{\mathbf{k}'-\mathbf{q},s'}(\tau)c_{\mathbf{k}'s'}(\tau)c_{\mathbf{k}-\mathbf{q},\sigma}(\tau)c^\dagger_{\mathbf{k},\sigma}(\tau')\rangle\rangle,\end{aligned} \tag{A.17}$$

where we pulled out factors not affected by the thermal average. This can then be rewritten as

$$\begin{aligned}\left(-\frac{\partial}{\partial\tau}-\xi_{\mathbf{k}}\right)\mathcal{G}(\mathbf{k},\tau-\tau') + \frac{1}{\nu}\sum_{\mathbf{q}\mathbf{k}'s'} V(\mathbf{q}) \\ \times\langle\langle\mathcal{T}_\tau c^\dagger_{\mathbf{k}'-\mathbf{q},s'}(\tau)c_{\mathbf{k}'s'}(\tau)c_{\mathbf{k}-\mathbf{q},\sigma}(\tau)c^\dagger_{\mathbf{k},\sigma}(\tau')\rangle\rangle = \delta(\tau-\tau'),\end{aligned} \tag{A.18}$$

where we have used that

$$\xi_{\mathbf{k}}\langle\langle\mathcal{T}_\tau c_{\mathbf{k}\sigma}(\tau)c^\dagger_{\mathbf{k}\sigma}(\tau')\rangle\rangle = -\xi_{\mathbf{k}}\mathcal{G}(\mathbf{k},\tau-\tau'). \tag{A.19}$$

Focusing on the four-operator object, we can simplify this using Wick factorization, so that

$$\begin{aligned}&\langle\langle\mathcal{T}_\tau c^\dagger_{\mathbf{k}'-\mathbf{q},s'}(\tau)c_{\mathbf{k}'s'}(\tau)c_{\mathbf{k}-\mathbf{q},\sigma}(\tau)c^\dagger_{\mathbf{k},\sigma}(\tau')\rangle\rangle \\ &\qquad\approx \langle\langle\mathcal{T}_\tau c^\dagger_{\mathbf{k}'-\mathbf{q},s'}(\tau)c_{\mathbf{k}'s'}(\tau)\rangle\rangle\langle\langle\mathcal{T}_\tau c_{\mathbf{k}-\mathbf{q},\sigma}(\tau)c^\dagger_{\mathbf{k},\sigma}(\tau')\rangle\rangle \\ &\qquad\quad - \langle\langle\mathcal{T}_\tau c^\dagger_{\mathbf{k}'-\mathbf{q},s'}(\tau)c_{\mathbf{k}-\mathbf{q},\sigma}(\tau)\rangle\rangle\langle\langle\mathcal{T}_\tau c_{\mathbf{k}'s'}(\tau)c^\dagger_{\mathbf{k},\sigma}(\tau')\rangle\rangle \\ &\qquad\quad + \langle\langle\mathcal{T}_\tau c^\dagger_{\mathbf{k}'-\mathbf{q},s'}(\tau)c^\dagger_{\mathbf{k},\sigma}(\tau')\rangle\rangle\langle\langle\mathcal{T}_\tau c_{\mathbf{k}'s'}(\tau)c_{\mathbf{k}-\mathbf{q},\sigma}(\tau)\rangle\rangle,\end{aligned} \tag{A.20}$$

where the minus sign arises from an odd number of fermion exchanges. Moving forward, all expressions are evaluated in the Wick-factorization approximation described in Sec. 2.2. To further simplify this, we assume that long-wavelength phonons give a zero potential. We can therefore neglect the pairing that occurs at $\mathbf{q}=0$ which makes the first term vanish. The second term is only nonzero when $\mathbf{k}'=\mathbf{k}$ and $s'=\sigma$, and it simplifies to

$$-\delta_{\mathbf{k}'\mathbf{k}}\delta_{s'\sigma}\langle\langle\mathcal{T}_\tau c^\dagger_{\mathbf{k}-\mathbf{q},\sigma}(\tau)c_{\mathbf{k}-\mathbf{q},\sigma}(\tau)\rangle\rangle\langle\langle\mathcal{T}_\tau c_{\mathbf{k}\sigma}(\tau)c^\dagger_{\mathbf{k},\sigma}(\tau')\rangle\rangle = \delta_{\mathbf{k}'\mathbf{k}}\delta_{s'\sigma}n_{\mathbf{k}-\mathbf{q}}\mathcal{G}(\mathbf{k},\tau-\tau'), \tag{A.21}$$

where we used that

$$\langle\langle c^\dagger_{\mathbf{k}\sigma}(\tau)c_{\mathbf{k}\sigma}(\tau)\rangle\rangle = n_{\mathbf{k}}. \tag{A.22}$$

Here, we have used the convention where the annihilation operators are placed to the right whenever there is a τ ordering of two operators occurring at the same imaginary time. This convention follows the convention used to write down the Hamiltonian in Eq. (3.6). The third term is only nonzero when $\mathbf{k}'=-\mathbf{k}+\mathbf{q}$ and $s'=-\sigma$. For this term, we need to consider two cases $\sigma=\uparrow$ and $\sigma=\downarrow$. First, we consider the case with $\sigma=\uparrow$, we find

$$\begin{aligned}&\delta_{\mathbf{k}',-\mathbf{k}+\mathbf{q}}\delta_{s',-\sigma}\langle\langle\mathcal{T}_\tau c^\dagger_{-\mathbf{k},\downarrow}(\tau)c^\dagger_{\mathbf{k},\uparrow}(\tau')\rangle\rangle\langle\langle\mathcal{T}_\tau c_{-\mathbf{k}+\mathbf{q},\downarrow}(\tau)c_{\mathbf{k}-\mathbf{q},\uparrow}(\tau)\rangle\rangle \\ &= -\delta_{\mathbf{k}',-\mathbf{k}+\mathbf{q}}\delta_{s',-\sigma}\langle\langle\mathcal{T}_\tau c^\dagger_{\mathbf{k},\uparrow}(\tau')c^\dagger_{-\mathbf{k},\downarrow}(\tau)\rangle\rangle\langle\langle\mathcal{T}_\tau c_{-\mathbf{k}+\mathbf{q},\downarrow}(\tau)c_{\mathbf{k}-\mathbf{q},\uparrow}(\tau)\rangle\rangle \\ &= -\delta_{\mathbf{k}',-\mathbf{k}+\mathbf{q}}\delta_{s',-\sigma}\mathcal{F}^\dagger(\mathbf{k},\tau'-\tau)\mathcal{F}(\mathbf{k}-\mathbf{q},0),\end{aligned} \tag{A.23}$$

where we exchanged the two electron operators in the first thermal average. The second spin case to consider is $\sigma = \downarrow$. This gives

$$\begin{aligned}
&\delta_{\mathbf{k}',-\mathbf{k}+\mathbf{q}}\delta_{s',-\sigma}\langle\langle \mathcal{T}_\tau c^\dagger_{-\mathbf{k},\uparrow}(\tau)c^\dagger_{\mathbf{k},\downarrow}(\tau')\rangle\rangle\langle\langle \mathcal{T}_\tau c_{-\mathbf{k}+\mathbf{q},\uparrow}(\tau)c_{\mathbf{k}-\mathbf{q},\downarrow}(\tau)\rangle\rangle \\
&= -\delta_{\mathbf{k}',-\mathbf{k}+\mathbf{q}}\delta_{s',-\sigma}\langle\langle \mathcal{T}_\tau c^\dagger_{-\mathbf{k},\uparrow}(\tau)c^\dagger_{\mathbf{k},\downarrow}(\tau')\rangle\rangle\langle\langle \mathcal{T}_\tau c_{\mathbf{k}-\mathbf{q},\downarrow}(\tau)c_{-\mathbf{k}+\mathbf{q},\uparrow}(\tau)\rangle\rangle \\
&= -\delta_{\mathbf{k}',-\mathbf{k}+\mathbf{q}}\delta_{s',-\sigma}\mathcal{F}^\dagger(-\mathbf{k},\tau-\tau')\mathcal{F}(-\mathbf{k}+\mathbf{q},0),
\end{aligned} \tag{A.24}$$

where we exchanged the two electron operators in the second thermal average. In the conventional BCS case, $\mathcal{F}$ and $\mathcal{F}^\dagger$ do not depend on the sign of their momentum and τ arguments. Because of this, Eqs. (A.23) and (A.24) are identical. The second term of Eq. (A.18) consisting of the four-operator object, simplifies as

$$\begin{aligned}
&\frac{1}{\nu}\sum_{\mathbf{q}\mathbf{k}'s'} V(\mathbf{q})\langle\langle \mathcal{T}_\tau c^\dagger_{\mathbf{k}'-\mathbf{q},s'}(\tau)c_{\mathbf{k}'s'}(\tau)c_{\mathbf{k}-\mathbf{q},\sigma}(\tau)c^\dagger_{\mathbf{k},\sigma}(\tau')\rangle\rangle \\
&\qquad = \frac{1}{\nu}\sum_{\mathbf{q}} V(\mathbf{q})\Big[\mathcal{G}(\mathbf{k},\tau-\tau')n_{\mathbf{k}-\mathbf{q}} - \mathcal{F}(\mathbf{k}-\mathbf{q},0)\mathcal{F}^\dagger(\mathbf{k},\tau-\tau')\Big].
\end{aligned} \tag{A.25}$$

Defining the gap function as in Eq. (3.12) and following the reasoning above that definition, the equation of motion can be written as

$$\left(-\frac{\partial}{\partial\tau} - \xi_{\mathbf{k}}\right)\mathcal{G}(\mathbf{k},\tau-\tau') + \Delta(\mathbf{k})\mathcal{F}^\dagger(\mathbf{k},\tau-\tau') = \delta(\tau-\tau') \tag{A.26}$$

A.3 Equation of Motion for the Anomalous Green's Function

Computing the τ derivative of Eq. (3.5) gives

$$\begin{aligned}
\frac{\partial}{\partial\tau}\mathcal{F}(\mathbf{k},\tau-\tau') &= \frac{\partial}{\partial\tau}\Big[\Theta(\tau-\tau')\langle\langle c^\dagger_{\mathbf{k}\uparrow}(\tau)c^\dagger_{-\mathbf{k}\downarrow}(\tau')\rangle\rangle - \Theta(\tau'-\tau)\langle\langle c^\dagger_{-\mathbf{k}\downarrow}(\tau')c^\dagger_{\mathbf{k}\uparrow}(\tau)\rangle\rangle\Big] \\
&= \delta(\tau-\tau')\langle\langle c^\dagger_{\mathbf{k}\uparrow}(\tau)c^\dagger_{-\mathbf{k}\downarrow}(\tau')\rangle\rangle + \Theta(\tau-\tau')\left\langle\left\langle \frac{\partial c^\dagger_{\mathbf{k}\uparrow}(\tau)}{\partial\tau}c^\dagger_{-\mathbf{k}\downarrow}(\tau')\right\rangle\right\rangle \\
&\quad + \delta(\tau'-\tau)\langle\langle c^\dagger_{-\mathbf{k}\downarrow}(\tau')c^\dagger_{\mathbf{k}\uparrow}(\tau)\rangle\rangle - \Theta(\tau'-\tau)\left\langle\left\langle c^\dagger_{-\mathbf{k}\downarrow}(\tau')\frac{\partial c^\dagger_{\mathbf{k}\uparrow}(\tau)}{\partial\tau}\right\rangle\right\rangle.
\end{aligned} \tag{A.27}$$

The delta functions are symmetric in their arguments, and these two terms can therefore be simplified as follows

$$\begin{aligned}
&\delta(\tau-\tau')\langle\langle c^\dagger_{\mathbf{k}\uparrow}(\tau)c^\dagger_{-\mathbf{k}\downarrow}(\tau')\rangle\rangle + \delta(\tau'-\tau)\langle\langle c^\dagger_{-\mathbf{k}\downarrow}(\tau')c^\dagger_{\mathbf{k}\uparrow}(\tau)\rangle\rangle \\
&= \delta(\tau-\tau')\left\langle\left\langle\left\{c^\dagger_{\mathbf{k}\uparrow}(\tau), c^\dagger_{-\mathbf{k}\downarrow}(\tau')\right\}\right\rangle\right\rangle \\
&= 0,
\end{aligned} \tag{A.28}$$

where we have used $\langle\langle a+b\rangle\rangle = \langle\langle a\rangle\rangle + \langle\langle b\rangle\rangle$ and where we also used that the delta function enforces equal time, so that we can use the anticommutation relation for

fermions. The other two terms of Eq. (A.27) can be written as

$$\begin{aligned}\left\langle\!\left\langle \mathcal{T}_\tau \frac{\partial c^\dagger_{\mathbf{k}\uparrow}(\tau)}{\partial\tau} c^\dagger_{-\mathbf{k}\downarrow}(\tau') \right\rangle\!\right\rangle &= \Theta(\tau-\tau') \left\langle\!\left\langle \frac{\partial c^\dagger_{\mathbf{k}\uparrow}(\tau)}{\partial\tau} c^\dagger_{-\mathbf{k}\downarrow}(\tau') \right\rangle\!\right\rangle \\ &\quad - \Theta(\tau'-\tau) \left\langle\!\left\langle c^\dagger_{-\mathbf{k}\downarrow}(\tau') \frac{\partial c^\dagger_{\mathbf{k}\uparrow}(\tau)}{\partial\tau} \right\rangle\!\right\rangle .\end{aligned} \tag{A.29}$$

Using these two results in Eq. (A.27) gives

$$\frac{\partial}{\partial\tau}\mathcal{F}(\mathbf{k},\tau-\tau') = \left\langle\!\left\langle \mathcal{T}_\tau \frac{\partial c^\dagger_{\mathbf{k}\uparrow}(\tau)}{\partial\tau} c^\dagger_{-\mathbf{k}\downarrow}(\tau') \right\rangle\!\right\rangle . \tag{A.30}$$

Using the result of Eq. (A.12) in Eq. (A.29), we find

$$\begin{aligned}\frac{\partial}{\partial\tau}\mathcal{F}(\mathbf{k},\tau-\tau') &= \xi_{\mathbf{k}} \langle\!\langle c^\dagger_{\mathbf{k}\uparrow}(\tau) c^\dagger_{-\mathbf{k}\downarrow}(\tau') \rangle\!\rangle \\ &\quad + \frac{1}{\nu}\sum_{\mathbf{q}\mathbf{k}'s'} V(\mathbf{q}) \langle\!\langle c^\dagger_{\mathbf{k}-\mathbf{q},\uparrow}(\tau) c^\dagger_{\mathbf{k}'+\mathbf{q},s'}(\tau) c_{\mathbf{k}'s'}(\tau) c^\dagger_{-\mathbf{k}\downarrow}(\tau') \rangle\!\rangle .\end{aligned} \tag{A.31}$$

We can rewrite this as

$$\left(-\frac{\partial}{\partial\tau}+\xi_{\mathbf{k}}\right)\mathcal{F}^\dagger(\mathbf{k},\tau-\tau') + \frac{1}{\nu}\sum_{\mathbf{k}\mathbf{k}'s} V(\mathbf{q}) \langle\!\langle \mathcal{T}_\tau c^\dagger_{\mathbf{k}-\mathbf{q},\uparrow}(\tau) c^\dagger_{\mathbf{k}'+\mathbf{q},s'}(\tau) c_{\mathbf{k}'s'}(\tau) c^\dagger_{-\mathbf{k}\downarrow}(\tau') \rangle\!\rangle = 0. \tag{A.32}$$

We can simplify the four-operator object using Wick factorization, so that

$$\begin{aligned}&\langle\!\langle \mathcal{T}_\tau c^\dagger_{\mathbf{k}-\mathbf{q},\uparrow}(\tau) c^\dagger_{\mathbf{k}'+\mathbf{q},s'}(\tau) c_{\mathbf{k}'s'}(\tau) c^\dagger_{-\mathbf{k}\downarrow}(\tau') \rangle\!\rangle \\ &\qquad \approx \langle\!\langle \mathcal{T}_\tau c^\dagger_{\mathbf{k}-\mathbf{q},\uparrow}(\tau) c^\dagger_{\mathbf{k}'+\mathbf{q},s'}(\tau) \rangle\!\rangle \langle\!\langle \mathcal{T}_\tau c_{\mathbf{k}'s'}(\tau) c^\dagger_{-\mathbf{k}\downarrow}(\tau') \rangle\!\rangle \\ &\qquad\quad - \langle\!\langle \mathcal{T}_\tau c^\dagger_{\mathbf{k}-\mathbf{q},\uparrow}(\tau) c_{\mathbf{k}'s'}(\tau) \rangle\!\rangle \langle\!\langle \mathcal{T}_\tau c^\dagger_{\mathbf{k}'+\mathbf{q},s'}(\tau) c^\dagger_{-\mathbf{k}\downarrow}(\tau') \rangle\!\rangle \\ &\qquad\quad + \langle\!\langle \mathcal{T}_\tau c^\dagger_{\mathbf{k}-\mathbf{q},\uparrow}(\tau) c^\dagger_{-\mathbf{k}\downarrow}(\tau') \rangle\!\rangle \langle\!\langle \mathcal{T}_\tau c^\dagger_{\mathbf{k}'+\mathbf{q},s'}(\tau) c_{\mathbf{k}'s'}(\tau) \rangle\!\rangle ,\end{aligned} \tag{A.33}$$

where the minus sign arises from an odd number of fermion exchanges. Moving forward, all expressions are evaluated in the Wick-factorization approximation described in Sec. 2.2. To further simplify this, we assume that long-wavelength phonons give a zero potential. We can therefore neglect the pairing that occurs at $\mathbf{q}=0$ which makes the first term vanish. The nonzero contributions are

$$\begin{aligned}\delta_{\mathbf{k},-\mathbf{k}'}\delta_{s'\downarrow}\mathcal{F}^\dagger(\mathbf{k}-\mathbf{q},0)\mathcal{G}(-\mathbf{k},\tau-\tau') - \delta_{\mathbf{k}',-\mathbf{k}-\mathbf{q}}\delta_{s'\uparrow}n_{\mathbf{k}-\mathbf{q}}\mathcal{F}^\dagger(\mathbf{k},\tau-\tau') \\ + \delta_{\mathbf{q},0}n_{\mathbf{k}'}\mathcal{F}^\dagger(\mathbf{k},\tau-\tau').\end{aligned} \tag{A.34}$$

The second term vanishes because of the arguments made above Eq. (3.12) of Sec. (3.1), and the last term vanishes because it requires $\mathbf{q}=0$. Inserting this into Eq. (A.32) and using the definition of the gap function in Eq. (3.12), the equation of motion can be written as

$$\left(-\frac{\partial}{\partial\tau}+\xi_{\mathbf{k}}\right)\mathcal{F}^\dagger(\mathbf{k},\tau-\tau') + \Delta^\dagger(\mathbf{k})\mathcal{G}(\mathbf{k},\tau-\tau') = 0. \tag{A.35}$$

A.4 Normal and Anomalous Green's Functions from the Coupled Equations of Motion

The equations of motion given in Eqs. (A.26) and (A.35) are two coupled equations, and Fourier transforming them gives

$$(i\omega_n - \xi_{\mathbf{k}})\mathcal{G}(\mathbf{k}, i\omega_n) + \Delta(\mathbf{k})\mathcal{F}^\dagger(\mathbf{k}, i\omega_n) = 1, \tag{A.36}$$

$$(i\omega_n + \xi_{\mathbf{k}})\mathcal{F}^\dagger(\mathbf{k}, i\omega_n) + \Delta(\mathbf{k})\mathcal{G}(\mathbf{k}, i\omega_n) = 0, \tag{A.37}$$

where we have assumed that the gap function is real. These equations can be solved algebraically. We begin by solving for $\mathcal{F}^\dagger$ in Eq. (A.37) and get

$$\begin{aligned}
&(i\omega_n + \xi_{\mathbf{k}})\mathcal{F}^\dagger(\mathbf{k}, i\omega_n) + \Delta(\mathbf{k})\mathcal{G}(\mathbf{k}, i\omega_n) = 0 \\
&\implies \mathcal{F}^\dagger(\mathbf{k}, i\omega_n) = -\frac{\Delta(\mathbf{k})}{(i\omega_n + \xi_{\mathbf{k}})}\mathcal{G}(\mathbf{k}, i\omega_n).
\end{aligned} \tag{A.38}$$

We use this in Eq. (A.36) and solve for $\mathcal{G}$. This gives

$$\begin{aligned}
&(i\omega_n - \xi_{\mathbf{k}})\mathcal{G}(\mathbf{k}, i\omega_n) + \Delta(\mathbf{k})\frac{-\Delta(\mathbf{k})}{(i\omega_n + \xi_{\mathbf{k}})}\mathcal{G}(\mathbf{k}, i\omega_n) = 1 \\
&\implies \mathcal{G}(\mathbf{k}, i\omega_n)\left[i\omega_n - \xi_{\mathbf{k}} - \frac{\Delta^2(\mathbf{k})}{(i\omega_n + \xi_{\mathbf{k}})}\right] = 1 \\
&\implies \mathcal{G}(\mathbf{k}, i\omega_n)\left[-\frac{\omega_n^2 + \xi_{\mathbf{k}}^2 + \Delta^2(\mathbf{k})}{(i\omega_n + \xi_{\mathbf{k}})}\right] = 1 \\
&\implies \mathcal{G}(\mathbf{k}, i\omega_n) = -\frac{i\omega_n + \xi_{\mathbf{k}}}{\omega_n^2 + \xi_{\mathbf{k}}^2 + \Delta^2(\mathbf{k})}.
\end{aligned} \tag{A.39}$$

We can now use this in Eq. (A.38) to get

$$\begin{aligned}
\mathcal{F}^\dagger(\mathbf{k}, i\omega_n) &= -\frac{\Delta(\mathbf{k})}{(i\omega_n + \xi_{\mathbf{k}})}\left[-\frac{i\omega_n + \xi_{\mathbf{k}}}{\omega_n^2 + \xi_{\mathbf{k}}^2 + \Delta^2(\mathbf{k})}\right] \\
&= \frac{\Delta(\mathbf{k})}{\omega_n^2 + \xi_{\mathbf{k}}^2 + \Delta^2(\mathbf{k})}.
\end{aligned} \tag{A.40}$$

The solutions to the equations of motion for $\mathcal{G}$ and $\mathcal{F}^\dagger$ are therefore given by

$$\mathcal{G}(\mathbf{k}, i\omega_n) = -\frac{i\omega_n + \xi_{\mathbf{k}}}{\omega_n^2 + \xi_{\mathbf{k}}^2 + \Delta^2(\mathbf{k})}, \tag{A.41}$$

$$\mathcal{F}^\dagger(\mathbf{k}, i\omega_n) = \frac{\Delta(\mathbf{k})}{\omega_n^2 + \xi_{\mathbf{k}}^2 + \Delta^2(\mathbf{k})}. \tag{A.42}$$

In the conventional BCS case with a real gap, the anomalous Green's functions satisfy $\mathcal{F} = \mathcal{F}^\dagger$. This can be verified by deriving the corresponding equation of motion for $\mathcal{F}$.

B

Evaluation of the Sample-State Sums in the DPE Counting Rate

In this Appendix, we give the algebraic steps used to simplify the sample contribution to the DPE counting rate. Starting from the transition amplitude in Eq. (4.30) and inserting it into the counting-rate expression in Eq. (4.12), one obtains terms of the form

$$\frac{1}{Z}\sum_{i,f} e^{-\beta E_i}\mathcal{K}^\dagger\mathcal{K} = \langle\!\langle c^\dagger_{\mathbf{p}'\sigma'_2}(t'_2)c^\dagger_{-\mathbf{p}'\sigma'_1}(t'_1)c_{-\mathbf{p}\sigma'_1}(t_1)c_{\mathbf{p}\sigma'_2}(t_2)\rangle\!\rangle, \tag{B.1}$$

$$\frac{1}{Z}\sum_{i,f} e^{-\beta E_i}\mathcal{R}^\dagger\mathcal{R} = \langle\!\langle c^\dagger_{\mathbf{p}'\sigma'_1}(t'_2)c^\dagger_{-\mathbf{p}'\sigma'_2}(t'_1)c_{-\mathbf{p}\sigma'_2}(t_1)c_{\mathbf{p}\sigma'_1}(t_2)\rangle\!\rangle, \tag{B.2}$$

$$\frac{1}{Z}\sum_{i,f} e^{-\beta E_i}\mathcal{R}^\dagger\mathcal{K} = \langle\!\langle c^\dagger_{\mathbf{p}'\sigma'_1}(t'_2)c^\dagger_{-\mathbf{p}'\sigma'_2}(t'_1)c_{-\mathbf{p}\sigma'_1}(t_1)c_{\mathbf{p}\sigma'_2}(t_2)\rangle\!\rangle, \tag{B.3}$$

$$\frac{1}{Z}\sum_{i,f} e^{-\beta E_i}\mathcal{K}^\dagger\mathcal{R} = \langle\!\langle c^\dagger_{\mathbf{p}'\sigma'_2}(t'_2)c^\dagger_{-\mathbf{p}'\sigma'_1}(t'_1)c_{-\mathbf{p}\sigma'_2}(t_1)c_{\mathbf{p}\sigma'_1}(t_2)\rangle\!\rangle, \tag{B.4}$$

where $\mathcal{K}$, $\mathcal{R}$, and their respective Hermitian conjugate are defined in Eqs. (4.27) and (4.28). The purpose of this appendix is to show how these terms can be written in terms of normal and anomalous Green's functions.

Let us define

$$c(1) = c_{-\mathbf{p}\sigma'_1}(t_1), \qquad c(3) = c_{\mathbf{p}\sigma'_1}(t_2), \tag{B.5}$$

$$c(2) = c_{-\mathbf{p}\sigma'_2}(t_1), \qquad c(4) = c_{\mathbf{p}\sigma'_2}(t_2). \tag{B.6}$$

Then, the above terms can be written as

$$\frac{1}{Z}\sum_{i,f} e^{-\beta E_i}\mathcal{K}^\dagger\mathcal{K} = \langle\!\langle c^\dagger(4')c^\dagger(1')c(1)c(4)\rangle\!\rangle,$$

$$\frac{1}{Z}\sum_{i,f} e^{-\beta E_i}\mathcal{R}^\dagger\mathcal{R} = \langle\!\langle c^\dagger(3')c^\dagger(2')c(2)c(3)\rangle\!\rangle,$$

$$\frac{1}{Z}\sum_{i,f} e^{-\beta E_i}\mathcal{R}^\dagger\mathcal{K} = \langle\!\langle c^\dagger(3')c^\dagger(2')c(1)c(4)\rangle\!\rangle,$$

$$\frac{1}{Z}\sum_{i,f} e^{-\beta E_i}\mathcal{K}^\dagger\mathcal{R} = \langle\!\langle c^\dagger(4')c^\dagger(1')c(2)c(3)\rangle\!\rangle.$$

These terms can be simplified using Wick's theorem

$$\begin{aligned}\frac{1}{Z}\sum_{i,f} e^{-\beta E_i}\mathcal{K}^\dagger\mathcal{K} \approx\ & \langle\!\langle c^\dagger(4')c^\dagger(1')\rangle\!\rangle\langle\!\langle c(1)c(4)\rangle\!\rangle \\ & - \langle\!\langle c^\dagger(4')c(1)\rangle\!\rangle\langle\!\langle c^\dagger(1')c(4)\rangle\!\rangle \\ & + \langle\!\langle c^\dagger(4')c(4)\rangle\!\rangle\langle\!\langle c^\dagger(1')c(1)\rangle\!\rangle,\end{aligned} \tag{B.7}$$

$$\begin{aligned}\frac{1}{Z}\sum_{i,f} e^{-\beta E_i}\mathcal{R}^\dagger\mathcal{R} \approx\ & \langle\!\langle c^\dagger(3')c^\dagger(2')\rangle\!\rangle\langle\!\langle c(2)c(3)\rangle\!\rangle \\ & - \langle\!\langle c^\dagger(3')c(2)\rangle\!\rangle\langle\!\langle c^\dagger(2')c(3)\rangle\!\rangle \\ & + \langle\!\langle c^\dagger(3')c(3)\rangle\!\rangle\langle\!\langle c^\dagger(2')c(2)\rangle\!\rangle,\end{aligned} \tag{B.8}$$

$$\begin{aligned}\frac{1}{Z}\sum_{i,f} e^{-\beta E_i}\mathcal{R}^\dagger\mathcal{K} \approx\ & \langle\!\langle c^\dagger(3')c^\dagger(2')\rangle\!\rangle\langle\!\langle c(1)c(4)\rangle\!\rangle \\ & - \langle\!\langle c^\dagger(3')c(1)\rangle\!\rangle\langle\!\langle c^\dagger(2')c(4)\rangle\!\rangle \\ & + \langle\!\langle c^\dagger(3')c(4)\rangle\!\rangle\langle\!\langle c^\dagger(2')c(1)\rangle\!\rangle,\end{aligned} \tag{B.9}$$

$$\begin{aligned}\frac{1}{Z}\sum_{i,f} e^{-\beta E_i}\mathcal{K}^\dagger\mathcal{R} \approx\ & \langle\!\langle c^\dagger(4')c^\dagger(1')\rangle\!\rangle\langle\!\langle c(2)c(3)\rangle\!\rangle \\ & - \langle\!\langle c^\dagger(4')c(2)\rangle\!\rangle\langle\!\langle c^\dagger(1')c(3)\rangle\!\rangle \\ & + \langle\!\langle c^\dagger(4')c(3)\rangle\!\rangle\langle\!\langle c^\dagger(1')c(2)\rangle\!\rangle.\end{aligned} \tag{B.10}$$

The first term in each expression contains anomalous correlations, while the remaining two terms contain normal correlations. We therefore separate the following derivation into two parts: first the anomalous contribution, and then the normal contribution.

B.1 Anomalous Contribution

Since we consider a superconducting sample with the symmetries $S = +1$, $P^* = +1$, $O = +1$, and $T^* = -1$, we can simplify the first terms of Eqs. (B.7), (B.8), (B.9) and (B.10) as follows

$$\frac{1}{Z}\sum_{i,f} e^{-\beta E_i}\mathcal{K}^\dagger\mathcal{K} \approx \langle\!\langle c^\dagger_{\mathbf{p}'\sigma_2'}(t_2')c^\dagger_{-\mathbf{p}'\sigma_1'}(t_1')\rangle\!\rangle\langle\!\langle c_{-\mathbf{p}\sigma_1'}(t_1)c_{\mathbf{p}\sigma_2'}(t_2)\rangle\!\rangle \tag{B.11}$$

$$\begin{aligned}\frac{1}{Z}\sum_{i,f} e^{-\beta E_i}\mathcal{R}^\dagger\mathcal{R} &\approx \langle\!\langle c^\dagger_{\mathbf{p}'\sigma_1'}(t_2')c^\dagger_{-\mathbf{p}'\sigma_2'}(t_1')\rangle\!\rangle\langle\!\langle c_{-\mathbf{p}\sigma_2'}(t_1)c_{\mathbf{p}\sigma_1'}(t_2)\rangle\!\rangle \\ &= \langle\!\langle c^\dagger_{\mathbf{p}'\sigma_2'}(t_2')c^\dagger_{-\mathbf{p}'\sigma_1'}(t_1')\rangle\!\rangle\langle\!\langle c_{-\mathbf{p}\sigma_1'}(t_1)c_{\mathbf{p}\sigma_2'}(t_2)\rangle\!\rangle,\end{aligned} \tag{B.12}$$

$$\begin{aligned}\frac{1}{Z}\sum_{i,f} e^{-\beta E_i}\mathcal{R}^\dagger\mathcal{K} &\approx \langle\!\langle c^\dagger_{\mathbf{p}'\sigma_1'}(t_2')c^\dagger_{-\mathbf{p}'\sigma_2'}(t_1')\rangle\!\rangle\langle\!\langle c_{-\mathbf{p}\sigma_1'}(t_1)c_{\mathbf{p}\sigma_2'}(t_2)\rangle\!\rangle \\ &= \langle\!\langle c^\dagger_{\mathbf{p}'\sigma_2'}(t_2')c^\dagger_{-\mathbf{p}'\sigma_1'}(t_1')\rangle\!\rangle\langle\!\langle c_{-\mathbf{p}\sigma_1'}(t_1)c_{\mathbf{p}\sigma_2'}(t_2)\rangle\!\rangle,\end{aligned} \tag{B.13}$$

$$\frac{1}{Z}\sum_{i,f} e^{-\beta E_i}\mathcal{K}^\dagger\mathcal{R} \approx \langle\!\langle c^\dagger_{\mathbf{p}'\sigma_2'}(t_2')c^\dagger_{-\mathbf{p}'\sigma_1'}(t_1')\rangle\!\rangle\langle\!\langle c_{-\mathbf{p}\sigma_2'}(t_1)c_{\mathbf{p}\sigma_1'}(t_2)\rangle\!\rangle$$
$$= \langle\!\langle c^\dagger_{\mathbf{p}'\sigma_1'}(t_2')c^\dagger_{-\mathbf{p}'\sigma_2'}(t_1')\rangle\!\rangle\langle\!\langle c_{-\mathbf{p}\sigma_2'}(t_1)c_{\mathbf{p}\sigma_1'}(t_2)\rangle\!\rangle. \tag{B.14}$$

From the definition of the greater anomalous Green's function in Eqs. (4.31) and (4.32), we see that

$$\begin{aligned}\langle\!\langle c^\dagger_{\mathbf{p}'\sigma_1'}(t_1')c^\dagger_{-\mathbf{p}'\sigma_2'}(t_2')\rangle\!\rangle\langle\!\langle c_{-\mathbf{p}\sigma_2'}(t_1)c_{\mathbf{p}\sigma_1'}(t_2)\rangle\!\rangle &= \Big[iF^{\dagger>}(\mathbf{p}',t_1',t_2')\Big]\Big[iF^{>}(\mathbf{p},t_1,t_2)\Big]\\ &= -F^{\dagger>}(\mathbf{p}',t_1',t_2')F^{>}(\mathbf{p},t_1,t_2).\end{aligned} \tag{B.15}$$

Having applied Wick's theorem, we work henceforth within the resulting factorized approximation and use equality signs for the corresponding expressions. With this simplification, the anomalous part of the counting rate can be written as

$$\begin{aligned}P^{(2)}_{\text{anom}} = \frac{1}{\Delta t}\int_{-\Delta t/2}^{\Delta t/2}\mathrm{d}t_2\int_{t_2}^{\infty}\mathrm{d}t_1\int_{-\Delta t'/2}^{\Delta t'/2}\mathrm{d}t_2'\int_{t_2'}^{\infty}\mathrm{d}t_1'\sum_{\mathbf{p},\mathbf{p}'}\mathcal{A}\mathcal{A}^\dagger\gamma(\mathbf{p})\gamma^\dagger(\mathbf{p}')\\ \times\Big[V(\mathbf{p}+\mathbf{k}')-V(\mathbf{p}-\mathbf{k}')\Big]\Big[V(\mathbf{p}'+\mathbf{k}')-V(\mathbf{p}'-\mathbf{k}')\Big]\\ \times\Big[-F^{\dagger>}(\mathbf{p}',t_2',t_1')\Big]F^{>}(\mathbf{p},t_1,t_2).\end{aligned} \tag{B.16}$$

In equilibrium, the real-time Green's functions are time-translation invariant and therefore depend only on relative time. Hence,

$$F^{>}(\mathbf{p},t,t') = F^{>}(\mathbf{p},t-t'). \tag{B.17}$$

B.2 Normal Contribution

To simplify the contribution to the normal part, we use the definition in Eq. (4.36), and not that

$$-\langle\!\langle\cdots\rangle\!\rangle\langle\!\langle\cdots\rangle\!\rangle = (iG^<)(-iG'^<) = G^<G'^<, \tag{B.18}$$
$$\langle\!\langle\cdots\rangle\!\rangle\langle\!\langle\cdots\rangle\!\rangle = (-iG^<)(-iG'^<) = -G^<G'^<. \tag{B.19}$$

Then, from the $\mathcal{K}^\dagger\mathcal{K}$ term, we get the contribution

$$\begin{aligned}&G^<_{\sigma_1'\sigma_2'}(-\mathbf{p},t_1;\mathbf{p}',t_2')G^<_{\sigma_2'\sigma_1'}(\mathbf{p},t_2;-\mathbf{p}',t_1') - G^<_{\sigma_2'\sigma_2'}(\mathbf{p},t_2;\mathbf{p}',t_2')G^<_{\sigma_1'\sigma_1'}(-\mathbf{p},t_1;-\mathbf{p}',t_1')\\ &= \delta_{\mathbf{p},-\mathbf{p}'}\delta_{\sigma_1'\sigma_2'}G^<(\mathbf{p},t_1-t_2')G^<(-\mathbf{p},t_2-t_1') - \delta_{\mathbf{p}\mathbf{p}'}G^<_{\sigma_2'}(\mathbf{p},t_2-t_2')G^<_{\sigma_1'}(-\mathbf{p},t_1-t_1').\end{aligned} \tag{B.20}$$

From the $\mathcal{R}^\dagger\mathcal{R}$ term, we get the contribution

$$\begin{aligned}&G^<_{\sigma_2'\sigma_1'}(-\mathbf{p},t_1;\mathbf{p}',t_2')G^<_{\sigma_1'\sigma_2'}(\mathbf{p},t_2;-\mathbf{p}',t_1') - G^<_{\sigma_1'\sigma_1'}(\mathbf{p},t_2;\mathbf{p}',t_2')G^<_{\sigma_2'\sigma_2'}(-\mathbf{p},t_1;-\mathbf{p}',t_1')\\ &= \delta_{\mathbf{p},-\mathbf{p}'}\delta_{\sigma_1'\sigma_2'}G^<(\mathbf{p},t_1-t_2')G^<(-\mathbf{p},t_2-t_1') - \delta_{\mathbf{p}\mathbf{p}'}G^<_{\sigma_1'}(\mathbf{p},t_2-t_2')G^<_{\sigma_2'}(-\mathbf{p},t_1-t_1').\end{aligned} \tag{B.21}$$

From the $\mathcal{R}^\dagger\mathcal{K}$ term, we get the contribution

$$G^<_{\sigma_1'\sigma_1'}(-\mathbf{p},t_1;\mathbf{p}',t_2')G^<_{\sigma_2'\sigma_2'}(\mathbf{p},t_2;-\mathbf{p}',t_1') - G^<_{\sigma_2'\sigma_1'}(\mathbf{p},t_2;\mathbf{p}',t_2')G^<_{\sigma_1'\sigma_2'}(-\mathbf{p},t_1;-\mathbf{p}',t_1')$$
$$= \delta_{\mathbf{p},-\mathbf{p}'}G^<_{\sigma_1'}(\mathbf{p},t_1-t_2')G^<_{\sigma_2'}(-\mathbf{p},t_2-t_1') - \delta_{\mathbf{p}\mathbf{p}'}\delta_{\sigma_1'\sigma_2'}G^<(\mathbf{p},t_2-t_2')G^<(-\mathbf{p},t_1-t_1'). \tag{B.22}$$

From the $\mathcal{K}^\dagger\mathcal{R}$ term, we get the contribution

$$G^<_{\sigma_2'\sigma_2'}(-\mathbf{p},t_1;\mathbf{p}',t_2')G^<_{\sigma_1'\sigma_1'}(\mathbf{p},t_2;-\mathbf{p}',t_1') - G^<_{\sigma_1'\sigma_2'}(\mathbf{p},t_2;\mathbf{p}',t_2')G^<_{\sigma_2'\sigma_1'}(-\mathbf{p},t_1;-\mathbf{p}',t_1')$$
$$= \delta_{\mathbf{p},-\mathbf{p}'}G^<_{\sigma_2'}(\mathbf{p},t_1-t_2')G^<_{\sigma_1'}(-\mathbf{p},t_2-t_1') - \delta_{\mathbf{p}\mathbf{p}'}\delta_{\sigma_1'\sigma_2'}G^<(\mathbf{p},t_2-t_2')G^<(-\mathbf{p},t_1-t_1'). \tag{B.23}$$

With these simplifications, the normal part of the counting rate can then be written as

$$\begin{aligned}
P^{(2)}_{\text{norm}} = \frac{1}{\Delta t}\int_{-\Delta t/2}^{\Delta t/2}\mathrm{d}t_2\int_{t_2}^{\infty}\mathrm{d}t_1\int_{-\Delta t'/2}^{\Delta t'/2}\mathrm{d}t_2'\int_{t_2'}^{\infty}\mathrm{d}t_1'\sum_{\mathbf{p},\mathbf{p}'}\mathcal{A}\mathcal{A}^\dagger\gamma(\mathbf{p})\gamma^\dagger(\mathbf{p}')\\
\times\Big\{V(\mathbf{p}+\mathbf{k}')V(\mathbf{p}'+\mathbf{k}')\Big[\delta_{\mathbf{p},-\mathbf{p}'}\delta_{\sigma_1'\sigma_2'}G^<(\mathbf{p},t_1-t_2')G^<(-\mathbf{p},t_2-t_1')\\
-\delta_{\mathbf{p}\mathbf{p}'}G^<_{\sigma_2'}(\mathbf{p},t_2-t_2')G^<_{\sigma_1'}(-\mathbf{p},t_1-t_1').\Big]\\
+V(\mathbf{p}-\mathbf{k}')V(\mathbf{p}'-\mathbf{k}')\Big[\delta_{\mathbf{p},-\mathbf{p}'}\delta_{\sigma_1'\sigma_2'}G^<(\mathbf{p},t_1-t_2')G^<(-\mathbf{p},t_2-t_1')\\
-\delta_{\mathbf{p}\mathbf{p}'}G^<_{\sigma_1'}(\mathbf{p},t_2-t_2')G^<_{\sigma_2'}(-\mathbf{p},t_1-t_1').\Big]\\
-V(\mathbf{p}+\mathbf{k}')V(\mathbf{p}'-\mathbf{k}')\Big[\delta_{\mathbf{p},-\mathbf{p}'}G^<_{\sigma_1'}(\mathbf{p},t_1-t_2')G^<_{\sigma_2'}(-\mathbf{p},t_2-t_1')\\
-\delta_{\mathbf{p}\mathbf{p}'}\delta_{\sigma_1'\sigma_2'}G^<(\mathbf{p},t_2-t_2')G^<(-\mathbf{p},t_1-t_1').\Big]\\
-V(\mathbf{p}-\mathbf{k}')V(\mathbf{p}'+\mathbf{k}')\Big[\delta_{\mathbf{p},-\mathbf{p}'}G^<_{\sigma_2'}(\mathbf{p},t_1-t_2')G^<_{\sigma_1'}(-\mathbf{p},t_2-t_1')\\
-\delta_{\mathbf{p}\mathbf{p}'}\delta_{\sigma_1'\sigma_2'}G^<(\mathbf{p},t_2-t_2')G^<(-\mathbf{p},t_1-t_1').\Big]\Big\}.
\end{aligned} \tag{B.24}$$

B.3 Fourier Transform of the Normal Contribution

Because Eq. (4.53) follows two time structures, namely, the one in Eq. (4.54) and the one in q. (4.55), we choose to split this into two calculations. These can be put together at the end. We will use the Fourier transform

$$G^<(\mathbf{p},t-t') = \frac{1}{2\pi}\int_{-\infty}^{\infty}\mathrm{d}\omega\, e^{-i\omega(t-t')}G^<(\mathbf{p},\omega). \tag{B.25}$$

We begin with the first relative-time structure.

$$G^<(\mathbf{p},t_1-t_2')G^<(-\mathbf{p},t_2-t_1')$$

Using the Fourier transform in Eq. (B.25) we can write the integrals as

$$\begin{aligned}&\frac{1}{\Delta t}\int_{-\Delta t/2}^{\Delta t/2}\mathrm{d}t_2\int_{t_2}^{\infty}\mathrm{d}t_1\int_{-\Delta t'/2}^{\Delta t'/2}\mathrm{d}t_2'\int_{t_2'}^{\infty}\mathrm{d}t_1'\sum_{\mathbf{p}}\mathcal{A}\mathcal{A}^{\dagger}\gamma(\mathbf{p})\gamma^{\dagger}(-\mathbf{p})\\&\times\frac{1}{4\pi^2}\int_{-\infty}^{\infty}\mathrm{d}\omega\int_{-\infty}^{\infty}\mathrm{d}\omega'\,e^{-i\omega(t_1-t_2')}e^{-i\omega'(t_2-t_1')}G^{<}(\mathbf{p},\omega)G^{<}(-\mathbf{p},\omega').\end{aligned}\tag{B.26}$$

Some of these integrals require regularization in order to ensure convergence, and we will introduce this regularization later, when we evaluate these integrals We will therefore treat these integrals as regulated. This allows us to simplify this further by changing the order of integration and using the explicit expression of $\mathcal{A}$ found in Eq. (4.29), to

$$\begin{aligned}&\frac{1}{4\pi^2\Delta t}\int_{-\infty}^{\infty}\mathrm{d}\omega\int_{-\infty}^{\infty}\mathrm{d}\omega'\int_{-\Delta t/2}^{\Delta t/2}\mathrm{d}t_2\int_{t_2}^{\infty}\mathrm{d}t_1\int_{-\Delta t'/2}^{\Delta t'/2}\mathrm{d}t_2'\int_{t_2'}^{\infty}\mathrm{d}t_1'\sum_{\mathbf{p}}\gamma(\mathbf{p})\gamma^{\dagger}(-\mathbf{p})\\&\times e^{i(\epsilon_{\mathbf{p}}-\omega_{\mathbf{q}}-\omega')t_2}e^{i(-\epsilon_{\mathbf{p}}+2\epsilon_{\mathbf{k}'}-\omega)t_1}e^{i(-\epsilon_{\mathbf{p}}+\omega_{\mathbf{q}}+\omega')t_2'}e^{i(\epsilon_{\mathbf{p}}-2\epsilon_{\mathbf{k}'}+\omega)t_1'}G^{<}(\mathbf{p},\omega)G^{<}(-\mathbf{p},\omega').\end{aligned}\tag{B.27}$$

We introduce the relative-time variables

$$s=t_1-t_2,\qquad s'=t_1'-t_2',$$

and focus on the time integrals. The time integrals are then given by

$$\begin{aligned}&\frac{1}{\Delta t}\int_{-\Delta t/2}^{\Delta t/2}\mathrm{d}t_2\int_{0}^{\infty}\mathrm{d}s\int_{-\Delta t'/2}^{\Delta t'/2}\mathrm{d}t_2'\int_{0}^{\infty}\mathrm{d}s'\\&\times e^{i(-\omega_{\mathbf{q}}+2\epsilon_{\mathbf{k}'}-\omega-\omega')t_2}e^{i(-\epsilon_{\mathbf{p}}+2\epsilon_{\mathbf{k}'}-\omega)s-\eta s}e^{i(\omega_{\mathbf{q}}-2\epsilon_{\mathbf{k}'}+\omega+\omega')t_2'}e^{i(\epsilon_{\mathbf{p}}-2\epsilon_{\mathbf{k}'}+\omega')s'-\eta s'},\end{aligned}\tag{B.28}$$

where we introduced the regularization factor η to ensure convergence. To calculate the integrals over s and s' we use the result

$$\int_0^{\infty}\mathrm{d}t\,e^{ixt-\eta t}=\frac{i}{x+i\eta}.\tag{B.29}$$

Then the integral over s integrates to

$$\int_0^{\infty}\mathrm{d}s\,e^{i(-\epsilon_{\mathbf{p}}+2\epsilon_{\mathbf{k}'}-\omega)s-\eta s}=\frac{i}{-\epsilon_{\mathbf{p}}+2\epsilon_{\mathbf{k}'}-\omega+i\eta},\tag{B.30}$$

and the integral over s' integrates to

$$\int_0^{\infty}\mathrm{d}s'\,e^{i(\epsilon_{\mathbf{p}}-2\epsilon_{\mathbf{k}'}+\omega')s'-\eta s'}=\frac{i}{\epsilon_{\mathbf{p}}-2\epsilon_{\mathbf{k}'}+\omega'+i\eta}=\frac{-i}{-\epsilon_{\mathbf{p}}+2\epsilon_{\mathbf{k}'}-\omega'-i\eta}.\tag{B.31}$$

We now have the two integrals over t_2 and t_2' left. Here we notice that

$$\begin{aligned}&\frac{1}{\Delta t}\int_{-\Delta t/2}^{\Delta t/2}\mathrm{d}t_2\int_{-\Delta t'/2}^{\Delta t'/2}\mathrm{d}t_2'\,e^{i(-\omega_{\mathbf{q}}+2\epsilon_{\mathbf{k}'}-\omega-\omega')t_2}e^{i(\omega_{\mathbf{q}}-2\epsilon_{\mathbf{k}'}+\omega+\omega')t_2'}\\&=\frac{1}{\Delta t}\int_{-\Delta t/2}^{\Delta t/2}\mathrm{d}t_2\int_{-\Delta t'/2}^{\Delta t'/2}\mathrm{d}t_2'\,e^{i(-\omega_{\mathbf{q}}+2\epsilon_{\mathbf{k}'}-\omega-\omega')t_2}e^{-i(-\omega_{\mathbf{q}}+2\epsilon_{\mathbf{k}'}-\omega-\omega')t_2'}\\&=\frac{1}{\Delta t}\left|\int_{-\Delta t/2}^{\Delta t/2}\mathrm{d}t_2\,e^{i(-\omega_{\mathbf{q}}+2\epsilon_{\mathbf{k}'}-\omega-\omega')t_2}\right|^2\end{aligned}\tag{B.32}$$

and this integral is calculated using the relation

$$\int_{-\Delta t/2}^{\Delta t/2} \mathrm{d}t'\, e^{ixt'} = \frac{2\sin\left(x\Delta t/2\right)}{x}. \tag{B.33}$$

Using this, we get

$$\begin{aligned}\frac{1}{\Delta t}\left|\int_{-\Delta t/2}^{\Delta t/2} \mathrm{d}t_2\, e^{i(-\omega_{\mathbf{q}}+2\epsilon_{\mathbf{k}'}-\omega-\omega')t_2}\right|^2 &= \frac{1}{\Delta t}\left|\frac{2\sin\left[(-\omega_{\mathbf{q}}+2\epsilon_{\mathbf{k}'}-\omega-\omega')\Delta t/2\right]}{-\omega_{\mathbf{q}}+2\epsilon_{\mathbf{k}'}-\omega-\omega'}\right|^2 \\ &= 2\frac{2}{\Delta t}\frac{\sin^2\left[(-\omega_{\mathbf{q}}+2\epsilon_{\mathbf{k}'}-\omega-\omega')\Delta t/2\right]}{(-\omega_{\mathbf{q}}+2\epsilon_{\mathbf{k}'}-\omega-\omega')^2} \\ &= 2\frac{\sin^2\left[(-\omega_{\mathbf{q}}+2\epsilon_{\mathbf{k}'}-\omega-\omega')\Delta t/2\right]}{(-\omega_{\mathbf{q}}+2\epsilon_{\mathbf{k}'}-\omega-\omega')^2\Delta t/2}.\end{aligned} \tag{B.34}$$

In the long-time limit, we can use Eq. (2.49) to find

$$\lim_{\Delta t\to\infty} 2\frac{\sin^2\left[(-\omega_{\mathbf{q}}+2\epsilon_{\mathbf{k}'}-\omega-\omega')\Delta t/2\right]}{(-\omega_{\mathbf{q}}+2\epsilon_{\mathbf{k}'}-\omega-\omega')^2\Delta t/2} = 2\pi\delta(-\omega_{\mathbf{q}}+2\epsilon_{\mathbf{k}'}-\omega-\omega'). \tag{B.35}$$

Putting these results back together gives us

$$\begin{aligned}&\frac{2\pi}{4\pi^2}\int_{-\infty}^{\infty}\mathrm{d}\omega\int_{-\infty}^{\infty}\mathrm{d}\omega'\,\delta(-\omega_{\mathbf{q}}+2\epsilon_{\mathbf{k}'}-\omega-\omega') \\ &\times\frac{i}{-\epsilon_{\mathbf{p}}+2\epsilon_{\mathbf{k}'}-\omega+i\eta}\frac{-i}{-\epsilon_{\mathbf{p}}+2\epsilon_{\mathbf{k}'}-\omega'-i\eta}G^<(\mathbf{p},\omega)G^<(-\mathbf{p},\omega'),\end{aligned} \tag{B.36}$$

and integrating out ω' gives

$$\frac{1}{2\pi}\int_{-\infty}^{\infty}\mathrm{d}\omega\,\frac{1}{-\epsilon_{\mathbf{p}}+2\epsilon_{\mathbf{k}'}-\omega+i\eta}\frac{1}{-\epsilon_{\mathbf{p}}+\omega_{\mathbf{q}}+\omega-i\eta}G^<(\mathbf{p},\omega)G^<(-\mathbf{p},-\omega_{\mathbf{q}}+2\epsilon_{\mathbf{k}'}-\omega). \tag{B.37}$$

The simplified Fourier transform of Eq. (B.26) is then given by

$$\begin{aligned}&\frac{1}{2\pi}\int_{-\infty}^{\infty}\mathrm{d}\omega\sum_{\mathbf{p}}\gamma(\mathbf{p})\gamma^\dagger(-\mathbf{p}) \\ &\times\frac{1}{-\epsilon_{\mathbf{p}}+2\epsilon_{\mathbf{k}'}-\omega+i\eta}\frac{1}{-\epsilon_{\mathbf{p}}+\omega_{\mathbf{q}}+\omega-i\eta}G^<(\mathbf{p},\omega)G^<(-\mathbf{p},-\omega_{\mathbf{q}}+2\epsilon_{\mathbf{k}'}-\omega).\end{aligned} \tag{B.38}$$

This concludes the Fourier transform of the first structure.

We continue with the second relative-time structure.

$$G^<(\mathbf{p},t_2-t_2')G^<(-\mathbf{p},t_1-t_1')$$

Using the Fourier transform in Eq. (B.25) we can write the integrals as

$$\begin{aligned}&\frac{1}{\Delta t}\int_{-\Delta t/2}^{\Delta t/2}\mathrm{d}t_2\int_{t_2}^{\infty}\mathrm{d}t_1\int_{-\Delta t'/2}^{\Delta t'/2}\mathrm{d}t_2'\int_{t_2'}^{\infty}\mathrm{d}t_1'\sum_{\mathbf{p}}\mathcal{A}\mathcal{A}^\dagger\gamma(\mathbf{p})\gamma^\dagger(\mathbf{p}) \\ &\times\frac{1}{4\pi^2}\int_{-\infty}^{\infty}\mathrm{d}\omega\int_{-\infty}^{\infty}\mathrm{d}\omega'\,e^{-i\omega(t_2-t_2')}e^{-i\omega'(t_1-t_1')}G^<(\mathbf{p},\omega)G^<(-\mathbf{p},\omega').\end{aligned} \tag{B.39}$$

Just as in the previous case, some of the integrals require regularization to ensure convergence, and since we will regularize these integrals later, we treat them as regularized. This is so we can simplify this further by changing the order of integration, and if we use the explicit expression of $\mathcal{A}$, found in Eq. (4.29), we can write this as

$$\begin{aligned}&\frac{1}{4\pi^2\Delta t}\int_{-\infty}^{\infty}\mathrm{d}\omega\int_{-\infty}^{\infty}\mathrm{d}\omega'\int_{-\Delta t/2}^{\Delta t/2}\mathrm{d}t_2\int_{t_2}^{\infty}\mathrm{d}t_1\int_{-\Delta t'/2}^{\Delta t'/2}\mathrm{d}t_2'\int_{t_2'}^{\infty}\mathrm{d}t_1'\sum_{\mathbf{p}}\gamma(\mathbf{p})\gamma^\dagger(\mathbf{p})\\&\times e^{i(\epsilon_{\mathbf{p}}-\omega_{\mathbf{q}}-\omega)t_2}e^{i(-\epsilon_{\mathbf{p}}+2\epsilon_{\mathbf{k}'}-\omega')t_1}e^{i(-\epsilon_{\mathbf{p}}+\omega_{\mathbf{q}}+\omega)t_2'}e^{i(\epsilon_{\mathbf{p}}-2\epsilon_{\mathbf{k}'}+\omega')t_1'}G^<(\mathbf{p},\omega)G^<(-\mathbf{p},\omega').\end{aligned}\tag{B.40}$$

We introduce the relative-time variables

$$s=t_1-t_2,\qquad s'=t_1'-t_2',\tag{B.41}$$

and the expression simplifies to

$$\begin{aligned}&\frac{1}{4\pi^2\Delta t}\int_{-\infty}^{\infty}\mathrm{d}\omega\int_{-\infty}^{\infty}\mathrm{d}\omega'\int_{-\Delta t/2}^{\Delta t/2}\mathrm{d}t_2\int_{0}^{\infty}\mathrm{d}s\int_{-\Delta t'/2}^{\Delta t'/2}\mathrm{d}t_2'\int_{0}^{\infty}\mathrm{d}s'\sum_{\mathbf{p}}\gamma(\mathbf{p})\gamma^\dagger(\mathbf{p})\\&\times e^{i(-\omega_{\mathbf{q}}+2\epsilon_{\mathbf{k}'}-\omega-\omega')t_2}e^{i(-\epsilon_{\mathbf{p}}+2\epsilon_{\mathbf{k}'}-\omega')s-\eta s}e^{-i(-\omega_{\mathbf{q}}+2\epsilon_{\mathbf{k}'}-\omega-\omega')t_2'}e^{i(\epsilon_{\mathbf{p}}-2\epsilon_{\mathbf{k}'}+\omega')s'-\eta s'}\\&\times G^<(\mathbf{p},\omega)G^<(-\mathbf{p},\omega').\end{aligned}\tag{B.42}$$

The s integral integrates to

$$\int_0^{\infty}\mathrm{d}s\,e^{i(-\epsilon_{\mathbf{p}}+2\epsilon_{\mathbf{k}'}-\omega')s-\eta s}=\frac{i}{-\epsilon_{\mathbf{p}}+2\epsilon_{\mathbf{k}'}-\omega'+i\eta},\tag{B.43}$$

and the s' integral integrates to

$$\int_0^{\infty}\mathrm{d}s'\,e^{i(\epsilon_{\mathbf{p}}-2\epsilon_{\mathbf{k}'}+\omega')s'-\eta s'}=\frac{i}{\epsilon_{\mathbf{p}}-2\epsilon_{\mathbf{k}'}+\omega'+i\eta}=\frac{-i}{-\epsilon_{\mathbf{p}}+2\epsilon_{\mathbf{k}'}-\omega'-i\eta}.\tag{B.44}$$

Multiplying the two results together gives

$$\frac{i}{-\epsilon_{\mathbf{p}}+2\epsilon_{\mathbf{k}'}-\omega'+i\eta}\times\frac{-i}{-\epsilon_{\mathbf{p}}+2\epsilon_{\mathbf{k}'}-\omega'-i\eta}=\left|\frac{1}{-\epsilon_{\mathbf{p}}+2\epsilon_{\mathbf{k}'}-\omega'+i\eta}\right|^2.\tag{B.45}$$

We notice that the t_2' exponential is just the complex conjugate of the t_2 exponential. We can therefore solve the two integrals as

$$\begin{aligned}&\frac{1}{\Delta t}\int_{-\Delta t/2}^{\Delta t/2}\mathrm{d}t_2\int_{-\Delta t'/2}^{\Delta t'/2}\mathrm{d}t_2'\,e^{i(-\omega_{\mathbf{q}}+2\epsilon_{\mathbf{k}'}-\omega-\omega')t_2}e^{-i(-\omega_{\mathbf{q}}+2\epsilon_{\mathbf{k}'}-\omega-\omega')t_2'}\\&=\frac{1}{\Delta t}\left|\int_{-\Delta t/2}^{\Delta t/2}\mathrm{d}t_2\,e^{i(-\omega_{\mathbf{q}}+2\epsilon_{\mathbf{k}'}-\omega-\omega')t_2}\right|^2\\&=\frac{1}{\Delta t}\left|\frac{2\sin\left[(-\omega_{\mathbf{q}}+2\epsilon_{\mathbf{k}'}-\omega-\omega')\Delta t/2\right]}{-\omega_{\mathbf{q}}+2\epsilon_{\mathbf{k}'}-\omega-\omega'}\right|^2\\&=2\frac{\sin^2\left[(-\omega_{\mathbf{q}}+2\epsilon_{\mathbf{k}'}-\omega-\omega')\Delta t/2\right]}{(-\omega_{\mathbf{q}}+2\epsilon_{\mathbf{k}'}-\omega-\omega')^2\Delta t/2},\end{aligned}\tag{B.46}$$

and in the limit as $\eta \to 0^+$ we get

$$\lim_{\eta\to 0^+} 2\frac{\sin^2\left[(-\omega_{\mathbf{q}} + 2\epsilon_{\mathbf{k}'} - \omega - \omega')\Delta t/2\right]}{(-\omega_{\mathbf{q}} + 2\epsilon_{\mathbf{k}'} - \omega - \omega')^2\Delta t/2} = 2\pi\delta(-\omega_{\mathbf{q}} + 2\epsilon_{\mathbf{k}'} - \omega - \omega'). \tag{B.47}$$

We therefore have

$$\begin{aligned}&\frac{2\pi}{4\pi^2}\int_{-\infty}^{\infty}\mathrm{d}\omega\int_{-\infty}^{\infty}\mathrm{d}\omega'\,\delta(-\omega_{\mathbf{q}} + 2\epsilon_{\mathbf{k}'} - \omega - \omega')\sum_{\mathbf{p}}\gamma(\mathbf{p})\gamma^\dagger(\mathbf{p})\\ &\times\left|\frac{1}{-\epsilon_{\mathbf{p}} + 2\epsilon_{\mathbf{k}'} - \omega' + i\eta}\right|^2 G^<(\mathbf{p},\omega)G^<(-\mathbf{p},\omega'),\end{aligned} \tag{B.48}$$

and integrating over ω' forces $\omega' = -\omega_{\mathbf{q}} + 2\epsilon_{\mathbf{k}'} - \omega$ such that we get

$$\frac{1}{2\pi}\int_{-\infty}^{\infty}\mathrm{d}\omega\,\sum_{\mathbf{p}}\gamma(\mathbf{p})\gamma^\dagger(\mathbf{p})\left|\frac{1}{\omega_{\mathbf{q}} - \epsilon_{\mathbf{p}} + \omega + i\eta}\right|^2 G^<(\mathbf{p},\omega)G^<(-\mathbf{p}, -\omega_{\mathbf{q}} + 2\epsilon_{\mathbf{k}'} - \omega), \tag{B.49}$$

which is the simplified Fourier transform of Eq. (B.39).

C

Frequency Symmetry of Anomalous Spectral Functions

In this appendix, we derive how the frequency symmetry of the anomalous Matsubara Green's function is reflected in the corresponding anomalous spectral function. The derivations are performed under the assumption that the anomalous Green's function $\mathcal{F}(i\omega_n)$ is Hermitian. The retarded and advanced anomalous Green's functions are obtained through the analytic continuations [4]

$$\mathcal{F}(i\omega_n \to \omega + i\eta) = F^R(\omega), \tag{C.1}$$

$$\mathcal{F}(i\omega_n \to \omega - i\eta) = F^A(\omega). \tag{C.2}$$

The appendix is organized into two sections, where the even-frequency and odd-frequency anomalous Green's functions are considered separately.

C.1 Even-Frequency Anomalous Green's Function

Consider that $\mathcal{F}(i\omega_n)$ is even in frequency,

$$\mathcal{F}(i\omega_n) = \mathcal{F}(-i\omega_n). \tag{C.3}$$

Then, from the analytic continuation in Eqs. (C.1) and (C.2), we must have

$$F^R(\omega) = \mathcal{F}(i\omega_n \to \omega + i\eta) = \mathcal{F}(-i\omega_n \to -\omega - i\eta) = F^A(-\omega), \tag{C.4}$$

and

$$F^A(\omega) = \mathcal{F}(i\omega_n \to \omega - i\eta) = \mathcal{F}(-i\omega_n \to -\omega + i\eta) = F^R(-\omega). \tag{C.5}$$

Using this relation together with Eq. (4.65), we find that

$$F^R(\omega) = \Big[F^A(\omega)\Big]^* = \Big[F^R(-\omega)\Big]^*. \tag{C.6}$$

From the definition of the anomalous spectral function in Eq. (4.63), we can write

$$\begin{aligned} A_F(\omega) &= -\frac{1}{\pi}\,\mathrm{Im}\,F^R(\omega) \\ &= -\frac{1}{\pi}\,\mathrm{Im}\Big[F^R(-\omega)\Big]^* \\ &= \frac{1}{\pi}\,\mathrm{Im}\,F^R(-\omega) \\ &= -A_F(-\omega) \end{aligned} \tag{C.7}$$

where we see that

$$A_F(\omega) = -A_F(-\omega) \tag{C.8}$$

is odd in frequency.

C.2 Odd-Frequency Anomalous Green's Function

For $\mathcal{F}(i\omega_n)$ odd in frequency, such that

$$\mathcal{F}(i\omega_n) = -\mathcal{F}(-i\omega_n). \tag{C.9}$$

We get from the analytic continuation in Eqs. (C.1) and (C.2) that

$$F^R(\omega) = \mathcal{F}(i\omega_n \to \omega + i\eta) = -\mathcal{F}(-i\omega_n \to -\omega - i\eta) = -F^A(-\omega), \tag{C.10}$$

and

$$F^A(\omega) = \mathcal{F}(i\omega_n \to \omega - i\eta) = -\mathcal{F}(-i\omega_n \to -\omega + i\eta) = -F^R(-\omega) \tag{C.11}$$

needs to hold. With this relation together with Eq. (4.65), we find that

$$F^R(\omega) = \Big[F^A(\omega)\Big]^* = \Big[-F^R(-\omega)\Big]^*. \tag{C.12}$$

From the definition of the anomalous spectral function in Eq. (4.63), we can write

$$\begin{aligned} A_F(\omega) &= -\frac{1}{\pi}\,\mathrm{Im}\,F^R(\omega) \\ &= -\frac{1}{\pi}\,\mathrm{Im}\Big[-F^R(-\omega)\Big]^* \\ &= \frac{1}{\pi}\,\mathrm{Im}\Big[F^R(-\omega)\Big]^* \\ &= -\frac{1}{\pi}\,\mathrm{Im}\,F^R(-\omega) \\ &= A_F(-\omega) \end{aligned} \tag{C.13}$$

where we see that

$$A_F(\omega) = A_F(-\omega) \tag{C.14}$$

is even in frequency.

D

Derivation of the Explicit Counting-Rate Contributions

In this appendix, we provide the derivations of the greater anomalous Green's function, the lesser normal Green's function, and the anomalous and normal contributions to the counting rate for the d-wave superconducting state considered in Ref. [10]. The derivations are performed for the case of zero center-of-mass momentum. The appendix is organized into four sections: the first two sections derive the greater anomalous and lesser normal Green's functions, respectively, while the final two sections derive the anomalous and normal contributions to the counting rate.

D.1 Derivation of the Greater Anomalous Green's Function

From Eq. (3.24) in Sec. 3.1 we have the following expression for the anomalous Green's function

$$F(\mathbf{p}, i\omega_n) = \frac{\Delta(\mathbf{p})}{\omega_n^2 + E_{\mathbf{p}}^2}. \tag{D.1}$$

Through analytic continuation, we get the retarded anomalous Green's function

$$F^R(\mathbf{p}, i\omega_n \to \omega + i\eta) = \frac{\Delta(\mathbf{p})}{E_{\mathbf{p}}^2 - (\omega + i\eta)^2} = -\frac{\Delta(\mathbf{p})}{2E_{\mathbf{p}}}\left(\frac{1}{\omega - E_{\mathbf{p}} + i\eta} - \frac{1}{\omega + E_{\mathbf{p}} + i\eta}\right), \tag{D.2}$$

and the advanced anomalous Green's function

$$F^A(\mathbf{p}, i\omega_n \to \omega - i\eta) = \frac{\Delta(\mathbf{p})}{E_{\mathbf{p}}^2 - (\omega - i\eta)^2} = -\frac{\Delta(\mathbf{p})}{2E_{\mathbf{p}}}\left(\frac{1}{\omega - E_{\mathbf{p}} - i\eta} - \frac{1}{\omega + E_{\mathbf{p}} - i\eta}\right). \tag{D.3}$$

To find the greater anomalous Green's function, we need to use Eq. (4.68) where we will assume that the corresponding equilibrium relations can also be applied to the anomalous Green's functions. Here, we need the imaginary part of the retarded anomalous Green's function. For the given anomalous Green's function in Eq. (D.1), the relation in Eq. (4.65) holds. Hence, we can use the standard relation

$$\operatorname{Im} z = \frac{z - \bar{z}}{2i}, \tag{D.4}$$

with $\bar{z}$ being the complex conjugate of z. Then,

$$\begin{aligned}\operatorname{Im} F^R(\mathbf{p},\omega) &= \frac{F^R(\mathbf{p},\omega) - F^A(\mathbf{p},\omega)}{2i} \\ &= -\frac{\Delta(\mathbf{p})}{4iE_\mathbf{p}}\left(\frac{1}{\omega - E_\mathbf{p} + i\eta} - \frac{1}{\omega - E_\mathbf{p} - i\eta} + \frac{1}{\omega + E_\mathbf{p} - i\eta} - \frac{1}{\omega + E_\mathbf{p} + i\eta}\right) \\ &= -2\pi i\frac{\Delta(\mathbf{p})}{4iE_\mathbf{p}}\left(\frac{1}{\pi}\frac{\eta}{(\omega + E_\mathbf{p})^2 + \eta^2} - \frac{1}{\pi}\frac{\eta}{(\omega - E_\mathbf{p})^2 + \eta^2}\right) \\ &= -\pi\frac{\Delta(\mathbf{p})}{2E_\mathbf{p}}\Big[\delta(\omega + E_\mathbf{p}) - \delta(\omega - E_\mathbf{p})\Big], \end{aligned} \tag{D.5}$$

where we have used that the regularization factor η is always to be understood in the limit $\eta \to 0^+$, so that Eq. (2.92) yields the Dirac delta functions. This can then be inserted into Eq. (4.68) to give

$$\begin{aligned} F^>(\mathbf{p},\omega) &= -2\pi i\frac{\Delta(\mathbf{p})}{2E_\mathbf{p}}\Big[1 - f(\omega)\Big]\Big[\delta(\omega + E_\mathbf{p}) - \delta(\omega - E_\mathbf{p})\Big] \\ &= 2\pi i\frac{\Delta(\mathbf{p})}{2E_\mathbf{p}}\Big\{\Big[1 - f(E_\mathbf{p})\Big]\delta(\omega - E_\mathbf{p}) - f(E_\mathbf{p})\delta(\omega + E_\mathbf{p})\Big\}, \end{aligned} \tag{D.6}$$

where we used $1 - f(\omega) = f(-\omega)$ together with the constraints imposed by the delta functions.

D.2 Derivation of the Lesser Green's Function

From Eq. (4.75) in Sec. 4.3 we have the following expression for the normal Green's function

$$\mathcal{G}(\mathbf{p}, i\omega_n) = \frac{u_\mathbf{p}^2}{i\omega_n - E_\mathbf{p}} + \frac{v_\mathbf{p}^2}{i\omega_n + E_\mathbf{p}}. \tag{D.7}$$

Through analytic continuation, we find the retarded Green's function as

$$G^R(\mathbf{p}, i\omega_n \to \omega + i\eta) = \frac{u_\mathbf{p}^2}{\omega - E_\mathbf{p} + i\eta} + \frac{v_\mathbf{p}^2}{\omega + E_\mathbf{p} + i\eta}. \tag{D.8}$$

In order to use Eq. (4.69), we first need to find the imaginary part of the retarded Green's function. We therefore introduce the variables

$$x^- = \omega - E_\mathbf{p}, \qquad x^+ = \omega + E_\mathbf{p}, \tag{D.9}$$

so that Eq. (D.8) can be written as

$$G^R(\mathbf{p},\omega) = \frac{u_\mathbf{p}^2}{x^- + i\eta} + \frac{v_\mathbf{p}^2}{x^+ + i\eta}. \tag{D.10}$$

We can then separate the real and imaginary part

$$\begin{aligned} G^R(\mathbf{p},\omega) &= \frac{u_\mathbf{p}^2(x^- + i\eta)}{(x^- + i\eta)(x^- - i\eta)} + \frac{v_\mathbf{p}^2(x^+ - i\eta)}{(x^+ + i\eta)(x^+ - i\eta)} \\ &= \frac{u_\mathbf{p}^2 x^-}{(x^-)^2 + \eta^2} + \frac{v_\mathbf{p}^2 x^+}{(x^+)^2 + \eta^2} + i\frac{-u_\mathbf{p}^2\eta}{(x^-)^2 + \eta^2} + i\frac{-v_\mathbf{p}^2\eta}{(x^+)^2 + \eta^2}, \end{aligned} \tag{D.11}$$

where we see that

$$\operatorname{Im} G^R(\mathbf{p},\omega) = -u_{\mathbf{p}}^2\pi\frac{1}{\pi}\frac{\eta}{(\omega-E_{\mathbf{p}})^2+\eta^2} - v_{\mathbf{p}}^2\pi\frac{1}{\pi}\frac{\eta}{(\omega+E_{\mathbf{p}})^2+\eta^2}. \tag{D.12}$$

Because the regularization factor η is always to be understood in the limit $\lim_{\eta\to 0^+}$, Eq. (2.92) simplifies this to

$$\operatorname{Im} G^R(\mathbf{p},\omega) = -\pi\Big[u_{\mathbf{p}}^2\delta(\omega-E_{\mathbf{p}}) + v_{\mathbf{p}}^2\delta(\omega+E_{\mathbf{p}})\Big]. \tag{D.13}$$

Then, from Eq. (4.69), we find the lesser Green's function to be

$$G^<(\mathbf{p},\omega) = 2\pi i f(\omega)\Big[u_{\mathbf{p}}^2\delta(\omega-E_{\mathbf{p}}) + v_{\mathbf{p}}^2\delta(\omega+E_{\mathbf{p}})\Big]. \tag{D.14}$$

D.3 Derivation of the Anomalous Counting-Rate Contribution

$$P_{\text{anom}}^{(2)} = 2\pi\delta(\omega_{\mathbf{q}}-2\epsilon_{\mathbf{k}'})\left|\frac{1}{2\pi}\sum_{\mathbf{p}} W_{\text{even}}(\mathbf{p},\mathbf{k}')\int_0^\infty \mathrm{d}s\, e^{i(\omega_{\mathbf{q}}-\epsilon_{\mathbf{p}})s}\int_{-\infty}^{\infty}\mathrm{d}\omega\, e^{-i\omega s}F^>(\mathbf{p},\omega)\right|^2. \tag{D.15}$$

We begin by inserting Eq. (D.6) into the anomalous contribution to the counting rate in Eq. (4.49). This gives

$$\begin{aligned} P_{\text{anom}}^{(2)} = 2\pi\delta(\omega_{\mathbf{q}}-2\epsilon_{\mathbf{k}'})\Bigg|\sum_{\mathbf{p}}\frac{\Delta(\mathbf{p})}{2E_{\mathbf{p}}}W_{\text{even}}(\mathbf{p},\mathbf{k}')\int_0^\infty \mathrm{d}s\, e^{i(\omega_{\mathbf{q}}-\epsilon_{\mathbf{p}})s} \\ \times\int_{-\infty}^{\infty}\mathrm{d}\omega\, e^{-i\omega s}\Big\{\Big[1-f(E_{\mathbf{p}})\Big]\delta(\omega-E_{\mathbf{p}}) - f(E_{\mathbf{p}})\delta(\omega+E_{\mathbf{p}})\Big\}\Bigg|^2, \end{aligned} \tag{D.16}$$

where the factor i vanish due to the modulus square. Integration over ω gives

$$\begin{aligned} P_{\text{anom}}^{(2)} = 2\pi\delta(\omega_{\mathbf{q}}-2\epsilon_{\mathbf{k}'})\Bigg|\sum_{\mathbf{p}}\frac{\Delta(\mathbf{p})}{2E_{\mathbf{p}}}W_{\text{even}}(\mathbf{p},\mathbf{k}')\int_0^\infty \mathrm{d}s\, e^{i(\omega_{\mathbf{q}}-\epsilon_{\mathbf{p}})s} \\ \times\Big\{e^{-iE_{\mathbf{p}}s}\Big[1-f(E_{\mathbf{p}})\Big] - e^{iE_{\mathbf{p}}s}f(E_{\mathbf{p}})\Big\}\Bigg|^2. \end{aligned} \tag{D.17}$$

The relative-time integral requires regularization to ensure convergence. We therefore introduce the regularization factor η that should be understood as the limit $\eta\to 0^+$. The relative-time integral can then be written as

$$\int_0^\infty \mathrm{d}s\, e^{i(\omega_{\mathbf{q}}-\epsilon_{\mathbf{p}}-E_{\mathbf{p}})s-\eta s}\Big[1-f(E_{\mathbf{p}})\Big] - \int_0^\infty \mathrm{d}s\, e^{i(\omega_{\mathbf{q}}-\epsilon_{\mathbf{p}}+E_{\mathbf{p}})s-\eta s}f(E_{\mathbf{p}}). \tag{D.18}$$

This can be integrated using the result of Eq. (2.84), so that we get

$$i\frac{1-f(E_{\mathbf{p}})}{\omega_{\mathbf{q}}-\epsilon_{\mathbf{p}}-E_{\mathbf{p}}} - i\frac{f(E_{\mathbf{p}})}{\omega_{\mathbf{q}}-\epsilon_{\mathbf{p}}+E_{\mathbf{p}}}. \tag{D.19}$$

Inserting this back into Eq. (D.17) gives

$$P^{(2)}_{\text{anom}} = 2\pi\delta(\omega_{\mathbf{q}} - 2\epsilon_{\mathbf{k}'})\Bigg|\sum_{\mathbf{p}} \frac{\Delta(\mathbf{p})}{2E_{\mathbf{p}}} W_{\text{even}}(\mathbf{p},\mathbf{k}') \times\left[\frac{f(E_{\mathbf{p}})}{\omega_{\mathbf{q}} - \epsilon_{\mathbf{p}} + E_{\mathbf{p}}} - \frac{1-f(E_{\mathbf{p}})}{\omega_{\mathbf{q}} - \epsilon_{\mathbf{p}} - E_{\mathbf{p}}}\right]\Bigg|^2, \tag{D.20}$$

where we again used $|i|^2 = 1$. Here, we have also utilized $|a-b|^2 = |b-a|^2$ to write it more in line with how they express it in Ref. [10]. To simplify this further, we approximate the effective electron–photon coupling matrix element as momentum independent, $\gamma(\mathbf{p}) \to \gamma_0$. Since this is to be compared to Ref. [10], we use their definition of the gap function

$$\Delta(\mathbf{p}) = \frac{\Delta_0}{2}\Big[\cos(p_x) - \cos(p_y)\Big]. \tag{D.21}$$

We may notice that this definition makes the gap function symmetric in $\mathbf{p}$, so that $\Delta(\mathbf{p}) = \Delta(-\mathbf{p})$. For the system in question, it also holds that $\epsilon_{\mathbf{p}} = \epsilon_{-\mathbf{p}}$, leading to $E_{\mathbf{p}} = E_{-\mathbf{p}}$. Then, we may simplify the kernel as follows

$$\begin{aligned}\sum_{\mathbf{p}} \gamma_0\Big[V(\mathbf{p}+\mathbf{k}') + V(\mathbf{p}-\mathbf{k}')\Big] &= \sum_{\mathbf{p}} \gamma_0\Big[V(-\mathbf{p}+\mathbf{k}') + V(\mathbf{p}-\mathbf{k}')\Big] \\ &= 2\gamma_0 \sum_{\mathbf{p}} V(\mathbf{k}'-\mathbf{p}),\end{aligned} \tag{D.22}$$

where we let $\mathbf{p} \to -\mathbf{p}$ in the first step and used that the effective Coulomb potential is symmetric. With this simplification, Eq. (D.20) becomes

$$P^{(2)}_{\text{anom}} = 8\pi\delta(\omega_{\mathbf{q}} - 2\epsilon_{\mathbf{k}'})\Bigg|\gamma_0 \sum_{\mathbf{p}} V(\mathbf{k}'-\mathbf{p}) \frac{\Delta(\mathbf{p})}{2E_{\mathbf{p}}} \times\left[\frac{f(E_{\mathbf{p}})}{\omega_{\mathbf{q}} + E_{\mathbf{p}} - \epsilon_{\mathbf{p}} + i\eta} - \frac{1-f(E_{\mathbf{p}})}{\omega_{\mathbf{q}} - E_{\mathbf{p}} - \epsilon_{\mathbf{p}} + i\eta}\right]\Bigg|^2. \tag{D.23}$$

D.4 Derivation of the Normal Counting-Rate Contribution

We begin by approximating the effective electron–photon coupling matrix element as momentum independent and real, $\gamma(\mathbf{p}) \to \gamma_0$ with $\gamma_0^\dagger = \gamma_0$. Because we are working in the opposite spin channel, the normal contribution to the counting rate

in Eq. (4.58) can be written as

$$\begin{aligned} P_{\text{norm}}^{(2)} = \frac{1}{2\pi}\int_{-\infty}^{\infty}\mathrm{d}\omega_1 \int_{-\infty}^{\infty}\mathrm{d}\omega_2 \sum_{\mathbf{p}}\gamma_0^2 \\ \times\Big\{\mathcal{D}_1\Big[-K(\mathbf{p}_+,-\mathbf{p}_+)G^<(\mathbf{p},\omega_1)G^<(-\mathbf{p},2\epsilon_{\mathbf{k}'}-\omega_{\mathbf{q}}-\omega_1) \\ - K(\mathbf{p}_-,-\mathbf{p}_-)G^<(\mathbf{p},\omega_1)G^<(-\mathbf{p},2\epsilon_{\mathbf{k}'}-\omega_{\mathbf{q}}-\omega_1)\Big] \\ + \mathcal{D}_2\Big[-K(\mathbf{p}_+,\mathbf{p}_+)G^<(\mathbf{p},\omega_2)G^<(-\mathbf{p},2\epsilon_{\mathbf{k}'}-\omega_{\mathbf{q}}-\omega_2) \\ - K(\mathbf{p}_-,\mathbf{p}_-)G^<(\mathbf{p},\omega_2)G^<(-\mathbf{p},2\epsilon_{\mathbf{k}'}-\omega_{\mathbf{q}}-\omega_2)\Big]\Big\}. \end{aligned} \tag{D.24}$$

Due to the symmetry arguments above Eq. (D.22) of Appendix D.3, it follows that the two coherence factors $u_{\mathbf{p}}$ and $v_{\mathbf{p}}$ are also symmetric in $\mathbf{p}$. With the explicit expression of the lesser Green's function in Eq. (D.14), we may notice that

$$G^<(\mathbf{p},\omega) = G^<(-\mathbf{p},\omega). \tag{D.25}$$

Thus, we can rename the dummy variable $\mathbf{p}\to-\mathbf{p}$ and use the symmetric property of the effective Coulomb potential to simplify Eq. (D.24) to

$$\begin{aligned} P_{\text{norm}}^{(2)} = \frac{2}{2\pi}\int_{-\infty}^{\infty}\mathrm{d}\omega_1 \int_{-\infty}^{\infty}\mathrm{d}\omega_2 \sum_{\mathbf{p}}\gamma_0^2 V(\mathbf{k}'-\mathbf{p})V(\mathbf{k}'-\mathbf{p}) \\ \times\Big\{\mathcal{D}_1\Big[-G^<(\mathbf{p},\omega_1)G^<(\mathbf{p},X-\omega_1)\Big] + \mathcal{D}_2\Big[-G^<(\mathbf{p},\omega_2)G^<(\mathbf{p},X-\omega_2)\Big]\Big\}. \end{aligned} \tag{D.26}$$

where we introduced the variable

$$X = 2\epsilon_{\mathbf{k}'} - \omega_{\mathbf{q}}. \tag{D.27}$$

From Eq. (D.14), we can write the product of the two lesser Green's functions as

$$\begin{aligned} -G^<(\mathbf{p},\omega_{1,2})G^<(\mathbf{p},X-\omega_{1,2}) = 4\pi^2 f(\omega_{1,2})f(X-\omega_{1,2}) \\ \times\Big\{u_{\mathbf{p}}^2u_{\mathbf{p}}^2\delta(\omega_{1,2}-E_{\mathbf{p}})\delta(X-\omega_{1,2}-E_{\mathbf{p}}) \\ + u_{\mathbf{p}}^2v_{\mathbf{p}}^2\delta(\omega_{1,2}-E_{\mathbf{p}})\delta(X-\omega_{1,2}+E_{\mathbf{p}}) \\ + v_{\mathbf{p}}^2u_{\mathbf{p}}^2\delta(\omega_{1,2}+E_{\mathbf{p}})\delta(X-\omega_{1,2}-E_{\mathbf{p}}) \\ + v_{\mathbf{p}}^2v_{\mathbf{p}}^2\delta(\omega_{1,2}+E_{\mathbf{p}})\delta(X-\omega_{1,2}+E_{\mathbf{p}})\Big\}. \end{aligned} \tag{D.28}$$

Since $\mathcal{D}_1$ and $\mathcal{D}_2$ are defined differently, and because the above expression includes four terms, we solve the integrals over $\omega_{1,2}$ separately.

Computing the integral with respect to ω_1

We proceed to compute

$$\begin{aligned}\int_{-\infty}^{\infty} \mathrm{d}\omega_1 \, \frac{f(\omega_1) f(X-\omega_1)}{(2\epsilon_{\mathbf{k}'} - \epsilon_{\mathbf{p}} - \omega_1 + i\eta)(\omega_{\mathbf{q}} - \epsilon_{\mathbf{p}} + \omega_1 - i\eta)} \\ \times \Big\{ u_{\mathbf{p}}^2 u_{\mathbf{p}}^2 \delta(\omega_1 - E_{\mathbf{p}}) \delta(X - \omega_1 - E_{\mathbf{p}}) \\ + u_{\mathbf{p}}^2 v_{\mathbf{p}}^2 \delta(\omega_1 - E_{\mathbf{p}}) \delta(X - \omega_1 + E_{\mathbf{p}}) \\ + v_{\mathbf{p}}^2 u_{\mathbf{p}}^2 \delta(\omega_1 + E_{\mathbf{p}}) \delta(X - \omega_1 - E_{\mathbf{p}}) \\ + v_{\mathbf{p}}^2 v_{\mathbf{p}}^2 \delta(\omega_1 + E_{\mathbf{p}}) \delta(X - \omega_1 + E_{\mathbf{p}}) \Big\}.\end{aligned} \tag{D.29}$$

To do this, we integrate each of the four terms separately. Beginning with the **first term**

$$\begin{aligned}&\int_{-\infty}^{\infty} \mathrm{d}\omega_1 \, \frac{u_{\mathbf{p}}^2 u_{\mathbf{p}}^2 f(\omega_1) f(X-\omega_1)}{(2\epsilon_{\mathbf{k}'} - \epsilon_{\mathbf{p}} - \omega_1 + i\eta)(\omega_{\mathbf{q}} - \epsilon_{\mathbf{p}} + \omega_1 - i\eta)} \delta(\omega_1 - E_{\mathbf{p}}) \delta(X - \omega_1 - E_{\mathbf{p}}) \\ &= \frac{u_{\mathbf{p}}^2 u_{\mathbf{p}}^2 f(E_{\mathbf{p}}) f(X - E_{\mathbf{p}})}{(2\epsilon_{\mathbf{k}'} - \epsilon_{\mathbf{p}} - E_{\mathbf{p}} + i\eta)(\omega_{\mathbf{q}} - \epsilon_{\mathbf{p}} + E_{\mathbf{p}} - i\eta)} \delta(X - 2E_{\mathbf{p}}) \\ &= \frac{u_{\mathbf{p}}^2 u_{\mathbf{p}}^2 f(E_{\mathbf{p}}) f(E_{\mathbf{p}})}{(\omega_{\mathbf{q}} - \epsilon_{\mathbf{p}} + E_{\mathbf{p}} + i\eta)(\omega_{\mathbf{q}} - \epsilon_{\mathbf{p}} + E_{\mathbf{p}} - i\eta)} \delta(\omega_{\mathbf{q}} - 2\epsilon_{\mathbf{k}'} + 2E_{\mathbf{p}}),\end{aligned} \tag{D.30}$$

where we used that the delta function imposes $X = 2E_{\mathbf{p}}$ and that $\delta(x) = \delta(-x)$ is symmetric. Furthermore, we inserted the explicit expression of X given by Eq. (D.27). The delta function then also imposes that $2\epsilon_{\mathbf{k}'} = \omega_{\mathbf{q}} + 2E_{\mathbf{p}}$, which we used. Once can see that the denominator takes the form of a modulus squared, hence we can write the expression as

$$\delta(\omega_{\mathbf{q}} - 2\epsilon_{\mathbf{k}'} + 2E_{\mathbf{p}}) \left| \frac{1}{\omega_{\mathbf{q}} - \epsilon_{\mathbf{p}} + E_{\mathbf{p}} + i\eta} \right|^2 u_{\mathbf{p}}^2 u_{\mathbf{p}}^2 f(E_{\mathbf{p}}) f(E_{\mathbf{p}}). \tag{D.31}$$

Continuing with the **second term**, we find

$$\begin{aligned}&\int_{-\infty}^{\infty} \mathrm{d}\omega_1 \, \frac{u_{\mathbf{p}}^2 v_{\mathbf{p}}^2 f(\omega_1) f(X-\omega_1)}{(2\epsilon_{\mathbf{k}'} - \epsilon_{\mathbf{p}} - \omega_1 + i\eta)(\omega_{\mathbf{q}} - \epsilon_{\mathbf{p}} + \omega_1 - i\eta)} \delta(\omega_1 - E_{\mathbf{p}}) \delta(X - \omega_1 + E_{\mathbf{p}}) \\ &= \frac{u_{\mathbf{p}}^2 v_{\mathbf{p}}^2 f(E_{\mathbf{p}}) f(X - E_{\mathbf{p}})}{(2\epsilon_{\mathbf{k}'} - \epsilon_{\mathbf{p}} - E_{\mathbf{p}} + i\eta)(\omega_{\mathbf{q}} - \epsilon_{\mathbf{p}} + E_{\mathbf{p}} - i\eta)} \delta(X) \\ &= \frac{u_{\mathbf{p}}^2 v_{\mathbf{p}}^2 f(E_{\mathbf{p}}) f(-E_{\mathbf{p}})}{(\omega_{\mathbf{q}} - \epsilon_{\mathbf{p}} - E_{\mathbf{p}} + i\eta)(\omega_{\mathbf{q}} - \epsilon_{\mathbf{p}} + E_{\mathbf{p}} - i\eta)} \delta(\omega_{\mathbf{q}} - 2\epsilon_{\mathbf{k}'}) \\ &= \frac{u_{\mathbf{p}}^2 v_{\mathbf{p}}^2 f(E_{\mathbf{p}}) \big[1 - f(E_{\mathbf{p}})\big]}{(\omega_{\mathbf{q}} - \epsilon_{\mathbf{p}} - E_{\mathbf{p}} + i\eta)(\omega_{\mathbf{q}} - \epsilon_{\mathbf{p}} + E_{\mathbf{p}} - i\eta)} \delta(\omega_{\mathbf{q}} - 2\epsilon_{\mathbf{k}'}).\end{aligned} \tag{D.32}$$

Here, we used the same kinds of simplifications as we did with the first term. Note that $\delta(X)$ imposes $X = 0$, which is why $f(X + E_{\mathbf{p}})$ could be simplified to $f(E_{\mathbf{p}})$. We have also used that $f(-E_{\mathbf{p}}) = 1 - f(E_{\mathbf{p}})$.

We compute the **third term**, which gives

$$\begin{aligned}
&\int_{-\infty}^{\infty} \mathrm{d}\omega_1 \, \frac{v_{\mathbf{p}}^2 u_{\mathbf{p}}^2 f(\omega_1) f(X-\omega_1)}{(2\epsilon_{\mathbf{k}'} - \epsilon_{\mathbf{p}} - \omega_1 + i\eta)(\omega_{\mathbf{q}} - \epsilon_{\mathbf{p}} + \omega_1 - i\eta)} \delta(\omega_1 + E_{\mathbf{p}}) \delta(X - \omega_1 + E_{\mathbf{p}}) \\
&= \frac{v_{\mathbf{p}}^2 u_{\mathbf{p}}^2 f(-E_{\mathbf{p}}) f(X+E_{\mathbf{p}})}{(2\epsilon_{\mathbf{k}'} - \epsilon_{\mathbf{p}} + E_{\mathbf{p}} + i\eta)(\omega_{\mathbf{q}} - \epsilon_{\mathbf{p}} - E_{\mathbf{p}} - i\eta)} \delta(X) \\
&= \frac{v_{\mathbf{p}}^2 u_{\mathbf{p}}^2 \big[1 - f(E_{\mathbf{p}})\big] f(E_{\mathbf{p}})}{(\omega_{\mathbf{q}} - \epsilon_{\mathbf{p}} + E_{\mathbf{p}} + i\eta)(\omega_{\mathbf{q}} - \epsilon_{\mathbf{p}} - E_{\mathbf{p}} - i\eta)} \delta(\omega_{\mathbf{q}} - 2\epsilon_{\mathbf{k}'}),
\end{aligned} \tag{D.33}$$

where we have used the same kinds of simplifications as we did for the first term.

We now compute the **fourth term**

$$\begin{aligned}
&\int_{-\infty}^{\infty} \mathrm{d}\omega_1 \, \frac{v_{\mathbf{p}}^2 v_{\mathbf{p}}^2 f(\omega_1) f(X-\omega_1)}{(2\epsilon_{\mathbf{k}'} - \epsilon_{\mathbf{p}} - \omega_1 + i\eta)(\omega_{\mathbf{q}} - \epsilon_{\mathbf{p}} + \omega_1 - i\eta)} \delta(\omega_1 + E_{\mathbf{p}}) \delta(X - \omega_1 + E_{\mathbf{p}}) \\
&= \frac{v_{\mathbf{p}}^2 v_{\mathbf{p}}^2 f(-E_{\mathbf{p}}) f(X+E_{\mathbf{p}})}{(2\epsilon_{\mathbf{k}'} - \epsilon_{\mathbf{p}} + E_{\mathbf{p}} + i\eta)(\omega_{\mathbf{q}} - \epsilon_{\mathbf{p}} - E_{\mathbf{p}} - i\eta)} \delta(X + 2E_{\mathbf{p}}) \\
&= \frac{v_{\mathbf{p}}^2 v_{\mathbf{p}}^2 f(-E_{\mathbf{p}}) f(-E_{\mathbf{p}})}{(\omega_{\mathbf{q}} - \epsilon_{\mathbf{p}} - E_{\mathbf{p}} + i\eta)(\omega_{\mathbf{q}} - \epsilon_{\mathbf{p}} - E_{\mathbf{p}} - i\eta)} \delta(\omega_{\mathbf{q}} - 2\epsilon_{\mathbf{k}'} - 2E_{\mathbf{p}}) \\
&= \frac{v_{\mathbf{p}}^2 v_{\mathbf{p}}^2 \big[1 - f(E_{\mathbf{p}})\big] \big[1 - f(E_{\mathbf{p}})\big]}{(\omega_{\mathbf{q}} - \epsilon_{\mathbf{p}} - E_{\mathbf{p}} + i\eta)(\omega_{\mathbf{q}} - \epsilon_{\mathbf{p}} - E_{\mathbf{p}} - i\eta)} \delta(\omega_{\mathbf{q}} - 2\epsilon_{\mathbf{k}'} - 2E_{\mathbf{p}}).
\end{aligned} \tag{D.34}$$

As with the first term, we notice that the denominator takes the form of a modulus squared. We therefore rewrite this as

$$\delta(\omega_{\mathbf{q}} - 2\epsilon_{\mathbf{k}'} - 2E_{\mathbf{p}}) \left| \frac{1}{\omega_{\mathbf{q}} - \epsilon_{\mathbf{p}} - E_{\mathbf{p}} + i\eta} \right|^2 v_{\mathbf{p}}^2 v_{\mathbf{p}}^2 \big[1 - f(E_{\mathbf{p}})\big] \big[1 - f(E_{\mathbf{p}})\big]. \tag{D.35}$$

Computing the integral with respect to ω_2

We want to compute

$$\begin{aligned}
\int_{-\infty}^{\infty} \mathrm{d}\omega_2 \left| \frac{1}{\omega_{\mathbf{q}} - \epsilon_{\mathbf{p}} + \omega_2 + i\eta} \right|^2 & f(\omega_2) f(X - \omega_2) \\
& \times \Big\{ u_{\mathbf{p}}^2 u_{\mathbf{p}}^2 \delta(\omega_2 - E_{\mathbf{p}}) \delta(X - \omega_2 - E_{\mathbf{p}}) \\
& \quad + u_{\mathbf{p}}^2 v_{\mathbf{p}}^2 \delta(\omega_2 - E_{\mathbf{p}}) \delta(X - \omega_2 + E_{\mathbf{p}}) \\
& \quad + v_{\mathbf{p}}^2 u_{\mathbf{p}}^2 \delta(\omega_2 + E_{\mathbf{p}}) \delta(X - \omega_2 - E_{\mathbf{p}}) \\
& \quad + v_{\mathbf{p}}^2 v_{\mathbf{p}}^2 \delta(\omega_2 + E_{\mathbf{p}}) \delta(X - \omega_2 + E_{\mathbf{p}}) \Big\}.
\end{aligned} \tag{D.36}$$

As before, we integrate each of the four terms separately. Beginning with the

first term

$$\begin{aligned}
&\int_{-\infty}^{\infty} \mathrm{d}\omega_2 \left| \frac{1}{\omega_\mathbf{q} - \epsilon_\mathbf{p} + \omega_2 + i\eta} \right|^2 u_\mathbf{p}^2 u_\mathbf{p}^2 f(\omega_2) f(X - \omega_2) \delta(\omega_2 - E_\mathbf{p}) \delta(X - \omega_2 - E_\mathbf{p}) \\
&= \left| \frac{1}{\omega_\mathbf{q} - \epsilon_\mathbf{p} + E_\mathbf{p} + i\eta} \right|^2 u_\mathbf{p}^2 u_\mathbf{p}^2 f(E_\mathbf{p}) f(X - E_\mathbf{p}) \delta(X - 2E_\mathbf{p}) \\
&= \delta(\omega_\mathbf{q} - 2\epsilon_{\mathbf{k}'} + 2E_\mathbf{p}) \left| \frac{1}{\omega_\mathbf{q} - \epsilon_\mathbf{p} + E_\mathbf{p} + i\eta} \right|^2 u_\mathbf{p}^2 u_\mathbf{p}^2 f(E_\mathbf{p}) f(E_\mathbf{p}),
\end{aligned} \tag{D.37}$$

where we used the symmetric property of the delta function, and that it imposes $X = 2E_\mathbf{p}$ for the simplifications in the last step.

Continuing with the **second term**, we find

$$\begin{aligned}
&\int_{-\infty}^{\infty} \mathrm{d}\omega_2 \left| \frac{1}{\omega_\mathbf{q} - \epsilon_\mathbf{p} + \omega_2 + i\eta} \right|^2 u_\mathbf{p}^2 v_\mathbf{p}^2 f(\omega_2) f(X - \omega_2) \delta(\omega_2 - E_\mathbf{p}) \delta(X - \omega_2 + E_\mathbf{p}) \\
&= \left| \frac{1}{\omega_\mathbf{q} - \epsilon_\mathbf{p} + E_\mathbf{p} + i\eta} \right|^2 u_\mathbf{p}^2 v_\mathbf{p}^2 f(E_\mathbf{p}) f(X - E_\mathbf{p}) \delta(X) \\
&= \delta(\omega_\mathbf{q} - 2\epsilon_{\mathbf{k}'}) \left| \frac{1}{\omega_\mathbf{q} - \epsilon_\mathbf{p} + E_\mathbf{p} + i\eta} \right|^2 u_\mathbf{p}^2 v_\mathbf{p}^2 f(E_\mathbf{p}) f(-E_\mathbf{p}) \\
&= \delta(\omega_\mathbf{q} - 2\epsilon_{\mathbf{k}'}) \left| \frac{1}{\omega_\mathbf{q} - \epsilon_\mathbf{p} + E_\mathbf{p} + i\eta} \right|^2 u_\mathbf{p}^2 v_\mathbf{p}^2 f(E_\mathbf{p}) \big[1 - f(E_\mathbf{p})\big],
\end{aligned} \tag{D.38}$$

where we used the same kinds of simplifications as we did for the first term, and the relation $f(-E_\mathbf{p}) = 1 - f(E_\mathbf{p})$.

We now compute the **third term**, which gives

$$\begin{aligned}
&\int_{-\infty}^{\infty} \mathrm{d}\omega_2 \left| \frac{1}{\omega_\mathbf{q} - \epsilon_\mathbf{p} + \omega_2 + i\eta} \right|^2 v_\mathbf{p}^2 u_\mathbf{p}^2 f(\omega_2) f(X - \omega_2) \delta(\omega_2 + E_\mathbf{p}) \delta(X - \omega_2 - E_\mathbf{p}) \\
&= \left| \frac{1}{\omega_\mathbf{q} - \epsilon_\mathbf{p} - E_\mathbf{p} + i\eta} \right|^2 v_\mathbf{p}^2 u_\mathbf{p}^2 f(-E_\mathbf{p}) f(X + E_\mathbf{p}) \delta(X) \\
&= \delta(\omega_\mathbf{q} - 2\epsilon_{\mathbf{k}'}) \left| \frac{1}{\omega_\mathbf{q} - \epsilon_\mathbf{p} - E_\mathbf{p} + i\eta} \right|^2 v_\mathbf{p}^2 u_\mathbf{p}^2 f(-E_\mathbf{p}) f(E_\mathbf{p}) \\
&= \delta(\omega_\mathbf{q} - 2\epsilon_{\mathbf{k}'}) \left| \frac{1}{\omega_\mathbf{q} - \epsilon_\mathbf{p} - E_\mathbf{p} + i\eta} \right|^2 v_\mathbf{p}^2 u_\mathbf{p}^2 \big[1 - f(E_\mathbf{p})\big] f(E_\mathbf{p}),
\end{aligned} \tag{D.39}$$

where we have used the same kinds of simplifications as we did for the first term.

Lastly, we compute the **fourth term**, giving

$$\begin{aligned}
&\int_{-\infty}^{\infty} \mathrm{d}\omega_2 \left|\frac{1}{\omega_{\mathbf{q}} - \epsilon_{\mathbf{p}} + \omega_2 + i\eta}\right|^2 v_{\mathbf{p}}^2 v_{\mathbf{p}}^2 f(\omega_2) f(X - \omega_2)\delta(\omega_2 + E_{\mathbf{p}})\delta(X - \omega_2 + E_{\mathbf{p}}) \\
&= \left|\frac{1}{\omega_{\mathbf{q}} - \epsilon_{\mathbf{p}} - E_{\mathbf{p}} + i\eta}\right|^2 v_{\mathbf{p}}^2 v_{\mathbf{p}}^2 f(-E_{\mathbf{p}}) f(X + E_{\mathbf{p}})\delta(X + 2E_{\mathbf{p}}) \\
&= \left|\frac{1}{\omega_{\mathbf{q}} - \epsilon_{\mathbf{p}} - E_{\mathbf{p}} + i\eta}\right|^2 v_{\mathbf{p}}^2 v_{\mathbf{p}}^2 f(-E_{\mathbf{p}}) f(-E_{\mathbf{p}})\delta(X + 2E_{\mathbf{p}}) \\
&= \delta(\omega_{\mathbf{q}} - 2\epsilon_{\mathbf{k}'} - 2E_{\mathbf{p}})\left|\frac{1}{\omega_{\mathbf{q}} - \epsilon_{\mathbf{p}} - E_{\mathbf{p}} + i\eta}\right|^2 v_{\mathbf{p}}^2 v_{\mathbf{p}}^2 \big[1 - f(E_{\mathbf{p}})\big]\big[1 - f(E_{\mathbf{p}})\big], \quad \text{(D.40)}
\end{aligned}$$

where we used the same kinds of simplifications as we did for the first term. We can now finalize the calculation.

Finalizing the calculations

Having computed the two integrals with respect to ω_1 and ω_2, respectively. We may notice that the terms in Eqs. (D.32), (D.33), (D.38), and (D.39), are proportional to the mixed occupation–vacancy factor $f(E_{\mathbf{p}})[1 - f(E_{\mathbf{p}})]$, whereas the remaining terms involve only occupation–occupation or vacancy–vacancy factors. We therefore split the normal contribution into two terms

$$P^{(2)}_{\mathrm{norm}} = P^{(2)}_{\mathrm{norm},1} + P^{(2)}_{\mathrm{norm},2}, \quad \text{(D.41)}$$

where we collect the occupation–occupation and vacancy–vacancy factors in $P^{(2)}_{\mathrm{norm},1}$, and the occupation–vacancy factors in $P^{(2)}_{\mathrm{norm},2}$. We begin with $P^{(2)}_{\mathrm{norm},1}$, where we collect the terms given in Eqs. (D.31), (D.35), (D.37), and (D.40), giving

$$\begin{aligned}
P^{(2)}_{\mathrm{norm},1} = 8\pi\gamma_0^2 \sum_{\mathbf{p}} \Bigg[&\delta(\omega_{\mathbf{q}} - 2\epsilon_{\mathbf{k}'} - 2E_{\mathbf{p}})\left|\frac{V(\mathbf{k}' - \mathbf{p})v_{\mathbf{p}}^2}{\omega_{\mathbf{q}} - \epsilon_{\mathbf{p}} - E_{\mathbf{p}} + i\eta}\right|^2 \big[1 - f(E_{\mathbf{p}})\big]\big[1 - f(E_{\mathbf{p}})\big] \\
&+ \delta(\omega_{\mathbf{q}} - 2\epsilon_{\mathbf{k}'} + 2E_{\mathbf{p}})\left|\frac{V(\mathbf{k}' - \mathbf{p})u_{\mathbf{p}}^2}{\omega_{\mathbf{q}} - \epsilon_{\mathbf{p}} + E_{\mathbf{p}} + i\eta}\right|^2 f(E_{\mathbf{p}}) f(E_{\mathbf{p}})\Bigg]. \quad \text{(D.42)}
\end{aligned}$$

Collecting the terms given in Eqs. (D.32), (D.33), (D.38), and (D.39), yields the occupation–vacancy contribution $P^{(2)}_{\mathrm{norm},2}$:

$$\begin{aligned}
P^{(2)}_{\mathrm{norm},2} = 4\pi\gamma_0^2 \sum_{\mathbf{p}} \delta(\omega_{\mathbf{q}} - 2\epsilon_{\mathbf{k}'})&\left|V(\mathbf{k}' - \mathbf{p})\frac{\Delta(\mathbf{p})}{2E_{\mathbf{p}}}\right|^2 f(E_{\mathbf{p}})\big[1 - f(E_{\mathbf{p}})\big] \\
&\times \Bigg\{ \frac{1}{(\omega_{\mathbf{q}} - \epsilon_{\mathbf{p}} - E_{\mathbf{p}} + i\eta)(\omega_{\mathbf{q}} - \epsilon_{\mathbf{p}} + E_{\mathbf{p}} - i\eta)} \\
&\quad + \frac{1}{(\omega_{\mathbf{q}} - \epsilon_{\mathbf{p}} + E_{\mathbf{p}} + i\eta)(\omega_{\mathbf{q}} - \epsilon_{\mathbf{p}} - E_{\mathbf{p}} - i\eta)} \\
&\quad + \left|\frac{1}{\omega_{\mathbf{q}} - \epsilon_{\mathbf{p}} + E_{\mathbf{p}} + i\eta}\right|^2 + \left|\frac{1}{\omega_{\mathbf{q}} - \epsilon_{\mathbf{p}} - E_{\mathbf{p}} + i\eta}\right|^2 \Bigg\}. \quad \text{(D.43)}
\end{aligned}$$

At first glance, the expression appears as if it could take complex values. To see the relevant structure, define

$$w = (\omega_{\mathbf{q}} - \epsilon_{\mathbf{p}} - E_{\mathbf{p}} + i\eta), \tag{D.44}$$

$$z = (\omega_{\mathbf{q}} - \epsilon_{\mathbf{p}} + E_{\mathbf{p}} + i\eta), \tag{D.45}$$

Then the quantity in braces in the summand has the structure

$$\frac{1}{w\bar{z}} + \frac{1}{\bar{w}z} + \left|\frac{1}{w}\right|^2 + \left|\frac{1}{z}\right|^2. \tag{D.46}$$

This can be written as

$$\left|\frac{1}{w} + \frac{1}{z}\right|^2, \tag{D.47}$$

where it is clear that this is indeed real valued. We use this factorization to write

$$\begin{aligned} P^{(2)}_{\text{norm},2} = 4\pi\gamma_0^2 \sum_{\mathbf{p}} \delta(\omega_{\mathbf{q}} - 2\epsilon_{\mathbf{k}'}) \left| V(\mathbf{k}' - \mathbf{p}) \frac{\Delta(\mathbf{p})}{2E_{\mathbf{p}}} \right|^2 f(E_{\mathbf{p}}) \Big[1 - f(E_{\mathbf{p}})\Big] \\ \times \left| \frac{1}{\omega_{\mathbf{q}} - \epsilon_{\mathbf{p}} + E_{\mathbf{p}} + i\eta} + \frac{1}{\omega_{\mathbf{q}} - \epsilon_{\mathbf{p}} - E_{\mathbf{p}} + i\eta} \right|^2. \end{aligned} \tag{D.48}$$

Thus, the normal contribution is given by Eq. (D.41), where the two terms are given in Eqs. (D.42) and (D.48).

DEPARTMENT OF PHYSICS AND ASTRONOMY
CHALMERS UNIVERSITY OF TECHNOLOGY
Gothenburg, Sweden
www.chalmers.se

CHALMERS
UNIVERSITY OF TECHNOLOGY